CHANNEL DYNAMICS IN ALPINE AND LOWLAND STREAMS ACROSS SPATIAL AND TEMPORAL SCALES: GRAND MESA, WESTERN COLORADO AND BRAZOS RIVER, CENTRAL TEXAS

A Dissertation

by

ADAM ALLEN LEE

Submitted to the Office of Graduate and Professional Studies of
Texas A&M University
in partial fulfillment of the requirements for the degree of

DOCTOR OF PHILOSOPHY

Chair of Committee,	John Giardino
Committee Members,	Franco Marcantonio
	John Vitek
	Georgianne Moore
Head of Department,	Michael Pope

May 2017

Major Subject: Geology

ABSTRACT

Rivers and streams develop landform morphology in equilibrium with the flow of water and sediment through the channel. This dissertation examines features in fluvial systems with different geomorphic regimes; step-pool streams in Grand Mesa, western Colorado, USA and the meandering Brazos River, east-central Texas, USA.

Grand Mesa streams are unique with headwaters located on one of the largest mesas in the world. Large reservoirs with regulated discharges drain into each stream. Significant differences were found for standard step-pool characteristics of step height, channel width and step wavelength between the streams of Grand Mesa and step-pool streams in mountain-peak alpine areas. The stage of channel evolution for step-pool streams shows the Grand Mesa channels as either approaching or having obtained an idealized channel form from distribution of energy within the system.

Rates of lateral channel migration occurring along a section of the middle Brazos River from the late 1920s to 2008 were mapped using aerial photographs, planimetric maps, and fieldwork. Flow regulation has greatly altered the discharge and suspended sediment characteristics of the river. Peak flows occurred more frequently prior to regulation, impacting the rate and style of migration. Rates of channel migration prior to regulation averaged 13 (+/- 3) m/year whereas migration after regulation averaged 4 (+/- 3) m/year. Total channel migration ranged from 1.09 to 11.53 m/year with an average of 3.28 m/year. The results support the difficulty in predicting the magnitude of channel meandering for large rivers.

Oxbow lakes are a major component of the fluvial system in lowland regions. After cutoff, the lake fills with sediment and requires an increasing river discharge to maintain a hydrologic connection. The relationship between the cutoff ratio, diversion angle and rate of sedimentation of twenty eight lakes located on the middle and lower Brazos River, central Texas, was examined. The time of cutoff was dated using historic maps and aerial photographs. Rates of sedimentation were determined using a digital elevation model and range from 0.02 to 0.4 meters per year. Field observations of river-to-lake connections with the rates of sedimentation determined a correlation between discharge events in the main channel and sediment deposited in the lake.

DEDICATION

Family…

Patient as the stars in the sky.

Always watching over…

Shining their light.

“Sky above prairie

Waves of grain all around us,

From black soil is Life.”

ACKNOWLEDGEMENTS

I would like to acknowledge the family, friends and folks that have supported and encouraged my studies all these many years; without their love and patience this document and this degree would be much less, or nothing. But it is something and I am something, because of them.

A hearty thanks to a most excellent teacher and mentor; Dr. John R. Giardino. His incredible breadth of knowledge, technical ability and advisement are greatly appreciated. Words are difficult to describe the gratitude for his efforts in my degree program. As we journey through life we intersect with people big and small on our timeline. Rick, you are a giant in my world. The storm was strong, but we made it to shore.

I thank Greg Malstaff and the staff of the Texas Water Development Board and the Instream Flow Program; their technical and financial support made this project, and the degree, possible. Roads unknown we travel; fortunate when others offer to light the way. Chevron Corporation also provided a one year research fellowship; many thanks!

Much thanks to my committee members: Drs. John Vitek, Georgianne Moore and Franco Marcantonio. It takes a village to raise one and Academia has its own language; thank you for the chance to step on the field.

The various staff and faculty of the Department of Geology and Geophysics at Texas A&M University, College Station. I greatly enjoyed my time there, a highlight of my life. Fancy findings are built upon the solid foundations constructed by others; to touch the Sun someone has to build the ladder. Thank you, craftsmen.

CONTRIBUTORS AND FUNDING SOURCES

This work was supervised by a dissertation committee consisting of Professor John Giardino and Professors John Vitek and Franco Marcantonio of the Department of Geology & Geophysics and Professors Inci Guneralp and Georgianne Moore of the Departments of Geography and Ecosystem Science & Management, respectively.

All work for the dissertation was completed by the student, under the advisement of Professor John Giardino of the Department of Geology & Geophysics.

This work was made possible in part by the Instream Flow Program in the Texas Water Development Board under Project Numbers 0904830898 and 0904830969. A fellowship was also provided by the Chevron Corporation through Texas A&M University. Funding was also provided by the Department of Geology & Geophysics at Texas A&M University in the form of numerous teaching assistantships.

Its contents are solely the responsibility of the authors and do not necessarily represent the official views of the Texas Water Development Board, Chevron Corporation or Texas A&M University.

TABLE OF CONTENTS

Page

LIST OF FIGURES

FIGURE Page

FIGURE Page

FIGURE Page

FIGURE Page

LIST OF TABLES

TABLE Page

1 INTRODUCTION

Nature, through organized chaos, presents a variety of landscapes and comprising landforms to the observer. Through space and time, matter and energy work in concert to provide a complex pattern of ever changing forms. The gravitational and molecular shear stresses working on the variety of Earth materials lead in turn to the cycles of weathering, erosion, transportation and deposition (Strahler, 1952). Of concern to this work is the process and pattern of fluvial channels on a planetary surface, specifically the surface of Earth. Matter in and along the stream is organized based on many factors within and without the channel boundary. This organizing is in constant flux, so that a seemingly stable landscape is undergoing modification, if even on the slightest scale or detail. In addition, the magnitude and frequency of events (Wolman and Miller, 1959), along with the geologic composition of an area, works to produce a vast array of forms in surface channels.

Under entropy, landscapes tend towards conserving energy with the least work done. Combined with factors interacting in a given landscape, any particular form in the landscape is attempting to reach equilibrium in erosion, transport and deposition of materials. With all forms in the landscape interacting with and against one another, equilibrium becomes dynamic, making adjustments within the landscape a constant (Hack, 1975) as the terrestrial surface of Earth is uplifted and subsequently lowered.

Of the factors affecting channel organization, and subsequent form, is the general relief of the region or area containing the channel. Stream channels in alpine and lowland areas work to dissipate energy and material, thus, creating highly specific

landforms to the particular region. Yet, both types of systems, the alpine and the lowland, are part of a continuum of fluvial processes and landscapes. Therefore, as this dissertation demonstrates, disparate fluvial forms are a response to similar channel conditions in different environments containing the channels. Through analysis of step-pool streams in Grand Mesa, Colorado and channel migration of the Brazos River in southeast Texas this work seeks to understand channel process and form. Specifically, the form of step-pools as relative to other, more traditional alpine systems containing step-pool streams; and channel migration in the context of various factors along the Brazos. These two different environments, alpine and lowland, give understanding to the general fluvial actions governing flow of surface water and the resultant landforms.

2 MORPHOLOGY OF STEP-POOL STREAMS ALONG GRAND MESA, COLORADO, USA

2.1 Overview

Step-pool streams are ubiquitous mountain features in which an alternating pattern of steps and pools, composed of large and small clasts, respectively, form in high gradient areas. The streams along the southern flanks of Grand Mesa, Colorado, one of the largest mesas in the world, are characterized by steep channel gradients, with steps composed of igneous clasts and woody debris and pools filled with finer sediments. The stream networks along Grand Mesa are unique in that they are fed by numerous, regulated, large reservoirs located on top of the mesa; in contrast to most first-order mountain step-pool streams originating at a high altitude and below an alpine peak.

The lengths of the step-pools vary from 1.2 to 3.7 meters. Step height varies from 0.07 to 0.61 meters. Particle sizes in a step range in size from 0.12 to 0.671 meters in diameter; pool sediments range from silt to > 0.61 meters in diameter. The stream geometry of Grand Mesa was compared to data from published studies on step-pool streams in mountain-peak landscapes of North America and Europe. Statistical tests found significant differences between the morphologic features of channel width and wavelength comparing the Grand Mesa and mountain-peak streams; with wider channels and greater wavelength on the mountain-peak streams. The step height and particle size of Grand Mesa have no significant difference compared to the step-pool streams of published studies in the scientific literature. The difference of channel width is likely attributable to the overall larger drainage areas and discharges of the mountain-peak

data. The average size of sediment particles comprising the steps is approximately equal between the two datasets. Step height, strongly controlled by the particle size comprising the steps, is equal between the Grand Mesa and alpine mountain-peak data.

In addition to natural, seasonal stream flow, the regulated reservoirs contribute releases of relatively large volumes of water. The overall contribution of the reservoirs, despite regular, nearly yearly releases, does little to change the overall discharge regime of step-pool streams along Grand Mesa. The total volume of water annually released from reservoirs averages 28,721 m^3/km^2, with the natural stream discharge ranging from 419,287 to 2,515,723 m^3/km^2. The releases from the reservoirs are neither of sufficient duration, magnitude nor frequency to alter channel geometry, as compared to natural seasonal discharge. From this work, high alpine reservoirs, which are uncommon in mountainous areas, do not significantly alter step-pool morphology, which is dominated by the morphologic characteristics of the watershed. These morphologic characteristics include channel slope, watershed area and channel width.

2.2 Introduction to Problem

Step-pool streams represent a distinctive channel pattern in mountainous regions (Montgomery and Buffington, 1997). Much of the work in step-pool morphology has been focused on understanding the processes governing formation and dimensions as well as how changes in slope, grain size, drainage area and discharge affect the channel characteristics (Grant et al., 1990; Abrahams et al., 1995; Zimmermann, 2008). The step-pool channel represents a geomorphic form balancing the erosive force of hydraulic processes with the resistance of substrate (Wohl and Wilcox, 2005). Boulders, large

woody debris (LWD) or erosion of bedrock comprise the structure of step-pools (Zimmermann, 2013).

Chin (1999) describes difficulty in discerning the role of discharge on step-pool formation; specifically, observing the flows needed to move the largest particles in the system. By analyzing the discharge values for the three streams, insight may be gained into the role played by discharge in the formation of step-pool sequences. The morphologic characteristics of step-pools along Grand Mesa can then be compared to those of step-pool sequences in other mountainous areas to understand better the processes acting on the formation. The main question, therefore, is; are the step-pools of Grand Mesa different in the morphologic characteristics than those of other regions, specifically streams originating from alpine mountain-peak topography? In addition, this study asks if the anthropogenic influenced (reservoir releases) discharge alters the basic geometry of step-pool streams?

Research in recent years seeks to place step-pool systems along an evolutionary progress in the geomorphic landscape (Chin and Phillips, 2007). Spatially divergent self-organization is defined either as minimizing or maximizing energy dissipation and/or entropy in a system. The broad concept includes the evolution of order and regularity in the total properties of a landscape through converging forms, and how those properties diverge into different landscapes of various forms (Phillips, 1999). The specific age and spatial extent of the basalt cap, approximately 9.92 Ma (Rex, 2007), atop Grand Mesa provide a temporal boundary on fluvial landscape evolution. The underlying rocks range in age from Eocene, ~40 Ma to upper Cretaceous, ~90 Ma. As comparison, the

mountain-peak landscapes reviewed in this study range in age from 5-7 Ma for the Cascades in western North America to 75-100 Ma for the central Rocky Mountains and ~100 Ma for the western Alps in central Europe.

In addition to allogenic tectonic and climatic controls, landscapes and geomorphic systems evolve in autogenic, or internal, organization (Chin & Phillips, 2007). The character of the basalt cap, specifically its well established age and large initial extent, may provide insight in the stage of evolution of a particular geomorphic region. Therefore, the step-pool streams of Grand Mesa have a defined temporal boundary and the morphologic properties may provide insight into the stage of evolution for alpine channels along the mesa.

Grand Mesa is a unique environment among landforms of the Colorado Plateau, especially those exposed to recent Pleistocene glaciations. Also unique to many of the step-pool environments commonly described in the published literature, the area has a high elevation with relatively flat topography at the top. Within the mesa topography over 220 lakes and numerous ponds fill depressions scoured from the prior glaciation. Ten surface water reservoirs, developed for irrigation purposes downstream, act as storage for potential energy to alter channel morphology downstream for the three streams observed for this study. Releases from reservoirs represent high-magnitude, low-frequency floods which the flows regimes are correlating to step-pool channels (Whittaker and Jaeggi, 1982). Therefore, the combination of a flat mesa and large reservoirs with periodic high-magnitude releases presents a unique geomorphic environment among high altitude 1st order streams. From this one can reasonably ask:

Do differences in step-pool morphology exist between the mesa and mountain-peak streams; and reservoir or non-reservoir alpine streams?

The goals of this work are:

1) Field survey and measurement the primary attributes of step-pool channels along the southern flank of Grand Mesa, CO
2) Compile and analyze the discharge data for the streams surveyed
3) Compile data on the primary attributes of step-pool streams from the scientific literature
4) Compare, graphically and statistically, the similarities and differences between the step-pool streams of Grand Mesa and those of mountain-peak systems

The main focus of this study is a comparison of the general morphology of alpine step-pool streams between Grand Mesa streams and other non-mesa mountain-peak streams. The unique situation of a flat mesa top and numerous large water reservoirs with controlled releases may contribute to significantly different step-pool morphology than streams in the more common mountain-peak regions. The null hypothesis of this study is: no significant differences exist between the average geometry of morphologic stream features of Grand Mesa and other mountain-peak areas. Alternately, examining the channel morphology and hydrology may exhibit differences in theses morphologies between mesa and mountain environments.

2.3 Literature Review

The dominant controls of channel slope and lateral confinements, which are influenced by the overall regional geomorphology, influence development of step-pool channels (Chin, 1989). Whereas streams in lower gradient watersheds meander or braid in the lateral dimension to dissipate energy (Chin 2002, Chin 2005), the higher slope gradients and narrower floodplains of alpine streams often results in channel meandering in the vertical dimension. This vertical meandering is manifest in step-pool and riffle pool channel morphologies (Ritter, 2006).

The main morphologic components of step-pool streams include channel width, step height and wavelength, or the distance between successive step crests (Abrahams, 1995; Chin, 1999). The wavelength is determined in large part by the slope and confinement of the channel. In watersheds of comparable size in similar physiographic settings, especially alpine, a more confined channel is generally narrower in bankfull width. In a channel system tending toward equilibrium of sediment and water transport, the steps prevent excessive erosion and channel degradation is checked by the channel steps forming along steep slopes (Heede, 1981; Chin and Wohl, 2005).

An important dependent variable from these main components is step wavelength, or the distance between successive step crests. Abrahams et al. (1995) hypothesized that step-pool morphology is formed through maximum resistance to flow, whereas Allen (1982) postulated that step-pool morphologies share a similar formation process as antidunes. Step wavelength, demonstrated by Chartrand and Whiting (2000), is a strong control on the overall morphology of step-pool channels.

The distance between step crests, or wavelength, is inverse to channel slope (Chin, 2008), with steeper slopes correlating to higher steps (Chin, 2008). Abrahams et al. (1995) describes the ratio of step height over pool length over slope as the channel shape with maximum resistance to flow. Zimmerman (2013) compares this ratio, H/L/S, to channel slope, with Canovaro et al., (2004); Church and Zimmermann, (2007); and Zimmermann (2009) finding that slopes of less than 7% form step-pool channels. The height of steps is also dependent on the particle sizes available to form steps. The average ratio of step height to the median diameter of step particle sizes (often cobble to boulder size), with consistent units, generally ranges from 1.0 to 1.5 (Chartrand and Whiting, 2000; Chin, 2008) with step height and particle size having consistent units. Particle sizes in step-pool systems often range from cobble to boulder size. Step wavelength increases further downstream in the transition to pool and riffle morphology. In free-flowing streams, channel width is a surrogate for drainage area, which correlates to average step height (Chin, 1999). The correlation between increasing channel width and drainage area is similar to the spacing between meanders and pool-riffle sequences; therefore, wavelengths are a function of discharge or channel width (Leopold and Wolman, 1957; Keller and Melhorn, 1978). Therefore, expressing step-pool spacing in units of channel width enables comparison with recent literature and allows interpretation of step-pool spacing in the context of gravel bed forms and adjustments in the fluvial landscapes (Chin, 1999). Particle size is a surrogate for slope and can be compared to step height and wavelength (Chin, 1999), with increasing particle size, which comprise the steps, resulting in larger step heights. As step height increases the

distance between successive steps, or wavelength, also increases to balance water and sediment in a given channel slope.

Halwas and Church (2002), McFarlane and Wohl (2003), and Wilcox and Wohl (2007) have shown variation in step-pool geometry according to major differences in geology or channel material. Halwas and Church (2002) described channel units in their investigations of the morphology of high-gradient streams in British Columbia, Canada. They examined the differences between bedrock, boulder, rapid, chute, riffle, glide and pool-channel systems. Halwas and Church (2002) found equivalent channel units in relatively equal regional settings. MacFarlane and Wohl (2003) compared step-pool morphologies of streams containing large amounts of large woody debris against those with relatively little large woody debris. Finding the presence, or lack, of LWD determines resistance of step-pools to the scouring effects of flow. Last, Wilcox and Wohl (2007) examined the velocity component of discharge along the longitudinal, cross-sectional and vertical dimensions showing that the discharge characteristics greatly influence step-pool hydraulics and subsequent channel forms.

Average step length increases with decreasing slope (Judd, 1964; Wertz, 1966; and Chin and Phillips, 2007). The steepness ratio, of step height (H) over wavelength (L) expressed as H/L, generally ranges from 0.06 to 0.20 for step-pool streams (Whittaker, 1987; Chin and Wohl, 2005). The spacing between steps, related to wavelength, generally ranges from one to four channel widths (Whittaker, 1987; Chin, 1989; 1999; Grant et al., 1990; Montgomery et al., 1995; Billi et al., 1998; Chin, 1999; Chartrand and Whiting, 2000; Wooldridge and Hickin, 2002; Curran and Wohl, 2003; Chin and Wohl,

2005; Chin and Phillips, 2007). A stepped bed profile often occurs along streams having a slope greater than 4-5% (Comiti, 2012) with Abrahams (1995) finding the steepness ratio, H/L, approximates to 1.5 times the slope. This relationship of steepness to slope defines the maximum flow resistance to develop step-pools in a channel (Lenzi, 2001).

Step-pool morphology transitions to riffles and pools as elevation decreases (Ritter, 2006) and distance between riffles increases downstream. With decreasing slope, this transition from a closely spaced step and pool channel to riffle and pool channel represents a reorganization of matter to accommodate changes in energy along the channel system.

2.4 Physical Setting

Grand Mesa, located in Delta and Grand Junction counties of western Colorado (Figure 2.1), is the largest mesa in the world with an elevation of approximately 3,050 meters. Located in western Colorado (latitude: 39^{o}04’00” N; longitude: 107^{o}56’12” W) Grand Mesa is an east-west trending landform with a basalt cap of ~10 Ma (Cole, 2007) overlying shale and sandstones of Jurassic and Cretaceous age (Cole and Sexton, 1981). The geology of Grand Mesa generally consists of Quaternary age alluvial and fluvial deposits underlain by sandstones and shales of Pleistocene to Cretaceous age, with further basement rock of Jurassic, Triassic and Precambrian origin (Fig. 2.2). The three study reaches drain a portion of the southern flank of Grand Mesa (Fig. 2.1). Cottonwood Creek, Youngs Creek and Horse Creek enter into Surface Creek which in turn flows into the Gunnison River near Delta, Colorado. The streams consist predominantly of basalt boulders and sediments derived from eroded sandstones and

shales. Further down the valley the streams consist of gravel and colluvium material.

The basalt cap covered an area of ~1943 square kilometers but subsequent erosion by predominantly fluvial and glacial processes has reduced the basalt cap to ~137 mi^2. Elevation differences between the mesa and the Colorado and Gunnison rivers are approximately 1,650 meters. Average thickness of the basalt cap ranges widely from 50 to 207 meters, with a maximum thickness of 240 meters (Cole and Sexton, 1981); and incision of the surrounding landscape averages approximately 0.17 meters per 1,000 years (Cole, 2001; Baker, 2002).

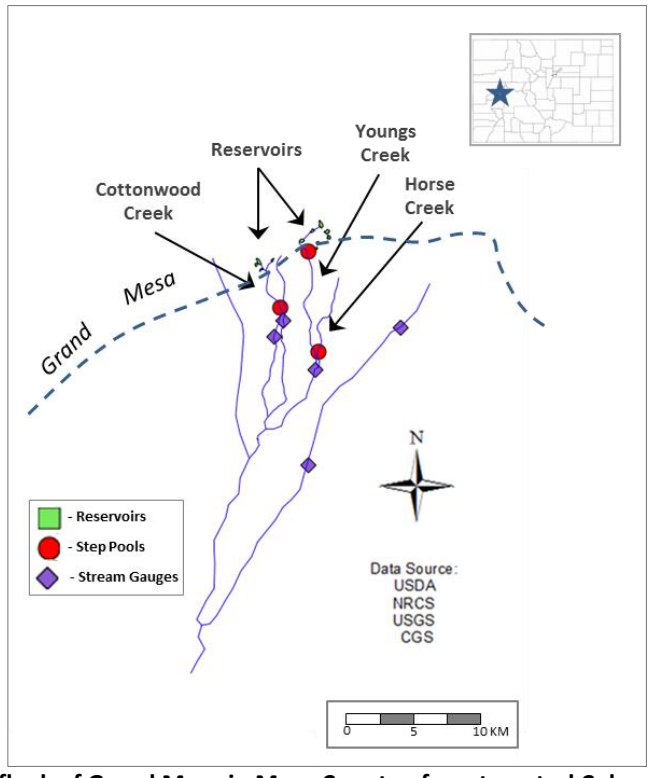

Figure 2.1. Southern flank of Grand Mesa in Mesa County of west-central Colorado. The three study sites are located in the upper half of the watershed. Historic and active gauge stations are located approximately 2-8 km downstream of the study locations. The reservoirs draining into the streams are the small green-colored polygons to the north of the mesa boundary line.

Subsequent erosion of the basaltic rock has created a series of geomorphic units of Quaternary age along the flanks of the mesa. A series of gravel units produced by stream and glacier transport underlie late Quaternary and Holocene alluvium and colluvial deposits (Hail, 1972) The Quaternary deposits range in thickness from 1 to 24 meters (Darling, 2007). Yeend (1969) classified surficial deposits into three major episodes of gravel and till deposition produced by late-Pleistocene glacial events of the Pinedale, Bull Lake and pre-Bull Lake episodes. Analysis of marine oxygen isotopes (MIS) place Pinedale in Late Wisconsin, MIS 2, Bull Lake in MIS 6 or earlier MIS 5d and pre-Bull Lake as pre-MIS 6 (Pierce, 2003). These isotopes categories correspond to glaciation of various ages. Pinedale glaciers culminated near the last maximum glacial extent at 21,000 years ago with MIS 2, and MIS 5d & 6 representing glacial deposits older than 55,000 years before present.

The Quaternary formations contain a large mix of basaltic sediments from the igneous cap atop the mesa. The stream headwaters and reservoirs are in glacial drift of basalt boulder till approximately Pinedale age. Where erosion has removed the basalt cap grayish fine-grained sandstones and siltstones of the Green River Formation of late Eocene age (Hail, 1972) outcrop among scattered the glacial drift. Included in this formation are minor deposits of marlstone and oil shales. Between the Tertiary basalt flows and Green River Formation lays the Uinta Formation, with a thickness of 60 meters (Ellis, 1989).

Occupying the interfluves between watersheds is the Wasatch Formation, early Eocene age, comprised of varies claystones and shale with interbedded sandstones and

conglomerates. Underlying the Wasatch Formation, the Mesaverde Formation the upper part contains brown to gray fine- to medium-grained sandstones with gray interbedded shale and a basal coal layer. Overlaying the Mesaverde are occasional conglomerate sandstones.

The southern flank of Grand Mesa, north of the town of Cedaredge, forms a topographic U-shape, with streams draining to the southwest towards the Gunnison River. The majority of the lower portion of the watersheds is comprised of young alluvial gravels. These gravels have numerous fans and pediments, with scattered deposits of basalt boulders from the mesa cap. Much of this material is glacial outwash of Pinedale age.

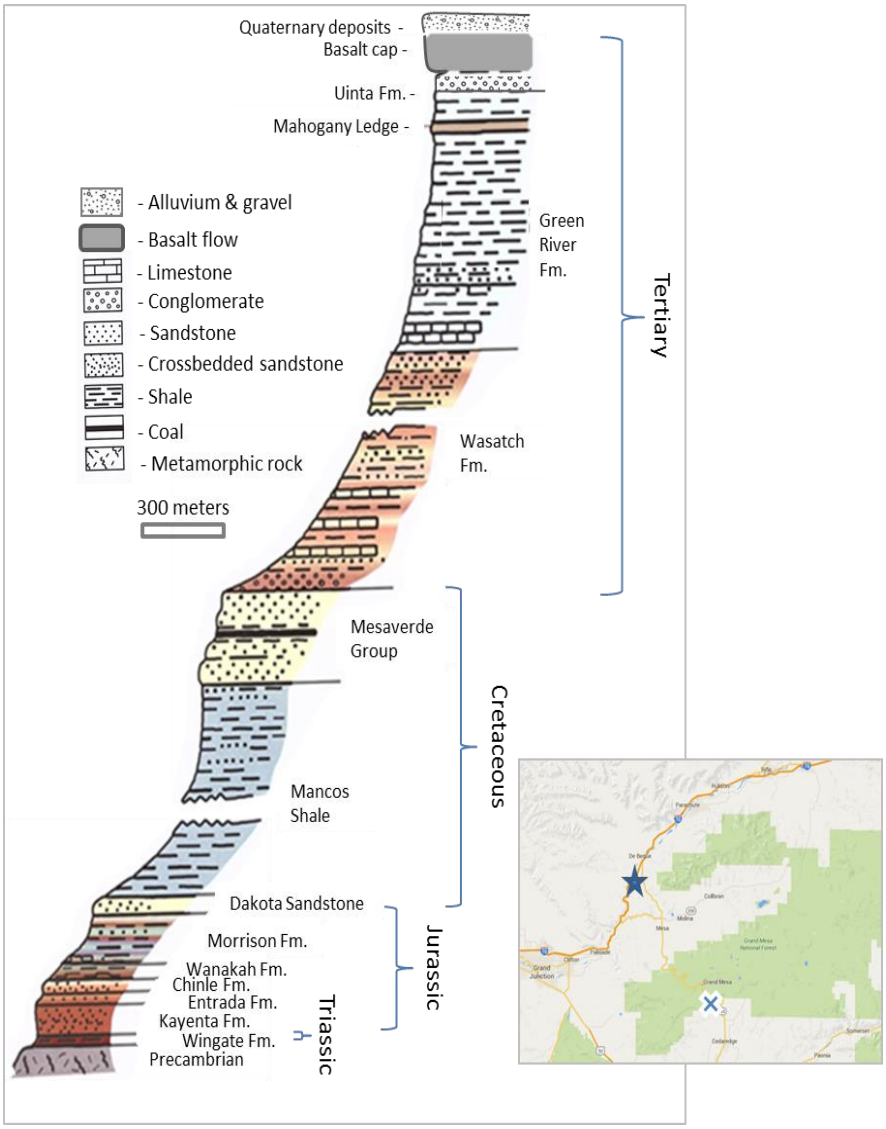

Figure 2.2 Stratigraphic column of Grand Valley along Interstate 70 along the northern flank of Grand Mesa (modified from Williams and Chronic, 2014). The stratigraphic column and study sites are marked with the blue star and cross, respectively, on the inset map.

Surface Creek, of which Cottonwood, Horse, Youngs and Kiser creeks drain into, is the major watershed of southern Grand Mesa and empties into the Gunnison River. The central valley of Surface Creek, comprised of Pinedale age alluvial sediments, is bounded on the east and west sides of the drainage with Mancos Shale topped with

gravels of middle Quaternary age of the Bull Lake episode.

Numerous reservoirs atop the mesa drain into streams flowing down the southern flank of Grand Mesa (Fig. 2.3). The reservoirs are predominantly located in the Uinta Formation, which underlies the major alluvial gravel and glacial drift deposits along the slopes of the mesa. The majority of the reservoirs have controlled outlets for releases into the natural streams and numerous diversion structures in the Grand Mesa watershed.

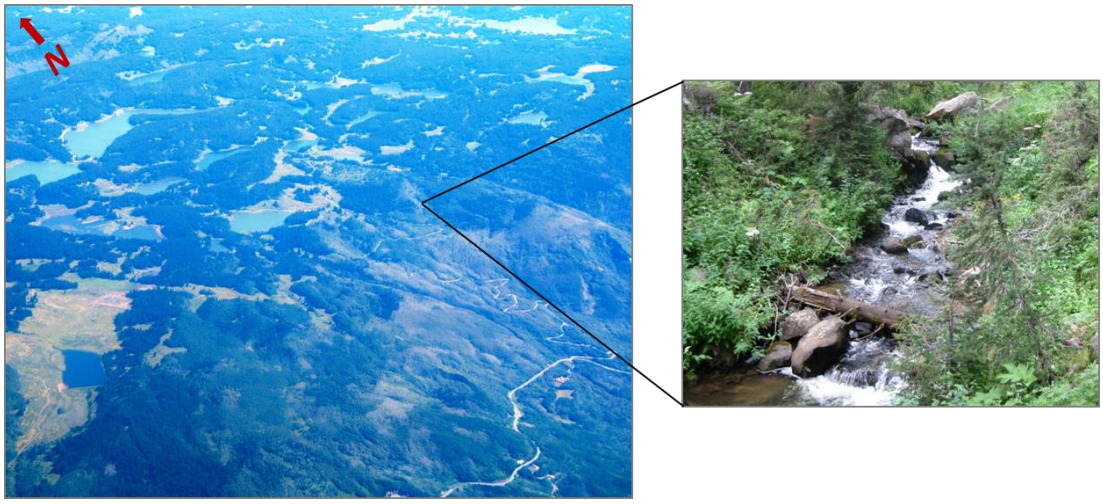

Figure 2.3. The left image is an oblique aerial photograph of the southern flanks of Grand Mesa. The red arrow points north. The numerous reservoirs atop the mesa are visible in the upper northern portion of the photograph. The photograph on the right shows a typical step-pool sequence in the high alpine streams of Grand Mesa. Large igneous boulders, with occasional logs, form the steps. The channel is approximately two meters wide.

The Colorado Decision Support System (CDSS) is an online database providing mapping and reports for water resources and structures in Colorado, including diversions, reservoirs, wells and pipelines. The southern portion of Grand Mesa, including the study reaches and the Surface Creek watershed, contain dozens of water diversion structures with many located near the headwaters of the step-pool streams.

2.5 Methods

2.5.1 Step-Pool Stream Morphology

United States Geological Survey (USGS) topographic maps and aerial photographs from the National Agricultural Imagery Program for the Cedaredge Area in Delta County, Colorado were used to locate high gradient slopes along the stream channels in which step-pools would likely be found. Specifically, streams were surveyed that had relative ease of access from US Highway 65, which travels up the valley along southern Grand Mesa. A single continuous reach in each stream was surveyed; with the start and end points based on changes in channel morphology, specifically slope changes where the channel transitioned from step-pool to pool-and-riffle morphology. Field surveys of reaches collected the stream geometry data using measuring tape and stadia survey rod. A global positioning system receiver located the step-pool reaches within the overall watershed. The surveyed reaches along Cottonwood, Youngs and Horse creeks were 26.6 (m), 32.9 (m) and 30.5 (m) in length, respectively. Eleven consecutive step-pool segments were surveyed in each stream.

The common step-pool morphologic parameters (Fig. 2.4) measured include: step height, pool length (spacing) and particle size (Grant et al., 1990; Wohl and Grodek, 1994; Chartrand and Whiting, 2000). Particle sizes for sediments in the pool were collected using the Wolman pebble count method (Wolman 1954; Leopold, 1970). Sediments were measured on each step along the B-axis where visible; the diameter of large woody debris (LWD) was measured where present in the steps. The surveyed reach of Youngs Creek is located at the highest altitude of the three study reaches and

contained more large woody debris, relative to Cottonwood and Horse creeks.

The upstream and downstream heights of steps were recorded to determine the volume of each pool. In addition, step width and pool width record the average channel width, which is a surrogate for channel discharge (Chin, 1999). The planform step thickness, or step length parallel to the direction of flow between successive steps was also measured to calculate the wavelength and overall length of the step-pool reaches.

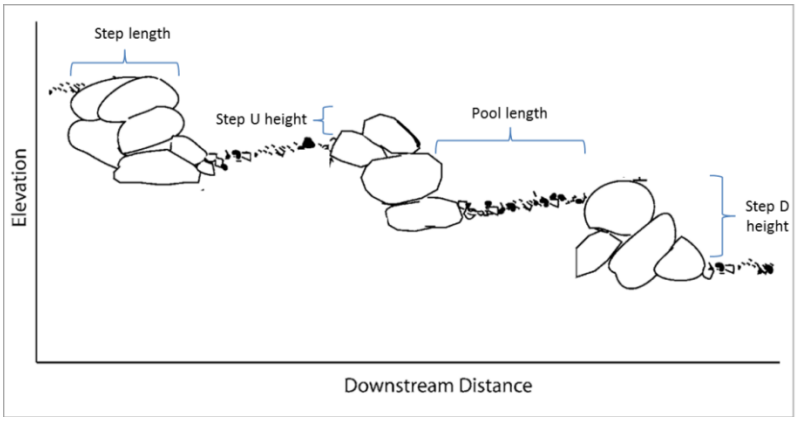

Figure 2.4. Schematic of typical step-pool profile (modified from Chin and Wohl, 2005). The upstream step height is represented with a 'U' and the downstream step height is represented with a 'D'. Wavelength is the distance between successive step crests. Width of the step-pool is the horizontal measurement taken across the step perpendicular to this image.

2.5.2 Step-Pool Data from Published Literature

Data on step-pool morphology in other alpine regions was compiled from the literature to graphically and statistically compare with the morphologies of the surveyed Grand Mesa streams. Studies were chosen that featured step-pool streams in regions with dominantly mountain-peak topography and did not contain surface water bodies at the stream headwaters. The published literature contains a range of studies focusing

predominantly on the morphology with emphasis on step-pool topography. The locations for the majority of the studies are the western United States and European Alps, with one study in New Zealand (Table 2.2). From these studies data on step-pool morphology was compiled with a focus on the variables of (1) channel width, (2) step height, (3) wavelength and (4) sediment particle size. The compiled data from the literature has a range of step-pool characteristics, including those with steps comprised of LWD and non-LWD, and alluvial, bedrock and mixed channels.

In addition data on drainage area and channel slope were compiled from the literature. These variables are important controls across the range of channel morphologies, including step-pools. Statistical tests were not performed on these data because the three streams surveyed along Grand Mesa (each having one data point for drainage area, discharge and channel slope) are not a sufficient sample size. The average, min and max of the mountain-peak data was compared to the Grand Mesa data for a descriptive comparison.

2.5.3 Stream Discharge along Grand Mesa

The stream discharge strongly affects channel morphology. The discharge data of Grand Mesa is a compilation of ten years of stream gauge data from the 1950s and 60s; whereas the discharge data from the literature is often collected during bankfull events when the step-pools are surveyed. Therefore, statistical comparison of discharge was not performed but comparing the range and averages are useful for understanding the results for the four channel variables.

Data from the USGS on daily average stream discharge is available from 1957 to

1969 for Cottonwood Creek, Youngs Creek and Kiser Creek. Kiser Creek is located in an adjacent watershed to the three streams in this study but at the time of field surveys was in overbank flood conditions from reservoir releases on the mesa. Therefore, Kiser Creek was not surveyed for step-pools. Nonetheless, Kiser Creek discharge data was included in this study because it has very similar overall watershed, climate and geologic conditions relative to the three surveyed streams.

The Colorado Water Conservation Board (CWCB) provides reports and data on water use through the Colorado Decision Support System (CDSS) website. Data on reservoir releases and mapped locations of water diversions from the reservoirs was compiled to compare to natural stream flow from the USGS gauging stations. Water diversions include surface ditches and pipelines predominantly used for agriculture in the Gunnison River Basin.

2.5.4 Statistical Analysis

Two statistical methods were used with the field data from the Grand Mesa streams and the data gathered from the published literature. The research focus of this study is a comparison of the standard geometric components (channel width, step height, wavelength and average sediment size) of Grand Mesa step-pool streams to step-pools of other areas; specifically step-pools occurring in high alpine, mountain-peak topography. The Pearson Product-Moment Correlation statistic compared the strength of correlation between independent and dependent variables for the Grand Mesa and mountain-peak step-pool streams. A parametric T-Test statistical method using unequal variances, with a 95% confidence, was used to compare the means of Grand Mesa step-pools to those of

mountain-peak streams for the main stream geometries of channel width, wavelength, step height and D_{50} sediment.

2.6 Results

2.6.1 Discharge

Surface discharge is an important component in determining step-pool wavelength and step height (Chin, 1999). The USGS operated a surface gauging station on two of the study streams and a third adjacent stream, Kiser Creek (not included in the field surveyed channels) from 1957 to 1969. For all three streams discharge never exceeds 3 m^3/s (Fig. 2.5). Though Horse Creek drains into Youngs Creek the stream gauge along Youngs Creek is above the confluence of the two creeks, therefore, Horse Creek discharge is not represented in the hydrographs.

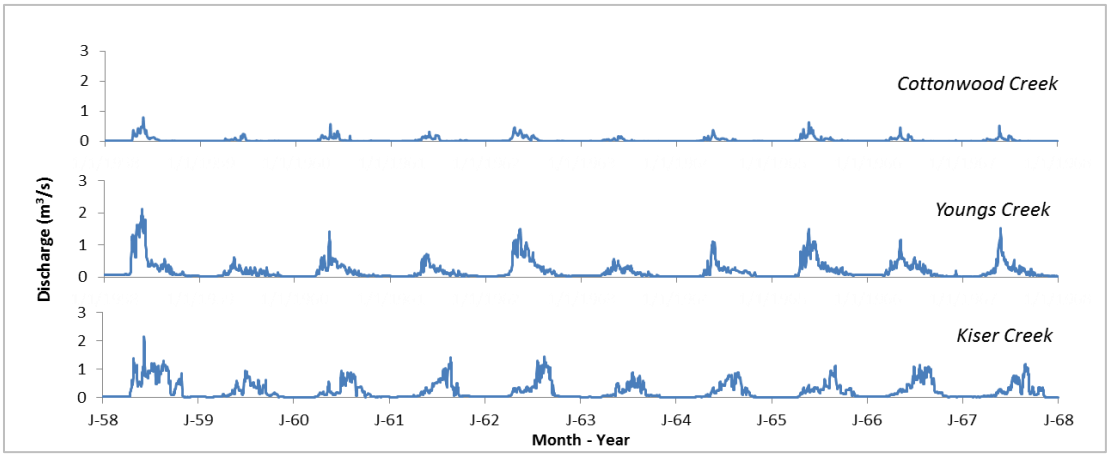

Figure 2.5. Historic daily discharge for three creeks along southern Grand Mesa. Cottonwood and Youngs creeks are included in the step-pool surveys, Kiser Creek was not surveyed in the field because of flooding. The discharge data was collected from January 1st, 1958 to January 1st, 1968.

During the field surveys, local water managers provided the current discharge at

the reservoir outlet into the step-pool streams. Kiser Creek, undergoing major release from the reservoir, had a discharge of 1 m^3/s, whereas Cottonwood Creek, Horse Creek and Youngs Creek had discharges of 0.008 m^3/s, 0.06 m^3/s and 0.2 m^3/s, respectively. The 1 m^3/s discharge at Kiser is greater than 97% of the stream discharge on Kiser Creek during the 1957-1967 gauging period (Fig. 2.5), representing significant overbank flooding for the stream.

Discharge during a specific year follows the general trend of alpine watersheds in the mountainous western United States with spring and summer snow melt greatly increasing discharge followed by low flow during the summer months. The earliest recorded reservoir release along these streams is 1973; therefore, no high discharges or floods from reservoir releases are recorded in the stream gauges. Cottonwood, Youngs and Kiser creeks drain into Surface Creek near the town of Cedaredge, which in turn flows into the Gunnison River near Delta, Colorado.

Moving downstream along the watersheds in this study is a number of additional stream gauges located on channels. The discharge values in the gauge records on Surface Creek and the Gunnison River do not show a marked increase corresponding to times of reservoir release. In addition to the complex interaction between surface and ground water along the length of a watershed, numerous diversion structures route the reservoir water to urban and agricultural uses. Although Horse Creek has no historic stream gauge for surface discharge data, the stream is of comparable size and adjacent to the Cottonwood Creek and Youngs Creek watersheds, therefore, Horse Creek should display similar surface hydrology characteristics. Reservoir releases for the three creeks occur

across a large range (Fig. 2.6) Releases from reservoirs are sporadic and dependent in part on rainfall amounts and land use patterns in the lower watersheds flanking Grand Mesa. For Cottonwood Creek several releases occur during a given year, whereas Youngs Creek has fewer but greater magnitude releases.

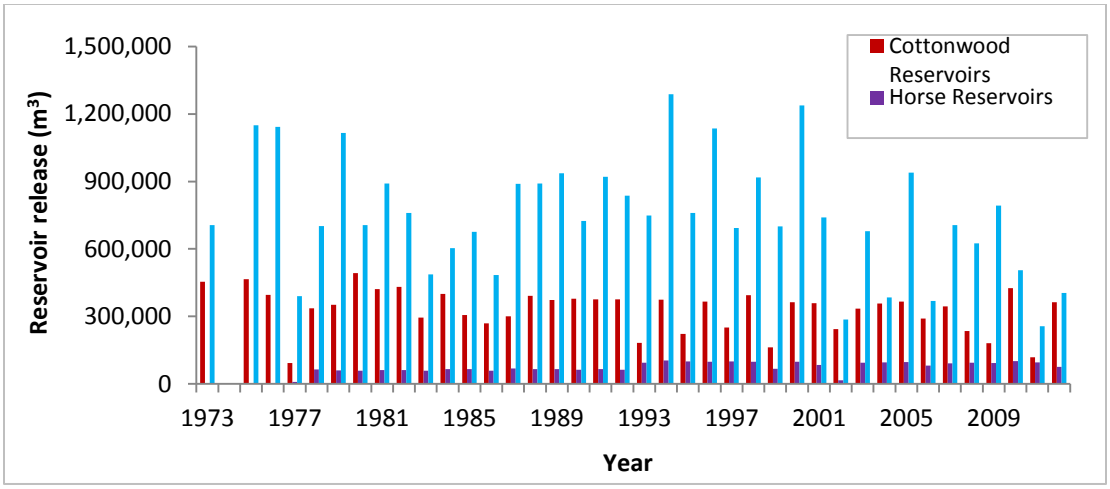

Figure 2.6. Reservoir releases for Cottonwood, Horse and Youngs creeks from 1973 to 2012. There are nine reservoirs discharging to the streams. The release values for a given year are cumulative, with many years containing multiple releases per reservoir.

Releases, to assist in irrigation operations further down the watersheds, from the reservoirs atop Grand Mesa typical occur from the beginning of June to the end of October for a given year, with occasional releases in May and late November. The majority of the reservoirs releases occurred from 1973 to 2012, based on the most recent data released by the CWCB. The two reservoirs on Horse Creek, the smallest stream and drainage area among the three streams of this study, had releases from 1993 to 2012 and 1977 to 2012, representing a shorter release period than either Cottonwood or Youngs creeks.

For the nine total reservoirs in the study, releases occurred on a nearly yearly basis, yet the CDSS only provides the *number of days* for a particular release for 24 percent of the total releases. Therefore, the record is incomplete concerning the maximum and minimum in discharge during all the recorded releases along Cottonwood, Horse and Youngs creeks. Reservoirs have relatively short release periods with fewer than one hundred days of release. The yearly time period of record between the reservoirs and streams is different and negates a direct comparison.

Release amounts for the reservoirs on Cottonwood, Horse and Youngs creeks vary greatly in total discharge for given water releases (Fig. 2.6). Cottonwood Creek reservoirs include Womack No. 1 and Womack No. 2. The maximum, minimum and average releases for Womack No. 1 reservoir are 270,132 m^3, 5,550 m^3 and 107,063 m^3 respectively. Womack No. 2 reservoir includes maximum, minimum and average releases of 214,625 m^3, 90,459 m^3 and 1,110 m^3, respectively. Horse Creek reservoirs include Eureka No. 1 and Eureka No. 2. Reservoir releases for Eureka No. 1 are a maximum, minimum and average of 36,757 m^3, 4,218 m^3, and 29,885 m^3, respectively; while Eureka No. 2 has a maximum, minimum and average of 70,678 m^3, 9,867 m^3, and 59,805 m^3.

Youngs Creek reservoirs include Goodenough, Mckoon, Ryan, Youngs No. 1 and Youngs No. 3. The maximum, minimum and average release values are, respectively, 192,274 m^3, 24,669 m^3 and 129,465 m^3 (Goodenough); 176,461 m^3, 1,850 m^3 and 74,705 m^3 (Mckoon); 64,140 m^3, 14,555 m^3 and 45,595 m^3 (Ryan); 849,621 m^3, 3897 m^3 and 430,373 m^3 (Youngs No. 1); 247,460 m^3, 21,585 m^3 and 144,943 m^3

(Youngs No. 2). Youngs No. 1 reservoir accounts for 50 to 100 percent of the releases from the five reservoirs draining to Youngs Creek.

Whereas the total volume of water for a given year is much greater during normal flow conditions, the magnitude of reservoir releases is much higher compared to the average stream discharge. The minimum and maximum stream discharge volumes are 497,688 m^3/year and 13,258,783 m^3/year, respectively, whereas reservoir release volumes average 137,000 cubic meters for a given year. The average daily discharge between reservoirs and natural stream flows is comparable, but the reservoir releases can be orders of magnitude greater than the discharge under normal surface flow conditions (Fig. 2.7). Conversely, the minimum daily discharge for the streams is an order of magnitude less than the daily discharge of reservoirs. For example, Youngs No. 1 Reservoir, draining into the Youngs Creek watershed, averages 65 days for a water release with an average of 4.5 m^3/s. Therefore, the reservoirs contribute higher discharge values during a short time for substantial bankfull and overbank flooding in the step-pool channels.

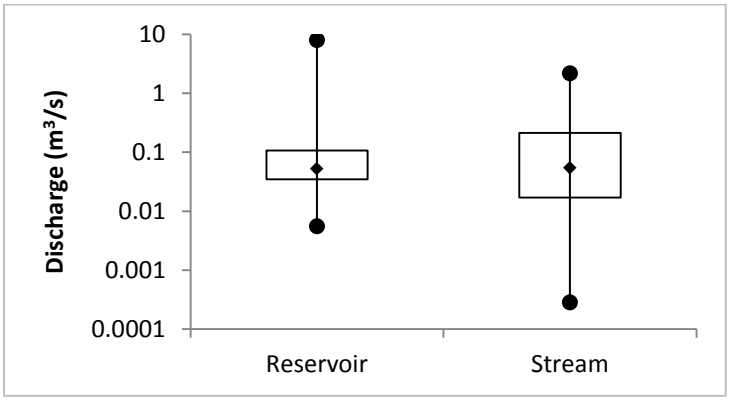

Figure 2.7. Boxplots of averaged daily discharge for reservoir releases and streams along Grand Mesa.

A large difference exists in volume of water between yearly reservoir releases (Fig. 2.6) and yearly stream discharge from the stream gauges. An important observation is the stream gauge data, dating from 1957 to 1967, was collected prior to recorded reservoir releases, which began in the early 1970s. Because of this difference in the time periods of hydrologic data, it is difficult to make direct comparisons of water in the channels versus water released from reservoirs. Several active gauging stations on Surface Creek and the Gunnison River, that include the time period of the reservoir releases, are further downstream in the watersheds of the southern flank of Grand Mesa but it is difficult to correlate reservoir release volumes with peaks in the active hydrographs of these gauges. In addition no active gauge is located on the short section of Surface Creek from the confluence the study streams to Surface Creek's exit to the Gunnison River. The drainage basin of Surface Creek has a large number of diversions which contribute to discrepancies between the stream gauge and reservoir releases. Mapping by the CWCB and provided by the CDSS plots several dozen active diversion locations within the Surface Creek and Ward Creek watersheds. These diversions make it difficult to estimate how much water is in the streams relative to the amount listed for a given reservoir release.

The drainage area of a reach is often used as a surrogate for discharge where flow records are unavailable (Chin, 1999). Watershed areas were calculated using the hydrologic tools in ArcGIS®. For calculating watersheds using a 10-meter resolution digital elevation model, collected by the USGS, the fill command in ArcHydro® was not used because this study wanted to preserve the reservoirs and lakes atop the mesa. The

longitudinal profile was calculated by dividing the total change in elevation from the upstream end to the downstream end of the study reach.

Discharge exerts strong controls on channel width, which in turn affects wavelength and step height (Leopold and Maddock, 1953 and Finnegan, 2005). The discharges of the mountain-peak channels from the literature were compared to those respective values from the Grand Mesa channels. Because there are only three data points for Grand Mesa statistical analysis were not preformed to compare the significance of difference for discharge. The average discharge of the Grand Mesa streams during the gauging period is 0.17 m^3/s, with a maximum and minimum of 2.15 m^3/s and 0.0003 m^3/s; respectively. The average discharge of the mountain-peak dataset is 8.09 m^3/s, with a maximum and minimum of 50.6 m^3/s and 0.01 m^3/s; respectively. Stream discharge and drainage area are logarithmically correlated as they increase in positive value. Drainage area for the three Grand Mesa streams ranges from 3.2 to 6.6 km^2 with an average of 4.7 km^2. From the published literature, drainage area ranges from 0.13 to 245 km^2 with an average of 29.2 km^2, and 80% of the values less than 20 km^2. From this, one observes the logarithmic increase is consistent between the Grand Mesa streams and the mountain-peak dataset.

2.6.2 Step-Pool Stream Morphology

Drainage areas and average step-pool morphology were surveyed for Cottonwood, Horse and Youngs creeks along southern Grand Mesa (Table 2.1). Channel width averages 1.35 m for Cottonwood Creek to 1.70 m for Youngs Creek to 2.04 m for Horse Creek m. Particle sizes average 0.16 m for Cottonwood Creek, 0.32 m for Youngs Creek and 0.33

m for Horse Creek. The total length of each study reach for Cottonwood Creek was 27 m, 43 m for Youngs Creek, and 31 m for Horse Creek. The step height of Cottonwood Creek averages 0.34 m, with 0.53 m and 0.68 m for Youngs Creek and Horse Creek, respectively. Step-pool wavelength averages 2.42 m, 3.00 m and 2.77 m for Cottonwood, Youngs and Horse creeks, respectively.

Table 2.1. Morphologic characteristics for three step-pool study reaches along southern Grand Mesa.

Stream	Drainage area (km^2)	Slope (m/m)	# of S-P Sequences	Channel width (m)	Step height (m)	Wavelength (m)	Particle size (m)	Length (m)
Cottonwood	3.18	0.085	11	1.35	0.34	2.42	0.16	27
Youngs	4.51	0.095	11	1.70	0.53	3.00	0.32	43
Horse	6.64	0.153	11	2.04	0.68	2.77	0.33	31

The drainage areas of the Cottonwood, Youngs and Horse creeks are 3.18 km^2, 4.51 km^2 and 6.64 km^2, respectively. Similar to discharge, the drainage area also influences channel width (Leopold and Maddock, 1953; Finnegan, 2005). Drainage areas for the mountain-peak channels average 29.2 km^2, with a maximum and minimum of 244.8 km^2 and 0.13 km^2, respectively.

Channel slope influences step wavelength and step height (Zimmermann, 2013). The channel slope of Cottonwood, Youngs and Horse creeks are 0.085, 0.095 and 0.153 m/m, respectively. The channel slopes for the mountain-peak data average 0.0712, with a maximum and minimum of 0.0148 and 0.18, respectively. As with discharge, there are not enough data points for drainage areas and channel slopes to perform a statistical comparison between the Grand Mesa and other mountain-peak data.

From field observations and measurements, the Youngs Creek study site is

higher on the shoulder of Grand Mesa, located in pine forests, with more LWD in the channels, specifically the steps. The study sites for Cottonwood Creek and Horse Creek study sites in brushy undergrowth lower on the flank of Grand Mesa. This greater presence of LWD in Youngs Creek does not contribute to large differences in the average geometry from the other two streams. The role of channel slope and available sediments for forming steps play a greater part in the geometry of Youngs Creek.

The variables of channel width, wavelength, step height and average particle size follow a normal distribution (Fig. 2.8). The histograms showing wavelength and step height histograms follow an approximate normal distribution that is skewed to the right; this is similar to other step-pool systems (Chin, 1999; Chartrand, 2000; Zimmermann, 2001). The normal distribution of these step-pool geometry components is common in the literature and allows the use of parametric statistical tests for comparing the geometry of Grand Mesa step-pool streams to the streams of other regions.

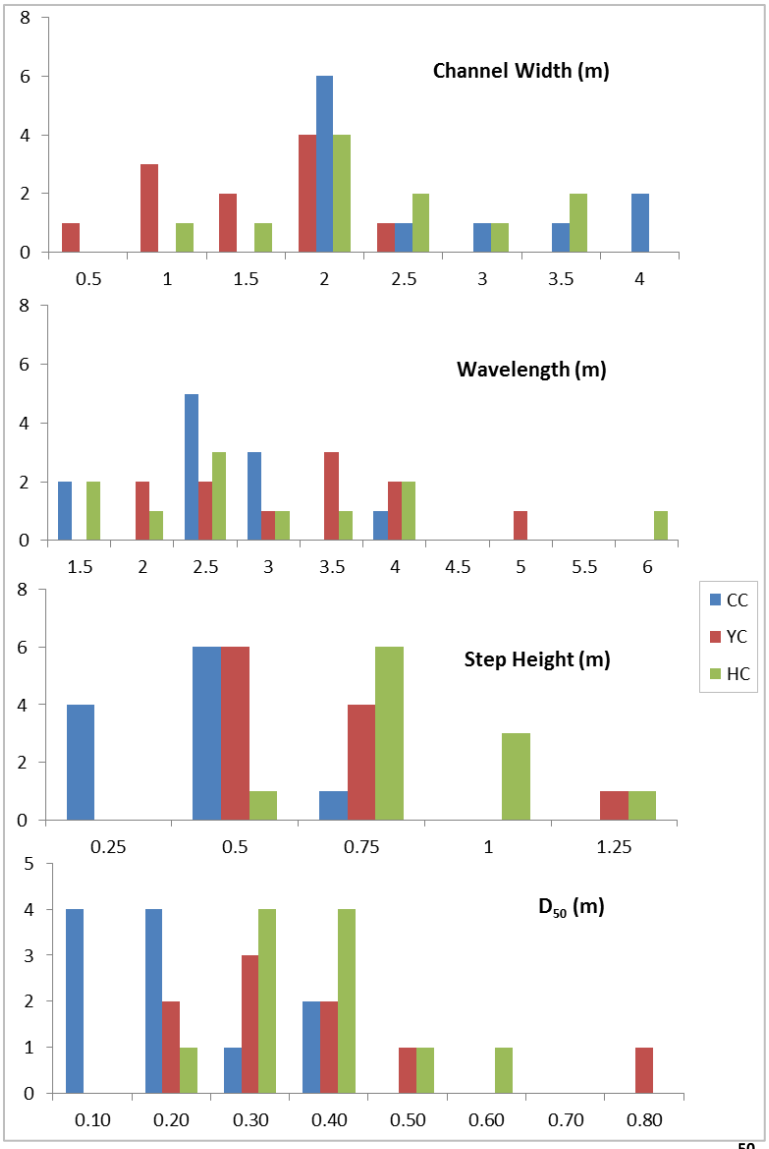

Figure 2.8. Histograms of channel width (m), wavelength (m) step height (m) and D^{50} sediment (m) for Cottonwood, Horse and Youngs creeks along Grand Mesa. The y-axis is height in meters.

Dividing wavelength by the average channel width of approximately 1.70 (m) the ratio is 1.5 to 1.8. This ratio of wavelength to channel width is consistent to other spacing of step-pool systems (Whittaker, 1987a; Grant et al., 1990) and much less than the pool-riffle spacing of 5 to 7 channel widths (Leopold et al., 1964; Keller and

Melhorn, 1978) in lower gradient streams. Therefore, from field surveys the step-pools of Grand Mesa resemble the step-pools of other watersheds.

The release amounts vary greatly between reservoirs (Fig. 2.6), therefore, the step-pool geometry between the streams of Grand Mesa may vary. A series of boxplots (Fig. 2.9) shows relatively little variation in the four step-pool variables. As stated earlier the increasing watershed area, channel slope and channel width also correspond to increasing average step height and average step-pool median sediment between the three streams. The variable of wavelength, important in defining step-pool reaches of a channel, decreases slightly with increasing watershed area, channel slope and channel width, but the range of wavelength is from 2.4 to 3.2.

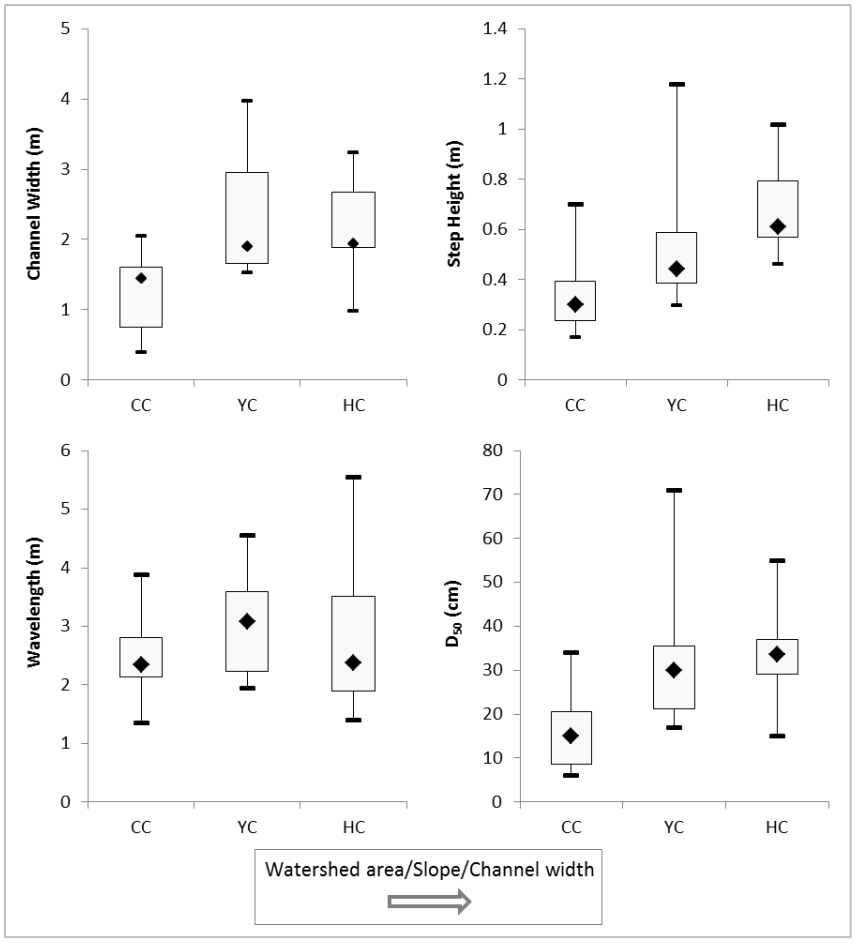

Figure 2.9. Boxplots of main channel variables for Grand Mesa step-pool streams. Watershed area, channel slope and channel width increase from Cottonwood Creek to Youngs Creek to Horse Creeks. Youngs Creek also has a greater average discharge relative to Cottonwood Creek during the gauging period. Horse Creek does not have gauged stream discharge data.

The step height for the three streams ranges from 0.2 (m) to 1.2 (m). The greatest variation is for Youngs Creek with a range of approximately 0.3 to 1.2 (m). The median value increases by approximately 0.1 (m) from one stream to the next.

The wavelength (Fig. 2.9) ranges from approximately 1.2 to 5.5 meters. The largest range for wavelength is for Horse Creek with wavelength values from 1.2 to 5.5 (m). The median values for Horse Creek, 2.8 (m), is slightly lower than that of Youngs

Creek, with a value of 3.0 (m). Data on step-pool geometry from eighteen studies from environments predominantly in North America and Europe were compiled to compare with the field surveys of Grand Mesa (Table 2.2).

Table 2.2. Author and location of step-pool data for comparison to Grand Mesa step-pool streams.

Author, Year	Study Location
Billi, 2014	Apennines Mountains, Italy, Europe
Chartrand, 2000	Central & west-central Idaho, USA
Chin, 1999	Santa Monica Mountains, California, USA
Curran, 2003	Central & southern Cascade Range, Washington, USA
Duckson, 1995	High Cascades, Oregon, USA
Duckson, 2001	High Cascades, Oregon, USA
Jimènez, 2013	Colorado Front Range, Colorado, USA
Lenzi, 2001	Rio Gordon, eastern Alps, Italy, Europe
Macfarlane, 2003	Western Cascades, Washington, USA
Milzow, 2006	Alpthal Basin, Swiss Alps, Switzerland, Europe
Molnar, 2010	Alpthal Basin, Swiss Alps, Switzerland, Europe
Recking, 2012	Southeastern Alps, France, Europe
Wilcox, 2007	Colorado Front Range, Colorado, USA
Wilcox, 2011	Rio Gordon, eastern Alps, Italy, Europe
Wohl, 2000	Christopher creek, Mogollon Rim, Central Arizona, USA
Wohl, 2004	Colorado Front Range, Colorado, USA
Wohl, 2005	Eastern & western South Island, New Zealand
Zimmermann, 2001	Rocky Mountains, British Columbia, Canada

Scatterplots of channel width versus average step height and average wavelength compare Grand Mesa to mountain-peak step-pool (Fig. 2.10). Step height decreases and wavelength increases downslope. Also, decreasing slope downstream correlates to lower particle size. Therefore, particle size is a surrogate for slope and can be compared to step height and wavelength (Chin, 1999). The steepness ratio of H/L is represented in the scatterplot of step height versus wavelength (Fig. 2.10.B), with the ratio of step height to wavelength ranging from 0.06-0.20. The R^2 values and trend lines plotted in Figure 2.10 are for the mountain-peak data from the review of literature.

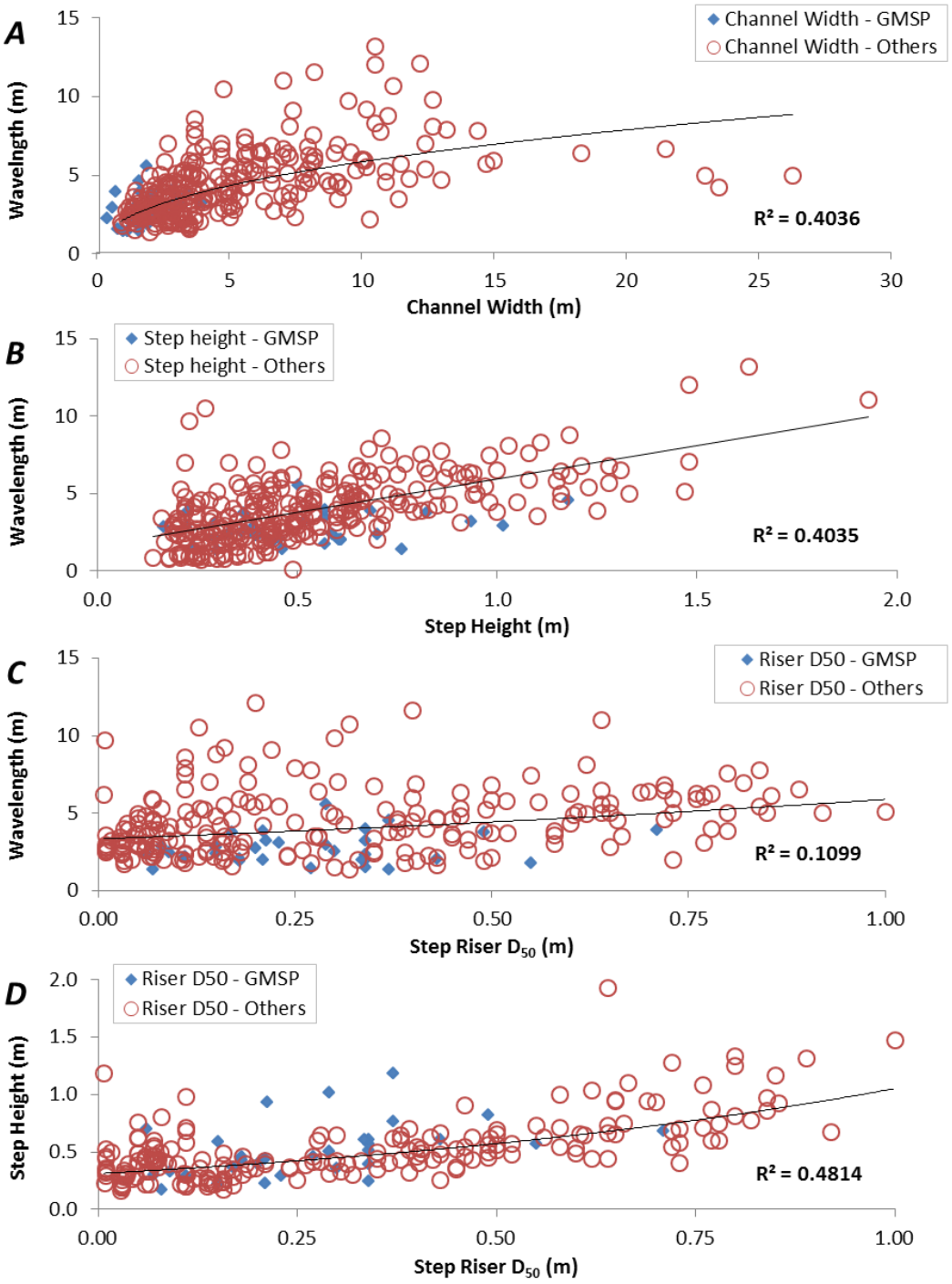

Figure 2.10. Scatterplots of prominent variables for comparing step-pools in various landscapes.

Figure 2.10.A, wavelength and channel width, follows a power function for the mountain-peak data with an R^2 of 0.4. Wavelength and step height (Fig. 2.10.B) follow a linear function with an R^2 of 0.4. A very weak ($R^2 = 0.1$) exponential correlation exists between wavelength and the sediment D_{50} of the step riser (Fig. 2.10.C). The correlation between step height and step riser sediment D_{50} (Fig. 2.10.D) follow an exponential function with an R^2 of 0.48. The Pearson product-moment correlation compares the strength of correlation between the main morphologic variables for the Grand Mesa and mountain-peak step-pool streams (Table 2.3).

Step height to wavelength (Fig. 2.10.B) follows a logarithmic function, with step height at a threshold of approximately 1.5 meters. The Grand Mesa streams plot near the mountain-peak data with no large outliers. The steepness ratio of H/L puts the Grand Mesa data around the upper range of 0.20. Therefore, the Grand Mesa streams have a high steepness factor owing more to the basalt boulders and cobbles that form the majority of a step within the streams.

The Grand Mesa median sediment falls within range of the wavelength and step height values for mountain-peak streams (Figs. 2.10.C and 2.10.D). The relation between step height and median sediment in the step follows an exponential function with step height increasing quickly as median sediment increases. In Figures 2.10.C and 2.10.D the Grand Mesa data plots along the mountain-peak points with no great outliers. Step height and wavelength, indicators of slope condition, correlate; and step height relates to median sediment; therefore, step-pool geometry in Grand Mesa is influenced more by

the typical variables of slope and material available for erosion and transport as opposed to changes in discharge at the headwaters.

As slope, drainage area and average discharge increase from Cottonwood to Youngs to Horse creeks, median step height increases and the range in wavelength also increases. The strongest relationship for step width/height and wavelength is for the non-reservoir stream, Horse Creek, whereas the size of step particles has little bearing on the step height and wavelength for any particular stream.

Table 2.3. Pearson product-moment correlation between variables of step-pool morphology for both Grand Mesa step-pools and step-pool systems of other studies.

Pearson Correlation	Channel Width & Wavelength	Step Height & Wavelength	D_{50} & Wavelength	D_{50} & Step Height
Grand Mesa	0.35	0.26	0.19	0.44
Mountain-Peak	0.52	0.64	0.29	0.69

The strength of correlations between channel width and wavelength for Grand Mesa and mountain-peak are in the medium range of 0.35 and 0.52, respectively. The step height and wavelength strength of correlations are 0.26 and 0.64 for the Grand Mesa and mountain-peak step-pool streams. The sediment D_{50} and wavelength strength of correlations for Grand Mesa and mountain-peak streams are 0.19 and 0.29, respectively. The sediment D_{50} and step height strength of correlations are 0.44 and 0.69 for the Grand Mesa and mountain-peak step-pool streams, respectively.

A two sample t-test, assuming unequal variances, compared the main variables of channel width, wavelength, step height and sediment D_{50} of the Grand Mesa to the mountain-peak step-pool streams (Table 2.4).

Table 2.4. Two sample t-tests assuming unequal variances for variables of step-pools.

Channel Geometry	Geomorphic Setting	n	Mean	Variance	p-value
Channel Width (m)	Grand Mesa	33	1.91	0.72	< 0.05
	Mountain-peak	269	5.44	19.3	
Wavelength (m)	Grand Mesa	33	2.72	0.96	< 0.05
	Mountain-peak	307	4.18	5.6	
Step Height (m)	Grand Mesa	33	0.52	0.05	0.67
	Mountain-peak	288	0.54	0.09	
Sediment D_{50} (m)	Grand Mesa	31	0.27	0.02	0.24
	Mountain-peak	226	0.31	0.07	

The number of samples for Grand Mesa is 31 to 33; the number of samples for mountain-peak channel width, wavelength, step height and median sediment are 269, 307, 288 and 226; respectively. A 95% confidence interval was used in the t-test. The channel width and wavelength have p-values less than 0.05, whereas step height and sediment D_{50} have a p-value of 0.67 and 0.24, respectively.

From the t-test, the null hypothesis is rejected for the variables of channel width and wavelength; the observed difference between the sample means of Grand Mesa step-pools and other step-pool streams in mountain-peak areas is statistically significant. Step height and median sediment fail to reject the null hypothesis; these two variables are not significantly different between the two geomorphic settings.

The magnitude and frequency of flows is important in high alpine streams. For example, using 1 m3/s, the flood discharge observed at Kiser Creek during field surveys, as a guideline for a high-magnitude flow, it is observed that 17% of daily averaged discharge values for reservoirs are greater than 1 m^3/s; whereas, only 2.9% of stream daily discharges from the USGS gauging period are greater than 1 m^3/s. Alternately, if

the total volume of water is calculated for a given year of stream discharge under non-reservoir conditions, the total volume of water is several orders of magnitude greater than the total reservoir volume released in any given year. Therefore, whereas the magnitudes of reservoir releases are greater at a given time, the overall water volume discharged by natural flow conditions is much larger. The frequency of high magnitude releases from reservoirs, combined with the numerous diversionary structures along the watersheds, is not sufficient to alter the overall geometry of step-pool streams along Grand Mesa.

An important note is the record of reservoir releases. The number of days per release is provided for only 24% of the reservoirs for calculating a daily discharge. The remaining 76% of reservoir releases, where the number of release days per discharge is unknown, may change the distribution of high and low flows down the streams. Also, the range between the 1st and 3rd quartiles is less for the reservoirs than for natural stream discharge. This corresponds to less variability in reservoir discharge. Despite this higher magnitude and less variable discharge, the frequency of reservoir releases do not have a significant effect on the geometry of step-pool streams along Grand Mesa.

2.6.3 Self-Organization and Evolution of Step-Pool Streams

The statistical tests show no significant difference in the morphology of Grand Mesa step-pools compared to those of other alpine mountain-peak areas. Reasons for this may be explained in how landscapes spatially organize through time. Spatially divergent self-organization is defined either as minimizing or maximizing energy dissipation and/or entropy in a system. The broad concept includes the evolution of order and regularity in

the total properties of a landscape through converging forms, and how those properties diverge into different landscapes of various forms (Phillips, 1999.)

As mentioned earlier, step-pool spacing generally ranges from one to four channel widths. Therefore, the idealized step-pool sequence of 25% steps and 75% pools, of the overall profile length, is a good approximation for all step-pool streams in a final self-organized evolution.

Testing for entropy, or maximum effort put forward by the fluvial system, requires comparing the topographic expression of a landscape at multiple time periods. Using the equation provided by Chin and Phillips (2007), entropy is calculated as:

$$H = -\sum(p_i \ln p_i) \quad (2.1)$$

whereby, *H* is entropy and *pi* is the percentage of a step or a pool length. Adding the *pi* of the step and pool for a reach will provide a value of the entropy in the system. Chin and Phillips (2007) provide the ratio of step to pools and associated entropy value for a surveyed stream and idealized stream (Fig. 2.11). The surveyed stream is plotted in Fig. 2.11 according to its position along the entropy-phase curve, and shows the channel is nearing the complete step-pool morphology end member and is expending less energy, i.e., less entropy, to organize the particles within the channel.

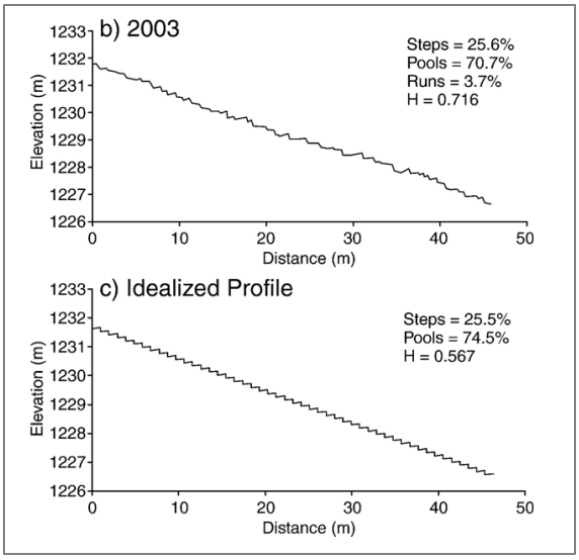

Figure 2.11. Well-developed and idealized step-pool sequence profiles (after Chin, 2007) in a reconstructed channel. Entropy in the system is represented by *H.* Note percentages of steps, pools and runs between the 2003 survey and an idealized profile.

As stated earlier, unlike most step-pool streams presented in the literature which begin along steep mountain flanks, the streams along Grand Mesa originate from a flat mesa with lakes that act as storage for potential energy above the step-pool systems. The survey results for step length and pool length are presented in Table 2.5.

Table 2.5. Step and pool length for three streams along southern Grand Mesa, Colorado. Note the entropy values listed in column "H".

Stream	Average Q (m^3/s)	Step Length (m)	%	Pool Length (m)	%	Total Length	H
Cottonwood	0.91247	4.98	18.76	21.58	81.25	26.56	0.483
Youngs	1.29249	8.62	26.22	24.26	73.78	32.88	0.575
Horse	1.9023	9.11	29.91	21.35	70.09	30.46	0.61

Using the surveyed data from the three streams along Grand Mesa, the author calculated the entropy at the study time using the above equation. The calculation for Cottonwood Creek is presented below:

Step-pool total length = 26.56 m

Step = 18.76%

Pools = 81.25%

Using the above equation (2.1):

pi1 = -0.168707

pi2 = -0.313937

Therefore, the sum of these values gives an H = 0.4826 for Cottonwood Creek. Applying the same process to streams two and three, Youngs Creek and Horse Creek respectively, give values of H = 0.5752 and H = 0.6101, respectively. These three H values place the Grand Mesa step-pool streams along the Channel Evolution at either just before phase 2 or approximately phase 5 (Fig. 2.12).

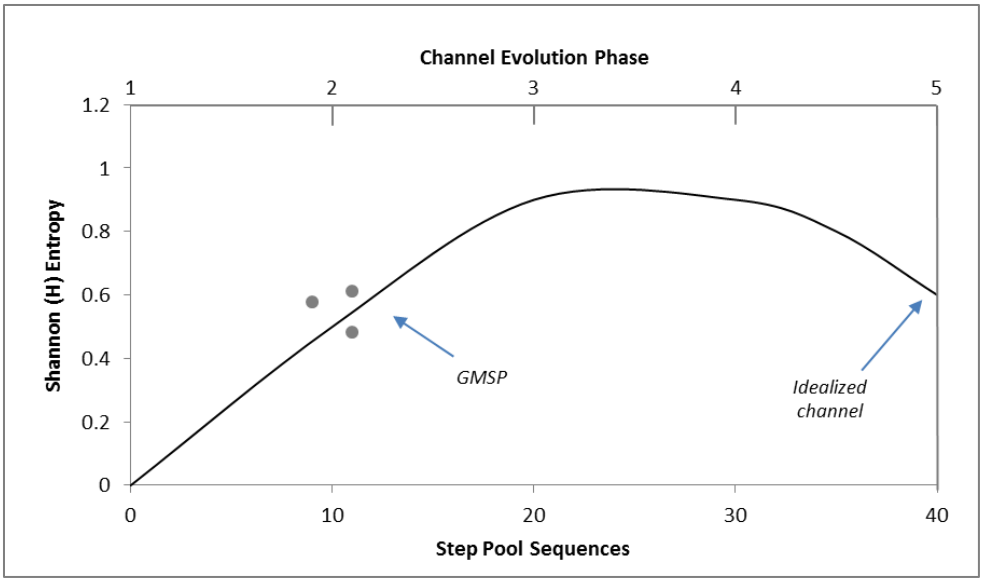

Figure 2.12. Entropy changes over time for the Andrews drainage subgrade with data points of the Grand Mesa streams, indicated by the three grey dots, falling on the upslope of the graph (modified after Chin and Phillips, 2007).

To determine the correct place along the entropy-evolution line, whether the Grand Mesa streams are phase 2 or phase 5, the geologic and geomorphic history must be understood. The mesa itself is capped by a basalt layer formed approximately 10 million years ago, and, therefore, streams have had time to adjust form to accommodate energy inputs. In addition, the author argues that given the relatively recent glaciation, and subsequent lake formation, may impact on the streams disorder and early evolution. Yet, at the same time, the steps and pools form the 1:4 spacing observed in other step-pool sequences (Chin, 1989; Grant et al., 1990; Montgomery et al., 1995; Chin, 1999; Chartrand and Whiting, 2000, Chin and Phillips, 2007). Therefore, the author argues step-pool streams along Grand Mesa that are drained by lakes are near the low-entropy early-evolution stage as presented by Chin and Phillips (2007).

Some comments of the validity of early, low-entropy step-pool streams in the Grand Mesa drainage area. Though the author plots the location of the entropy values for Grand Mesa step-pools as near the upslope phase of channel evolution (Fig. 2.12), several factors need to be addressed in this assessment of landscape evolution and organization. First, the author has no historical data on the condition and morphology of these step-pool streams along Grand Mesa. Therefore, it can be difficult to make assertions about current landscape organization when it is unknown what the baseline was for these fluvial systems. Second, the author may have performed the stream survey, which the data in Table 2.5 are derived from, incorrectly, in that several of the pools in each stream are nearly twice as long as the average pool length. This implies that a riffle, or run, is separating two pools, creating additional step-pool sequences. This would place those streams further along the line in Fig. 2.12 in a later evolutionary stage. This change in position would require a higher entropy level than currently exists in the Grand Mesa step-pool streams. Third, as discussed earlier, the anthropogenic influence from reservoir releases may impact the natural evolution of these streams.

The self-organization process should work to smooth or roughen channels, based upon the available stream power and channel slope. The pairings are increasing flow resistance and decreasing slope versus decreasing flow resistance and decreasing the vertical sinuosity. Step-pool streams are analogous to meandering streams; vertical migration (narrow floodplain and high-angle valley walls) vs. lateral migration (wide floodplain and low-angle valley walls). Therefore, much like a relationship between radius of curvature vs. rates of migration (i.e., stability of the channel planform), a

"vertical radius of curvature" exists to the wave-form of step-pools, vs. the movement of steps downstream, or the channel vertically.

To examine the stream power aspect of the system the author used the following equation provided by Chin and Phillips (2007):

$$P_{\text{reach}} = \gamma^{1.5} d^{1.5} S^{1.5} w f^{-0.5} L \quad (2.2)$$

where P_{reach} is the stream power for a reach, γ is unit weight (constant), d is mean depth, S is energy gradient slope, w is width, f is a friction factor and L is the reach length. The friction factor was determined using a Moody diagram (Moody, 1944) and associated Reynold's number for each of the three Grand Mesa stream reaches. The velocity component of the Reynold's number was calculated using the average discharge, gathered from gauging stations along the streams, and cross-sectional channel area for each stream. The density and dynamic viscosity component of the Reynolds number was calculated at a water temperature of 15 degrees Celsius. The calculated stream power was then compared to the H entropy (heat loss), friction factor (surrogate for channel roughness) and slope (surrogate for potential energy) values (Fig. 2.13).

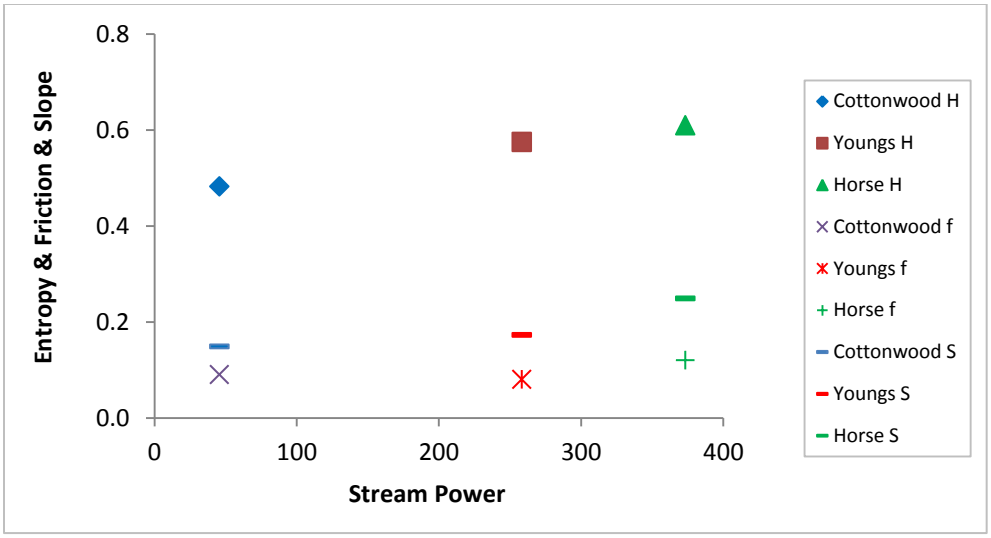

Figure 2.13. Stream power related to entropy (H), friction (f) and slope (S) for the three streams along the southern flank of Grand Mesa. As stream power increases, entropy, energy loss in the system, also increases. Overall channel slope also increases. The entropy (P), friction factor (f) and slope (S) are plotted on the Y-axis.

On this graph, as stream power increases, entropy, or heat loss through work, also increases. In addition, channel roughness, and resistance to flow, also increases. Therefore, increasing friction is associated with increasing slope, leading to energy loss through entropy. Also, stream power works to add entropy to the system. This translates to increased erosive ability of the stream to carry sediments further down the channel. At the same time, energy is lost to heat loss through entropy.

2.7 Discussion

2.7.1 Discharge

Thirty-two step and pool sequences in three streams along the southern flank of Grand Mesa were surveyed to describe the morphology and determine the main processes of formation. The effect of variable discharge from large reservoirs located above the

headwaters was investigated. The step-pool reaches surveyed exhibit similar morphologic characteristics as those described in other geographic regions. Step width is the dominant control on step height, whereas step width is the dominant control on step wavelength. The periodic reservoir releases, occurring on a nearly yearly basis atop Grand Mesa, are unique in alpine environments for high gradient channels. Unlike many studies involving high alpine fluvial systems where the headwater begins at a mountain-peak, the reservoirs atop the mesa provide storage for potential energy in water releases.

The discharge of Grand Mesa streams under natural flow conditions is similar to that of high-altitude alpine fluvial systems; low-flow conditions during fall and winter seasons followed by high flows in the spring and early summer as the snowpack melts. The releases from reservoirs have a greater magnitude of peak discharge, but the frequency of releases appears not enough to significantly alter the geometry of the step-pool streams.

2.7.2 Step-Pool Stream Morphology

The step-pool data from Grand Mesa were statistical compared to data from other step-pool systems (Table 2.1) in the literature. Three hundred and seven step-pool stream segments from eighteen different studies in the step-pool literature were graphically and statistically compared to step-pool streams at Grand Mesa, Colorado. Statistically, step-pool streams along Grand Mesa do exhibit large differences in the channel width and wavelength features as compared to step-pool systems in other high-altitude and alpine settings. No significant difference occurs between step height and sediment D_{50} in the Grand Mesa and mountain-peak datasets.

The strength of correlation observed between step height and wavelength and between median sediment and step height for mountain-peak step-pools may result from having a greater sample size as compared to the correlations for Grand Mesa step-pools.

Direct comparisons between the discharge of natural stream flow prior to 1970 and reservoir releases after 1970 are not appropriate because of the time-period difference and the large number of diversions transporting water away from stream channels at a high altitude in the stream headwaters on the mesa.

The study reach along Youngs Creek is immediately downstream of a large culvert. This may have influenced the discharge regime and step transport characteristics for these step-pools, helping to explain the large range in step height and step particle size. Cottonwood Creek also crossed a road several meters downstream of the last step-pool section surveyed. This may affect the morphology of the lower step-pool.

Step height and wavelength are controlled by channel slope, channel width and the median sediment (Zimmermann, 2013). From the statistical tests, wavelength rejects the null hypothesis; that the geometry of step-pool channels is equivalent between Grand Mesa and mountain-peak environments. This result follows that drainage area and discharge, which control channel width (Leopold and Maddock, 1953 and Finnegan, 2005), have averages of 4.8 km^2 and 29.2 km^2, and 0.17 m^3/s and 8.09 m^3/s for Grand Mesa and mountain-peak, respectively. Therefore, channel widths, which reject the null, are significantly different, which in turn creates unequal channel wavelengths between the step-pool two datasets.

Channel slopes are relatively equal between the datasets, furthering stressing the importance of drainage area and discharge on channel morphology. Rates of regional erosion, which along with tectonic uplift affect channel slopes, are comparable between the datasets. Grand Mesa has a regional rate of erosion of 0.17 meters per 1000 years (Cole, 2001). The European Alps and Rocky Mountains of the western United States, where the majority of step-pool data from the literature analyzed in this study was collected, have regional rates of erosion of 0.3-2.2 m/kyr and 0.04-1.0 m/kyr, respectively (Wittmann, 2007 and Herman, 2013). The Grand Mesa rates of erosion are near the low end of the range, which supports the low difference in slopes between Grand Mesa and the mountain-peak data.

Step height is strongly controlled by the sediment D_{50}, or median particle size comprising the steps. The median sediment fails to reject the null hypothesis; the particle size is roughly equivalent between Grand Mesa and mountain-peak streams. Therefore, step height is roughly equivalent between the two datasets. The steps are predominantly igneous cobbles and boulders from erosion of the basalt cap, with the processes producing similarly sized particles to those of other high alpine environments. Despite the unique physiography of Grand Mesa, the morphology of the fluvial basin and the driving force of the hydrological cycle control the overall step-pool morphology along Grand Mesa. As Chin (1999) reported, step-pools along Grand Mesa correspond to the overall step-pool morphology of high slope areas with positive relationships between wavelength and discharge, and between height and particle size. Chin and Wohl (2005) present a synthesis on the overall state of research with four primary areas of analyses of

form, quantifying processes, combing studies for broad explanations, and managing and restoring channels.

As stated earlier, Abrahams et al. (1995) showed 1.5*slope of the channel approximates to the channel steepness (expressed as H/L). The step-pools along Grand Mesa deviate little from the trend line of mountain-peak streams (Fig. 2.14). The slopes along the mesa are typical of slopes in mountain-peak landscapes.

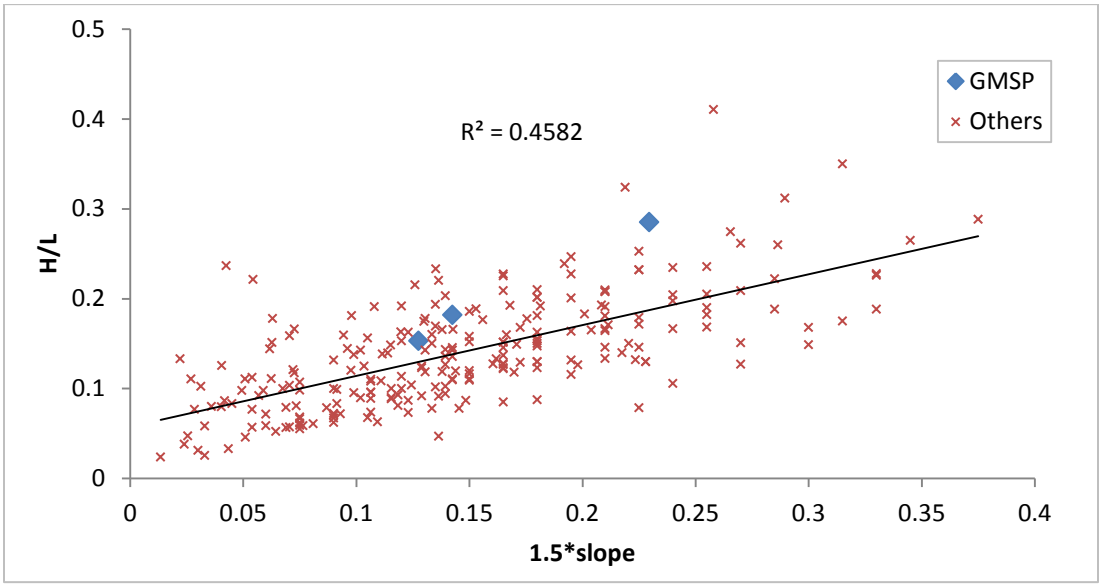

Figure 2.14. Abraham (1995) postulated that 1.5*slope approximates to steepness (H/L). Two of the Grand Mesa step-pool streams fall closely to the linear correlation for mountain-peak step-pool streams, while the third stream is within the limits of the non-Grand Mesa data.

From Figure 2.14, the geomorphic forms observed and compared from Grand Mesa and the mountain-peak literature reinforce the assertion that fundamental landscape processes are the main driving factors in development of step-pool channels, and the overall watershed, along Grand Mesa. Overall channel slope, which is a function

of the geologic material, soil and vegetation comprising the watershed, dominates development of step-pools, as compared to the flat mesa physiography and discharge.

This work does not differentiate between alluvial and bedrock channels in high alpine and mountain environments. For a given watershed area, bedrock channels have a higher channel gradient as compared to alluvial channels (Church, 2013; Massong and Montgomery, 2000). The majority of channels in mountainous environments vary between these two end members and the channel bottom is composed of a resistant bedrock surface with a layer of varying thickness and particle size as bed and suspended load. Reviewing the environments in which the mountain-peak data was collected, the majority of the systems are this mixed bedrock-alluvial type. Step-pool studies of true bedrock-only channels, such as those found in the bare sandstones of the Colorado Plateau, are a minority of the geologic literature. Therefore, it is an apt comparison between the streams of Grand Mesa and those of the channels reviewed from the literature for this study.

The specific age, ~10 million years, and large spatial extent of the basalt cap have provided a time boundary on landscape development in Grand Mesa. The streams have reached approximate equilibrium in transport of sediment and water. The influence of glaciation, including large-scale isostatic rebound of the landscape affecting slope and major shifts in climate over tens of thousands of years, is important in the configuration of watersheds. The headwater locations atop a flat mesa appear negligible in development of streams in the landscape. The slopes of the flanks of Grand Mesa are approximately similar to those in mountain-peak landscapes.

The relationship of channel width to wavelength (Fig. 2.10.A) is a power function with the majority of the data points clustering around a channel width of 4 meters and wavelength of 4 meters. The Grand Mesa data plots near the lower end of the spectrum with the streams having a lower channel width and wavelength. As none of the Grand Mesa streams are outliers, the relation between channel widths, a surrogate for discharge, and wavelength, the indicator of step-pool morphology along with step height, is typical to that of mountain-peak step-pool streams.

The statistical tests show no significant difference in the morphology of Grand Mesa step-pools compared to those of other alpine mountain-peak areas. Reasons for this may be explained in how landscapes spatially organize through time. Spatially divergent self-organization is defined either as minimizing or maximizing energy dissipation and/or entropy in a system. The broad concept includes the evolution of order and regularity in the total properties of a landscape through converging forms, and how those properties diverge into different landscapes of various forms (Phillips, 1999.)

The four primary attributes, and their relation to one another, are the main factors in detailing the differences, or lack of, between the specific streams observed along Grand Mesa and the general step-pool streams found in more typical mountain environments. As step width, height and wavelength for Grand Mesa are within the ranges of mountain-peak values there is no discernable difference at this scale. The difference observed in channel width and wavelength between the two datasets is attributable to the larger overall discharge and drainage areas of the mountain-peak data. Fundamentally, the sediment particle sizes are similar between the two sets of data,

resulting in little difference between the topographies. Overall, the general variables of the drainage basin (slope, hydro-cycle, drainage area, etc.) explain morphologies of channels, versus the specifics characteristics of physiographic provinces.

2.8 Conclusions

The purpose of this study is three-fold; first, to determine the effect of controlled discharge from reservoirs atop the mesa on the step-pool morphology. Second, to examine the channel geometry of several step-pool streams developed along a mesa and compare these streams to the ubiquitous mountain-peak step-pools common in the scientific literature. Third, this study sought to place the surveyed Grand Mesa step-pool streams along the continuum of internally organizing, or autogenic, fluvial systems in landscape evolution.

Using an overbank flooding value of 1 m^3/s, based on field surveys of the step-pool streams, it was observed that 17% of daily averaged discharge values for reservoirs are greater than 1 m3/s; whereas, only 2.9% of stream daily discharges from the USGS gauging period are greater than 1 m^3/s. The total volume of water released from reservoirs in a given year is a small portion of the overall volume of water discharging down the stream during natural flow conditions. The magnitude of discharge during a reservoir release is greater than the maximum discharge under natural conditions. The amount of water diverted for agricultural and industrial purposes from the reservoir release before reaching the surveyed step-pool segments is unknown. From the measurements of step-pool geometries and the comparison of total water volumes for reservoir and non-reservoir discharges it appears the step-pool streams are not largely

altered by changes in the hydrologic regime along southern Grand Mesa.

Field surveys of channel morphology were examined to determine the dependence between morphologic characteristics and the differences in step-pool morphology relative to other step-pool systems. The main channel attributes in step-pool morphology are channel width, step height, wavelength (distance between successive steps) and median sediment particle (D_{50}). The channel attributes of three Grand Mesa streams (Cottonwood Creek, Horse Creek and Youngs Creek) were graphed and statistically compared to mountain-peak step-pool systems from eighteen studies located predominantly in the western United States and European Alps. Statistical analysis of the two step-pool groups shows significant differences for the channel width and wavelength variables of the Grand Mesa and mountain-peak step-pool streams; whereas, there appears to be no significant difference between step height and median sediment of these systems. The observed difference in channel widths is attributable to the greater overall drainage areas and discharges of the mountain-peak data. This difference in channel widths contributes to the difference observed in step-pool wavelength. The channel slopes and step particle size are consistent between the two data sets, contributing to relatively equal step heights. In conclusion, the step-pool streams along the southern flank of Grand Mesa exhibit morphologic properties consistent with those of other alpine, but mountain-peak, topographies. The observed differences in geometries between the data sets are attributable to more general basin-wide differences, rather than the unique characteristics of the Grand Mesa area.

The data from this study were also compared to experimental step-pool streams. Despite the recent glaciation of Grand Mesa, the streams present have been developing since the basalt cap, topping the mesa, solidified and rain began. Therefore, the author submits that these step-pool sequences are near a low-entropy stage and represent standard step-pool sequences found on the mountain-peak and mesa landscape settings. In addition, high gradient step-pool streams contain more friction as work is applied to alter the gradient, by arranging the particles into appropriate steps and pools, removing sediment through downstream transport, until a threshold is reached where slope gradient is now such to lower the energy loss into a stable geomorphic system. This work helps lead to a more complete picture of step-pool stream development in high alpine areas, including mesa and mountain landscapes.

3 CHANNEL MIGRATIONS ALONG THE BRAZOS RIVER IN CENTRAL TEXAS

3.1 Overview[1]

Meander migration has been investigated from numerous perspectives over the years. These investigations have resulted in numerous approaches of applying this research to various rivers irrespective of size and style. Although these models are generalizations of a typical alluvial river, they do not fit all large rivers. On a scale of hundreds to thousands of kilometers in channel length the great variety in vegetation types, underlying bedrock geology and variety of channel features impose many variables and driving factors on channel movement across the floodplain.

Recent attempts to regulate Texas river basins necessitate detailed understanding of discharge-driven rates of migration for proper planning and management. One of the key elements needed for appropriate management is an understanding of the rate of migration of meanders on a river. Rates and magnitudes of lateral channel migration occurring along a section of the middle Brazos River from the late 1920s to 2008 were mapped using aerial photographs, planimetric maps, and fieldwork.

The middle Brazos River traverses from the Blackland Prairie to the Interior Coastal Plain physiographic provinces. The floodplain of the Brazos is composed of predominately silty sand with occasional outcrops of limestone. The study reach consists of 92 bends and 203 km of channel. Flow regulation, which has resulted in substantial decrease in channel migration since the late 1940s, has greatly altered the discharge and

[1] Reprinted with permission from "Rates of Channel Migration on the Brazos River" by John R. Giardino & Adam A. Lee, 2011. Texas Water Development Board Project Report, 127 p.

suspended sediment characteristics of the river. Discharge from the late 1920s to 1949 averaged 75 m^3/s whereas discharge averages 61 m^3/s since flow regulation began. Peak flows occurred more frequently prior to regulation, impacting the rate and style of migration.

Rates of channel migration prior to regulation averaged 13 (+/- 3) m/year whereas migration after regulation averages 4 (+/- 3) m/year. Total migration of the channel ranges from 1.09 to 11.53 m/year with an average of 3.28 m/year for the entire study time period. The results support the inherent difficulty in predicting magnitudes and direction of channel migration for large, irregular fluvial systems.

3.2 Introduction to Problem

Channel migration is a natural phenomenon presenting challenges for engineers, scientists, and managers on how to best accommodate societal needs with the structure and processes of nature. Management of rivers in Texas is concerned with maintaining sound ecologic environments in the major river basins. The Texas Instream Flow Program was established to further understanding of the chemical and physical processes in the river basins. Concerning geomorphology, the role of sediment transport and deposition, in combination with the hydrologic regime, form and maintain the habitats necessary for healthy river ecosystems (Texas Water development Board, 2008).

The mechanisms for changes in channel changes on the Brazos River are only partially understood. The scale of processes and the nonlinear interaction on large rivers such as the Brazos River make it difficult to isolate singular variables as the cause of

major changes in channel position. These complex interactions of processes make it difficult for land and resource managers to mitigate changes in this dynamic landscape.

Indicators of stability include rates of lateral channel migration and the nature of bank erosion. Lateral channel migration and bank erosion are influenced by a number of variables including land cover, hydrologic regime, bank composition and underlying geology, among others.

The fluvial system, including the main channel, is a physical system with a memory (Schumm, 1977). This memory is represented by the template of various landforms and geologic deposits on which contemporary processes operate. By examining this memory, I examined patterns of channel movements in relation to hydrologic characteristics to understand the effect of changes in hydrologic discharge regime on the rates and styles of lateral channel migration.

The nature of channel migration along the Brazos River in central Texas will be addressed with the following questions: First, what are the rates of channel migration along discrete sections of the main channel? Second, what is the effect or overall influence of major watershed parameters, i.e., bedrock geology, channel discharge and bank conditions, on rates and styles of migration of the channel?

The goals of this work are to:

1) Delineate a central section of the Brazos River to evaluate discrete channel segments for the major variables influencing migration of the main channel

2) Quantify the rates and qualify the styles of migration of the main channel of the Brazos River
3) Quantify the nature of the hydrologic regime within the main channel of the Brazos watershed
4) Examine the contribution of the major factors affecting the river, i.e., underlying geology, land use, surface hydrology and basic geomorphic change over time, to explain the style of meandering observed along the middle Brazos River

Through quantifying the rates of migration of the Brazos River and examining the various factors to this change an understanding and explanation of the river can contribute to understanding historical trends and predicting future developments.

3.3 Literature Review

3.3.1 Overview

All landscapes are subject to the independent drivers of climate and tectonics. Channelized water flow contributes a very small percentage to the overall global water budget, yet water flowing over the terrestrial surface is a major component of the change and evolution of landscapes. River processes across spatial and temporal scales, such as climate, tectonics, land cover/land use, and channel geometry (width, depth, and curvature) interact in complex ways to create a wide suite of channel forms in a given landscape (Knighton, 1998).

The migration of large alluvial rivers has received a great deal of attention in the fields of geomorphology, geology, hydrology and engineering (Dunne and Leopold,

1978). The range of work covers from the early definitions of channel-forming, or "bankfull", discharges discussed by Wolman and Leopold (1957) to complex modeling of meander characteristics for predictive purposes (Lancaster and Bras, 2002; Guneralp and Rhoads, 2010) Of particular interest is understanding the processes and associated rates that lead to the formation of the numerous features and forms found in fluvial environments. At broad spatial and temporal scales the interaction between fluvial processes, sediment yields and the rapid rate of human-induced land alteration globally (Kondolf, 2014) presents an immediate need for proper understanding of river mechanics and forms. Tremendous advances in remote sensing and geospatial data and technologies over the last several decades have facilitated studies of watersheds and rivers across both large and remote geographic areas (Clifford et al., 2016).

3.3.2 Meandering Channels

The meandering channel pattern, as opposed to straight or braided channels, is constitutes the majority of channelized fluvial forms. An extensive survey of the United States reveals approximately 90% of the total valley length contains meandering channels (Leopold et al., 1994). Ritter et al. (2006) provides a succinct explanation of the driving factors for the initiation of meanders. Water flow within the channel can be divided into two primary aspects: downstream, or primary, flow and a secondary flow perpendicular to the downstream direction. This secondary flow is the main driver in development of meanders. As water moves around a bend, centrifugal forces cause a slight elevation increase along the outside of the bend. This elevation increase creates a pressure gradient which in turn propagates a circular pattern of flow (Ritter et al., 2006).

Water moving along the surface towards the outer bank and along the bottom towards the point bar creates a helical flow as the water moves downstream. While this secondary flow can be further subdivided into more specific components the helical pattern is the primary driver in the meandering channel pattern.

With meandering contributing a large portion of the overall channel type, there is a variety of patterns within this group. Knighton (1999) lists three categories based on channel sinuosity with irregular, regular and tortuous meanders indicating greater degree of sinuous channel.

The stark regularity to which meanders form across the landscape can be readily described by the meander wavelength. The wavelength represents the downstream distance between two meander bends on the same side of the floodplain. This measurement is taken parallel to the tangent of the outer bank of the bend. The meander wavelength relates to many variables including the radius of curvature of a bend and discharge and width of the channel. Therefore, channel curvature and geometry exert an influence on flow within the channel (Ritter et al., 2006).

Numerous workers have employed methods for the measurement of meander migration using image overlays, such as aerial photographs and planimetric maps. Leopold (1973) and Gurnell et al. (1994) drew a series of transects perpendicular to the valley axis and measured the distance of channel movement for different time periods. Urban and Rhoads (2004) calculate changes in channel area per unit of channel length for each river-length unit, whereas Nicoll (2010) measured the distance between channel centerlines from different periods along the down-valley axis.

Briaud et. al. (2007) presents an overview on meander migration predictions, flume tests, risk analysis and various software modelling methods to address migration. Briaud et. al. (2002) presents the three commonly used approaches when predicting meander migration, with specific focus on the magnitude of channel movement. These methods are 1) empirical approach, 2) time-sequence maps and extrapolation approach, and 3) a fundamental modeling approach. The first approach uses correlation equations built using observed meander data, whereas the second uses observed movement of a given meander to predict subsequent migration. The third approach relies on modeling erosion processes at the soil-water interface and making future projections using recent hydrographs.

Two general types of meanders have been proposed by Kinoshita (1961); symmetric, low amplitude meanders that migrate in a consistent pattern downstream and high amplitude where different shifting at points along the bends creates a complex planform pattern. This relates to the importance of geometric properties, especially the radius of curvature, in understanding channel migration. Spatial lag is attributed to the development of asymmetric meanders because the rate of migration is related to the curvature at a point upstream (Ferguson, 1984). Numerous workers have shown the relationship between the rates of channel migration and channel curvature. Early efforts by Hickon and Nanson (1975, 1984) demonstrated that a radius of curvature where $2 < r_c/w < 3$ gives the maximum value of rates of migration, with decreases on either side of this limit (Buraas et al., 2014).

The action of meandering imparts a pattern of sinuosity on the landscape. As noted by Lazarus and Constantine (2012), sinuous channel forms occur in river systems where meandering is not active or very low. Traditionally, meandering is associated with internal flow dynamics in the fluid within the channel but Lazarus and Constantine (2012) demonstrate through modeling and natural observations that resistance to lateral and vertical channel movement is also related to the roughness of the surface over which a river flows. Resistant-dominated surfaces create higher sinuosity than slope-dominated surfaces. Schuurman et al. (2016) delineates a threshold between the magnitude and frequency of bar to floodplain conversion and the degree of sinuosity of meanders. Using flume experiments, both inflow disturbances and bar to floodplain conversions contribute to highly sinuous channels. The two end-members of channel form, single-thread channels and braided channel systems, display this connection between bar-floodplain formation and channel sinuosity. Single-thread channels, such as most large rivers in temperate lowland areas, develop prominent floodplains as the channel migrates across the floodplain. This migration results in few chute cutoffs, where a weak zone develops in the floodplain allowing a channel segment to avulse, as the floodplain and adjacent banks have a strong cohesion and the channel develops a high sinuosity.

The distinction should be made between channel migration and meander migration. For the purpose of this study, rates of migration were concerned with using the channel, rather than discrete meanders. Previous work on river migration along the Brazos (Gillespie, 1997) is concerned with rates of migration in discrete meanders, of which were defined by changes in inflection along the channel.

3.3.3 Reservoir and Impoundment Impacts on Rivers

In the United States, the large majority of dam and reservoir construction began in the second half of the 20th century. The conditions of the Dust Bowl of the 1930s placed pressure on land and resource managers to ensure the availability of adequate water supplies on a regular basis. In addition, the post-World War II economic and population boom created a need for regular supplies of water, including for electricity as suburban housing development became a dominant feature on the U.S. landscape. Flood control also contributed to the drive for dam building projects.

In the sciences of hydrology and geomorphology several developments facilitated enhanced understanding of these processes in fluvial landscapes. Coinciding with reservoir and dam construction was the installation of an extensive network of stream gauges for monitoring surface discharge across the U.S (Leopold et al., 1964). This network provided data over large geographic areas of water conditions and could be correlated to rainfall and flooding events. The second half of the 20th Century saw development in the geographic and geomorphic sciences as incorporating more quantitative theories and methods into practice (Gregory, 1985; McDowell, 2013). Much of geomorphology was highly descriptive but in combination with the advent of computing technology quantitative analysis has greatly expanded the base of knowledge. Technologically, aerial photography developed during the two World Wars, and satellite

observation during the Cold War, was slowly applied to studying the variety of features on Earth's surface, including fluvial systems. Though limited data exists in some areas as far back as the 1930s, the majority of historic aerial imagery coincided with the bulk of dam construction in the 1950s and 60s. This paucity of data over large areas prior to the 1950s highlights the importance of studies that can include quantitative measurements of channel form and adjustment prior to this period.

Reservoir construction has several impacts on floodplain geomorphology (Marren, 2014). Changes in sediment supply affect downstream floodplain development and increase the effects of floodplain-channel disconnect. River avulsions, specifically oxbow cutoff channels, are particularly suspect with decreased sediment supply altering the standard infilling of oxbows. Much of the research on reservoir changes to sediment supply focus on in-stream morphologies but overbank flooding and deposition is also altered and presents a research opportunity (Marren, 2014).

The impoundment of large volumes of water and sediment through reservoirs along the main channel is a component of the greater human-induced changes across fluvial landscapes. Rhoads et al. (2016) documented changes in the extent of channel networks and changes in planform in the Sangamon River basin in the Midwest of the United States. This river basin is heavily altered by conversion of the pre-European settlement tallgrass prairie to intensively managed agricultural landscapes. The anthromorphic changes have altered the river basin from predominantly biogeochemical transformations and storage of water and sediments before intense land use change to the current mode of intensified fluctuations of water, sediment and nutrients.

Schmidt et al. (2008) presents three metrics for assessing the downstream effects of dams. Examining the balance of changes in sediment supply and transport capacity may indicate a sediment deficit or surplus. Second, the Shields number represents the ability of downstream flows to incise channels with sediment deficiencies. Third, the ratio of downstream to upstream, from the dam, flood discharges is a measurement for the scale and rate of channel change with a focus on width.

The frequency and magnitude of discharge events of varying size also impacts the style of meandering on a river. The United States alone contains over 75,000 dams; with every major river altered by the one hundred thirty-seven very large dams, which store 1.2 km^3 or more of water (Graf, 2006). By analyzing the hydrologic data from stream gages on both the upstream and downstream reaches adjacent to dammed sections, Graf (2006) observed marked reductions in the annual peak discharges, ratio of annual maximum to mean flow and range of daily discharges by upwards of 60% and more. The temporal range of high and low flows and timing of the yearly maximum and minimum flows is altered by upwards of a half a year. River systems with the highest variability in natural flow amounts are often most susceptible to damming and impoundment as those watersheds are often in geographic areas with large human and natural pressure on water resources.

Graf (2006) furthermore discusses the geomorphic differences between regulated i.e., dammed) and unregulated reaches. These changes are a direct result in the alterations to the hydrologic regime as biotic and non-biotic matter and energy are reorganized in these systems. Similar to the changes in the hydrologic regime, the

streams and rivers of the western United States, specifically the interior watersheds have the largest change in the overall density of geomorphic features. In particular, Graf (2006) observed regulated reaches having 79% less active floodplain area, 3.6 times more inactive flood area, 50% smaller high flow channels, and 32% larger low flow channels.

The combination of aging infrastructure and societal desire for river restoration are the main drivers in dam removal. Efforts in recent decades to remove dams and impoundments from the fluvial landscape have provided opportunity for studying rapid and intense changes in the hydrologic, geomorphic and ecologic characteristics of the affected watersheds. An expedient qualitative method is to observe sediment transported downstream post-removal and its effect on the geomorphic units within the channel such as point bars, mid channel bars and flood overbank deposits (Doyle et al., 2002). Overall statistics on dam removal are provided by Bellmore et al. (2016). Their review of the literature finds over 1200 dams removed in the U.S. with fewer than 10% scientifically evaluated. Those evaluated had a short duration of study and limited or no monitoring before removal of the dam. In addition, the focus of research is predominantly on hydrologic and geomorphic aspects, with ample opportunity for understanding the interaction between physical and ecologic components.

3.3.4 Various Factors Affecting Meandering Rivers

Vegetation represents a strong control on the magnitude and frequency of channel migration. Several authors (Beeson, 1995; Abbe, 2003; and Gurnell, 2012) have examined the relationship between the extent and type of vegetation along a fluvial

system, and the forms of the channel. Beeson (1995) found non-vegetated streams in British Columbia are five times more likely to experience detectable erosion than vegetated streams after storms. Abbe (2003) describes the importance of loose wood in the channel, i.e., logjams, in adding complexity to the hydraulic, geomorphic and ecologic aspects of riparian areas. Gurnell (2012) provides an overview of the cycling of live and dead wood through floodplain riparian ecosystems. McBoom (2014) notes that whereas reservoirs as a result of damming do not greatly affect the characteristics of large woody debris in large rivers, consequences occur for riparian forest disturbance. The condition of riparian forest along rivers in turn can alter sediment erosion and deposition patterns. On large rivers, variability in the composition of bank material can occur over relatively short distances (Konsoer et al., 2016)

Channel banks, regardless of watershed drainage size, are less susceptible to erosion when herbaceous or woody plants are present in large areas (Micheli, 2004). Odgaard (1987) showed channels of the central United States with a forest vegetative cover migrate roughly half as fast as non-forested channels. By mapping and measuring this change in cover, it is to relate vegetation change to channel migration. Esfahani and Keshavarzi, (2010) showed that riparian vegetation should be planted at a width of 10% of the floodplain width for the channel.

Micheli et al. (2004) investigated the channel change between forested and agriculture land uses along the Sacramento River in central California. The Sacramento River is also a large alluvial system in a flat topographic area but has a different

sediment regime with significant sediment load from mountain drainage, leading to large sand and gravel in the main channel.

The influence of the underlying bedrock may exert a control on the magnitude and frequency of migration of the main channel. Bedrock geology works as a dominant control on channel form and processes for 'bedrock' (i.e., mountainous) and 'alluvial' (i.e., lowland) streams (Stark, 2003; Keen-Zerbert, 2007; Nittrouer, 2011). The morphology and composition of the floodplain can exert similar allogenic influence on the planform of surface channels. The majority of lowland floodplain studies of channels focused on the interaction between floodplains and the channelized components in the channel belt, i.e., the width from meander to meander along the downstream direction. Depending on the characteristics of the floodplain, parallel channels form during overbank discharge events (David et al., 2016). These channels flowing down valley with various bifurcations and confluences occur predominantly in fluvial systems with large floodplain-to-channel width ratios, high rates of main channel migration and often found in agricultural areas. These channels with intermittent active discharge are likely paleo-meanders from a previous chute cutoff.

3.3.5 Meandering In Relation To the Brazos River

The responses of large rivers, such as the Brazos River in western and central Texas, to changes in a particular variable are difficult to predict. The Brazos River has a large drainage basin that crosses distinct physiographic provinces, which contain a variety of unique geomorphic landforms. The Brazos, contrary to appearances with its large alluvial floodplain may respond significantly, in lateral movement, to changes in

bedrock geology, which transition in a linear fashion, through geologic time, down the channel. Whereas rivers actively meandering in bedrock banks often develop unpaired strath terraces (Johnson, 2015), alluvial or lowland rivers typically develop paired depositional terraces (Ritter, 2006). The presence of resistant bedrock in alluvial rivers may alter the paired terrace pattern. In a previous study of channel migration, Gillespie & Giardino (1997) found no correlation between the changes in alluvial sediments and channel migration along the Brazos River, but suggest underlying bedrock geology may influence the dynamics of channel migration. In addition, the uniform orientation (strike and dip) of rock units along the length of the channel makes testing the hypothesis, that bedrock can play a part in the migration of individual reaches of large alluvial rivers straightforward, relative to other large rivers.

The study reach of the Brazos River contains relatively homogeneous bank erodibility (Gillispie, 1992). The active channels within the floodplain are dominated by clays, silt and fine sands. Recent reservoir construction has lowered the overall magnitude and frequency of overbank flooding. The planform pattern and meander characteristics of rivers are influenced in part by overbank flooding, with sinuosity of the channel affected by a large amount of bank heterogeneity (Schwendel, 2015). Reconstruction of channel cross-sections from historic stream gauge data shows the Brazos River adjusting to post-reservoir sediment and water discharge (Heitmuller, 2014). The banks of the lower Brazos River have experienced bank encroachment since the 1970s. Along with recent flooding, channel aggradation has occurred, and built bank accretion deposits. These deposits indicate the channel returning to the 1- to 2- year

return period. Therefore, as the lower Brazos River adjustments to post-reservoir sediment and water, the middle Brazos River, of concern to this study, adjusts as well to changes in sediment and water regime. Kondolf (1997) details channel effects of dams and in-stream gravel mining along rivers in central California. Reaches downstream of impoundment and reservoirs are often sediment starved which in turn erodes channel bed and banks, produces down cutting or channel incision and coarsens the overall sediment load. Though the sediment of the Brazos River is predominantly fine to coarse sand, in-stream aggregate mining also has the potential for disruption in the geomorphic forms of the active floodplain. Dunn and Raines (2001) identify an overall decrease in the volume of sand in the suspended sediment load near the coastal outlet of the Brazos River, but found the effects of sand mining difficult to quantify. The channel incision, observed on the central and lower reaches of the Brazos River, increases the flood discharge needed to reconnect with overbank geomorphic forms and ecologic habitat.

In addition, browsing the collection of historic aerial photographs along the Brazos River displays a substantial change in woody plant cover. As discussed earlier, the presence of vegetation, specifically large woody plants, has a substantial impact on bank stability and erosion resistance. Many stretches of the Brazos River have undergone extensive land cover and land use changes over the last two centuries. Clear cutting of the forested riparian corridor for agricultural use in particular has increased erosion of the sandy and silty banks. This sediment is then transported downstream. Concurrently, since impoundment of the major reservoirs along the river, large volumes of sediment have become trapped within the reservoirs themselves. As a result of

impoundment, decreases in sediment supply to the barrier island system protecting the Texas coastal prairies occur (Mathewson and Minter, 1981). The sediment budget for the central and lower Brazos River is unbalanced, increasing the bank instability. As mentioned earlier, the advancement in geomorphic science over the last several decades provides insight into pre- and post-reservoir development along the Brazos River. The central watershed of the Brazos River was developed early in the settlement of Texas with railroad construction and heavy agriculture use substantially altering the landscape of the watershed, specifically along the major active floodplain of the main channel. Detailed surveys and mapping of the Brazos River floodplain provide data for comparing channel response post-reservoir construction.

3.4 Physical Setting

The Brazos River has a drainage area of approximately 137,000 km^2 and a length of 2,060 kilometers. The study reach is defined from just below the last major reservoir, Lake Waco, to the Brazos County line (Fig. 3.1). Three gaging stations (Waco, Highbanks, and Highway 21) along the main channel provide the hydrologic data used in this study. The southern extent of the reach was selected based on the stage-discharge relationship of increasing stage for an equivalent discharge. The river channel downstream of the Highway 21 gauging station is incised up to 20-30 meters with little lateral migration, as the channel cross the active floodplain from west to east.

Figure 3.1 displays the major geologic units along the study reach. The middle and lower alluvial floodplain is ~ 12.8 km wide near the Brazos County line. Horizontal layers of clay and silt overlain by overbank deposits constitute the majority of materials

forming the alluvial valley (Waters, 1995). Upland areas of Eocene age confine the broad alluvial valley (Phillips, 2006).

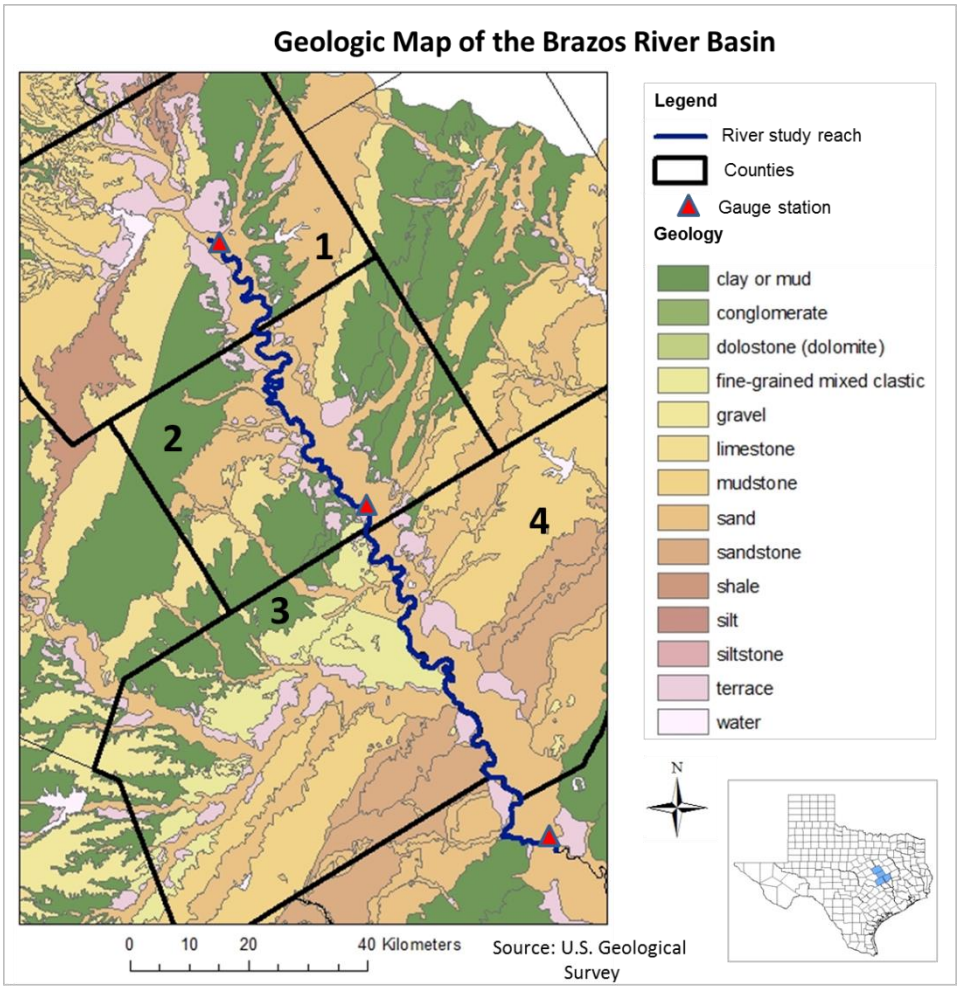

Figure 3.1. Map of the study reach along main channel of the Brazos River from southern Waco, TX (Waco gaging station) to near the Brazos County line (Highbank gaging station). Total length is approximately 200 kilometers. Geology of the Brazos River Basin. The inset numbers represent counties; 1) McLennan, 2) Falls, 3) Milam & 4) Robertson.

A variety of major geologic formations underlie the Brazos River valley (Fig. 3.1). The study reach extends from just south of the city of Waco to approximately the

northern Brazos County line. It is within this reach that the Brazos River floodplain expands to its full extent within the drainage basin.

Strata striking northeast to southwest underlie the study area. Outcrops consist of indurated sedimentary layers. Several major and minor aquifers underlie the floodplain area. The Texas Board of Water Engineers (2007) describes the northern aquifers north of the Falls County line as having negligible contributions to the Brazos River base flow; whereas the region between the northern Falls County line and the city of Bryan, which encompasses the majority of the study reach, appears to have a significant contribution to the baseflow discharge.

3.5 Methods

The major data components utilized in this study include vertical aerial photographs, planimetric maps, regional geologic and hydrogeological data, digital elevation models (DEMs), hydrologic data from three surface gauging stations, and field surveys. These data were integrated into a Geographic Information System (GIS) for compilation and analysis. This is a common data processing procedure used in a number of river morphology studies (Shields, 2000; Buckingham, 2007; Rhoades, 2009).

3.5.1 Hydrology

Data from three surface stream gauging stations were used in this analysis. The majority of hydrologic analysis data was based on data from the Waco gauging station (No. 8096500, latitude: 31.535833, longitude: 97.073056). It was selected because it covered the entire time period (1929-2010) for the study area. Because hydrologic records have

been kept since 1898, covering the entire time period under investigation, the collection of data from the Waco gauging station was utilized. The Highbank gauging station (No. 08098290, latitude: 31.133889, longitude: 96.824722) is located at the entrance of a major tributary along the main river channel. A third gauging station located at the bridge crossing of Highway 21 (No. 08108700, latitude: 30.626667, longitude: 96.543889) was used to represent the southern extent of the study reach.

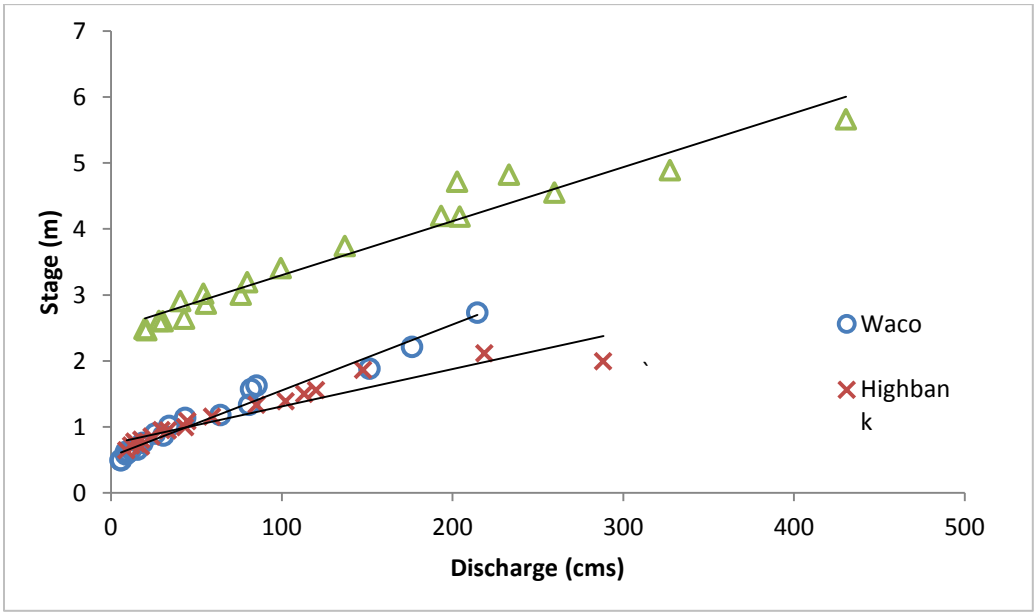

Figure 3.2. Brazos river incision increases downstream. The Waco gaging station is at the upper portion of the study reach. The Highbank gaging station is approximate midpoint of the study reach, while the Highway 21 gaging station is a short distance downstream of the southern extent of the study reach.

Figure 3.2, which includes data for only those dates with both discharge and stage values, shows a threefold increase in stage with an equivalent discharge between the two upstream gauge stations, Waco and Highbank, and the downstream gauge, Highway 21 gauge. Deepening of the main river channel at the Brazos County line

increases the stage height for an equivalent discharge. The Highway 21 forms the southern limit of the study reach. The amount of channel migration differs between the study and subsequent downstream reaches. Migration is neither as frequent nor as high downstream of the Highway 21 gaging station. Because of the relatively homogenous composition of the Brazos floodplain within the study reach changes in channel geometry most often occur lateral, or across valley, rather than vertical incision or accretion.

Surface hydrologic data gathered from the Waco gaging station along the main Brazos River channel were analyzed to determine discharge patterns affecting channel migration. Important flows incorporated into this evaluation of migration-discharge include the yearly maximum, mean and total channel discharge. These flow variables describe the hydrologic characteristics of the river channel for each particular time period. All hydrologic values are presented in units of cubic meter per second (m^3/s). Figure 3.3 displays changes in the overall channel discharge from 1910 to 2010. The pre-reservoir period, 1910-1950, shows greater discharge than the post-reservoir, 1950-2010, period.

Several major reservoirs (Table 3.1), including Possum Kingdom (1941), Lake Whitney (1951), Lake Granbury (1969) and Waco Lake (1965) constructed along the Brazos River, significantly alter the overall hydrologic regime of the river and affect channel response to discharge. Channel discharge at the Waco gaging station averaged 75 m^3/s/month prior to 1950 and 61 m^3/s/month after 1950. Figure 3.3 displays changes

in the mean and total discharge for 10-year increments at the Waco gaging station with significant decrease of 0.4 m^3/s/month in discharge after 1950.

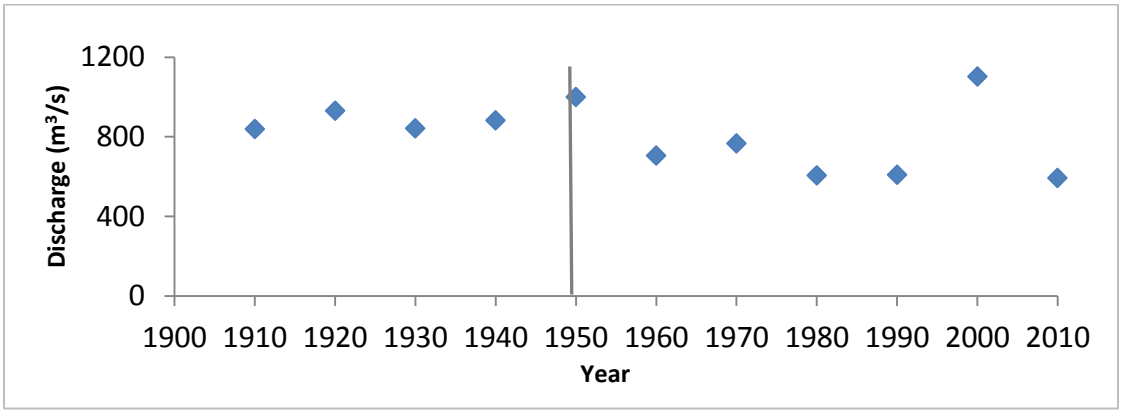

Figure 3.3. Total discharge at the Waco gaging station for ten year intervals. Discharge has a marked decrease after 1949, marked with a vertical line; multiple reservoirs were constructed over the following decades.

Table 3.1. Major reservoirs constructed upstream of the study reach.

Reservoir	Stream Impounded	Impoundment Date	Total Storage Capacity (m^3)
Possum Kingdom Lake	Brazos River	1941	893,555,100
Lake Whitney	Brazos River	1951	2,465,383,500
Belton Lake	Leon River	1954	1,345,597,560
Hubbard Creek Res.	Hubbard Creek	1962	635,981,400
Proctor Lake	Leon River	1963	461,388,600
Lake Waco	Bosque River	1965	895,651,200
Somerville Lake	Yegua Creek	1967	625,747,500
Stillhouse Hollow Lake	Lampasa River	1968	777,283,200
Lake Granbury	Brazos River	1969	296,709,120
Lake Limestone	Navasota River	1978	392,217,300
Lake Georgetown	San Gabriel River	1980	161,276,400
Granger Lake	San Gabriel River	1980	301,098,600
Aquilla Reservoir	Aquilla Creek	1983	180,018,000

It is apparent that a change occurs in the overall hydrology pre- and post-1950. The discharge has a relatively uniform flow pre-1950 but post-1950 a high fluctuation

occurs in the values. The pattern for discharge between the average and total is nearly identical. Thirteen constructed reservoirs, along the main channel and numerous tributaries impound a significant amount of water (Table 3.1). The largest storage capacity is on reservoirs constructed in the 1940s and 1950s, specifically Lake Whitney and Belton Lake.

3.5.2 Channel Migration

Methods for measuring channel migration are well documented in the scientific literature (Shields, 2000; Urban and Rhoads, 2004). Typically, aerial photography, satellite imagery, topographic maps and other planimetric data are integrated into a GIS for measurement and analysis. This present study is based primarily on aerial photography, including black and white, color, and false-color images to analyze channel movement (Fig. 3.4). Including all sources of data, the dates of channel coverage are 1929, 1941, 1951, 1955, 1958, 1960, 1965, 1968, 1972, 1974, 1978, 1982, 1988, 1993, 1995, 2004, 2008, and 2010, respectively. The data for all channel coverages preceding 1995 are not continuous along the study reach, but rather cover portions of the study reach throughout the counties of McLennan, Falls, Milam and Robertson. Therefore, the data was delineated based on the county level for analysis purposes. The coverage dates of 1995, 2004, 2005 and 2008 are continuous along the entire study reach. The southern two counties, Milam and Robertson, share the Brazos River as the county border.

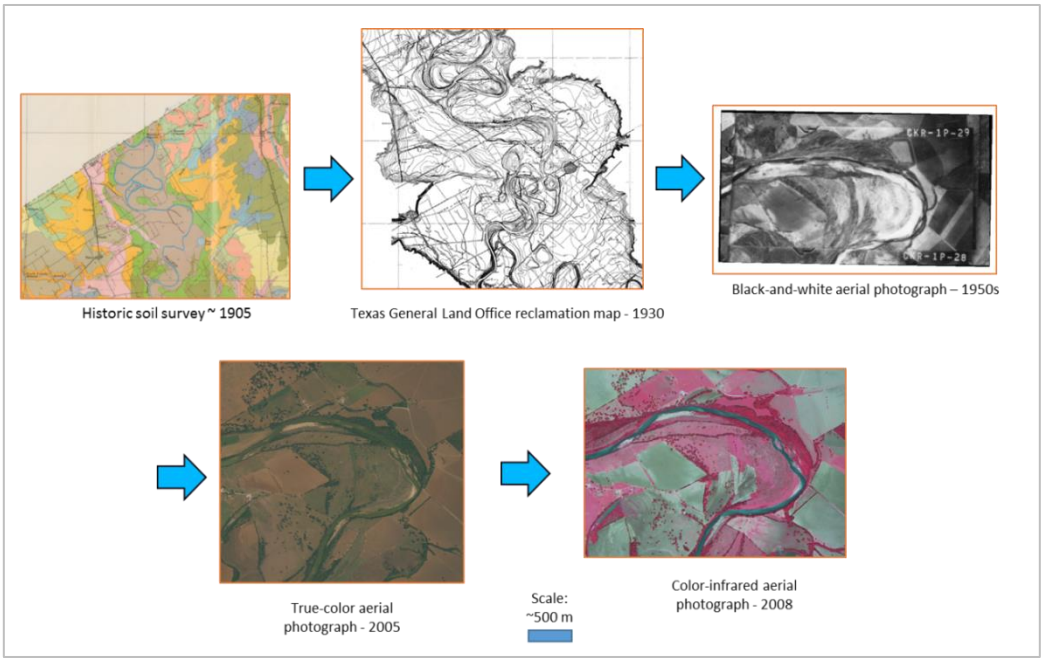

Figure 3.4. Data sources for planimetric measurement of channel migration.

Additional data sources were used, including topographic maps, engineering survey maps, and digital elevation models. Survey maps, produced by the Texas State Reclamation Department dating from the late 1920s, were obtained from the Texas General Land Office. United State Geological Survey topographic maps dated from 1978 were used for channel locations for Falls County only to provide an additional time period between 1968 and 1995. Measurements were made for 1968-1978, 1978-1995, and 1968-1995 to eliminate any spatial error from topographic maps.

Historic and contemporary aerial photographs, including the years 1941, 1951, 1955, 1958, 1960, 1965, 1968, 1972, 1974, 1982, 1988, 1993, 1995, 2004, 2008, and 2010, form the majority of channel migration values presented in this work; scales range from 1:20,000 to 1:60,000. The positions of the river channel were digitized using

editing tools available in the ArcGIS® software. A scale of 1:4,000 was used to digitize channel features. This scale provides sufficient spatial separation between terrestrial and aquatic areas. The majority of images are black-and-white photographs held by the US Department of Agriculture Farm Service Agency and the National Agricultural Imagery Program for recent images.

All pre-1996 aerial photographs lacked spatial coordinates and had to be georeferenced in the GIS. In total, 419 separate aerial photographs were georeferenced using ArcGIS® software. In addition, the Texas GLO reclamation maps were georeferenced by converting the lat-long coordinate system into Universal Transverse Mercator (UTM) system.

Georeferencing images require a transformation and resampling of the pixel data. Hughes (2006) recommends using a second-order polynomial transformation for orthorectification and a cubic convolution for pixel resampling. The transformation of a second-order quadratic applies a least-squares function between the ground control points (GCP) selected on the image and the coordinates present on the base image. The 2004 National Agricultural Imagery Program (NAIP) provided the base layer for ground control point (GCP) selection.

Ground control points are assigned to locations in the unregistered photograph to known locations on the georegistered photograph. The imagery is in false-color format whereby areas of heavy vegetation have a more intense red hue and water shows especially dark as compared to the surrounding landscape. These data are especially useful for delineating different geometries such as bank boundaries. The spatial

resolution for all aerial photographs ranges between one and three meters. *Time frame* refers to an individual photograph year, i.e., 1974; whereas *time period* refers to an interval between photograph years, i.e., 1968-1974, from which migration was measured.

The methodology for measuring total channel migration between years is similar to that presented in Hughes (2006) and Shields (2000). Channel boundaries were manually digitized using the editing tools available in ArcGIS®. Bank lines were drawn between the edge of vegetation and the exposed channel bank during high/low water periods (Richard et al., 2005). In locations where the water level was lower than expected, usually along large, sandy point bars, the channel boundary was delineated as the interface between established vegetation and dominantly sandy areas. Where tree crowns overhang banks, the bank line was drawn through the crown center (Winterbottom, 2000). The separate left and right bank line shapefiles were merged into a single shapefile; a centerline for each time frame was calculated using automatic tools in ArcGIS®. The resultant centerline shapefile was adjusted for errant channel center locations that may have been generated from the merged bank lines shapefile. The centerlines for respective years were overlayed and 'migration' polygons were generated between adjacent and sequential centerlines.

The respective total area of a migration polygon was divided by half the perimeter of that polygon, or the length of the migration polygon centerline (Fig. 3.5). Values below four meters of migration were eliminated because of potential spatial error in the georeferencing of images and manual digitizing. This procedure follows the

standard method from the literature. The spatial error is present in georeferencing aerial photographs as an artifact of the mathematical process of aligning the image to the reference grid. The root mean square error is lower at values of four meters and higher because of the equation threshold the software applies to the georeferencing. Table 3.2 references spatial error of the aerial photograph relative to the reference grid, whereas evaluating migration values of four meters or greater references spatial error within the georeferenced image.

The rate of migration was calculated using the following equation:

$$R_m = \frac{A}{L}/\mathrm{y} \tag{3.1}$$

where R_m is the rate of migration; A is the area of the polygon; L is the length of centerline Time 1 for each polygon; and y is the number of years between sequential channel centerlines.

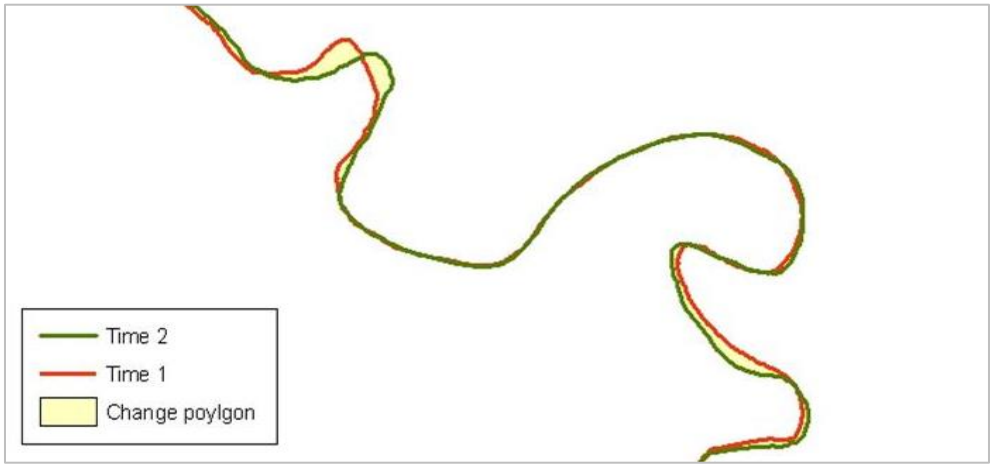

Figure 3.5. Method for measuring the amounts of channel migration. Time 1 and Time 2 lines represent channel centerlines for a particular year.

A migration value represents the average for a particular migration polygon and takes into account narrowing and widening of the migration polygon. The extreme values, high and low, for each individual polygon are not represented. This has the effect of smoothing the data. The migration value measured along a particular bend during a time period describes neither the smallest nor the largest amount of migration at that location, but rather the average migration for the lateral movement polygon.

To assess pre- and post-reservoir effects on channel migration and channel width an alternate migration method was employed for the entire study reach (Fig. 3.6). We used the method used by Leopold (1973) and others (Gurnell, 1994) to analyze the 1929, 1950s, and 2004 planimetric data.

The method involves delineating a series of transects perpendicular to the river floodplain and measuring the distance between the points of intersection between the channel centerline and transect for subsequent time frames. I generated 180 migration values for the 1929 to 1954 and 1954 to 2004 datasets, respectively. The 180 values were measured at points along the river bends midway between the inflection points of a particular bend. The inflection points of a channel occur where the river changes course along a tangent adjacent to the channel. The migration distance for pre- and post-reservoir time periods was calculated using the following equation:

$$D_m = T_1 - T_2 \tag{3.2}$$

where D_m is the distance the channel migrated, and T_1 and T_2 are the time periods of subsequent channel migration.

Time periods between the 1950s and 2004, i.e., 1972, 1988, etc., were not used in the analysis of channel migration differences between the major pre- and post-reservoir construction time periods. Transects were placed one kilometer apart. This method eliminates bias in selecting migration locations, but features of particular interest, such as avulsions or abrupt changes in a small area, may not be recorded.

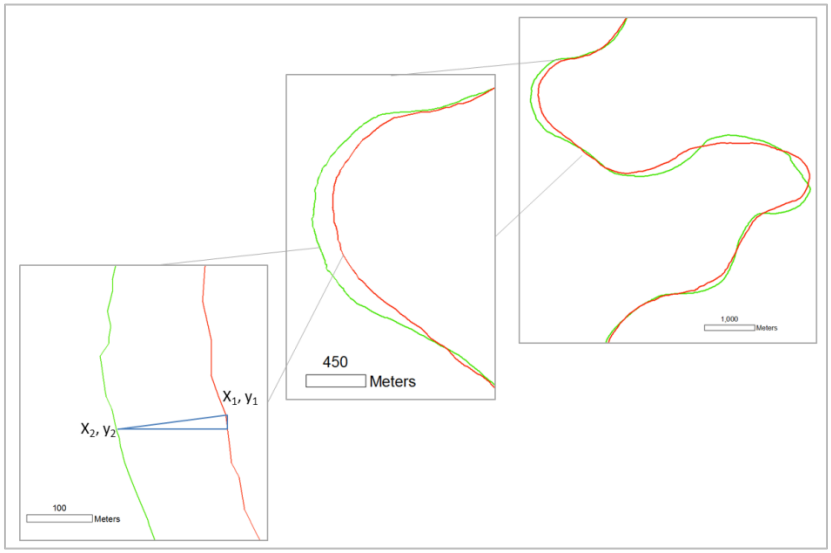

Figure 3.6. Secondary method for measuring channel migration used to determine pre- and post-reservoir magnitudes and rates of migration. Red line represents channel position pre-reservoir, while the green line represents the channel position post-reservoir.

The geospatial coordinates for the inflection point along the meander bend were captured for each time period. Using the right triangle I could quickly determine the distance between subsequent inflection points. The following formula calculates the distance between inflection points:

$$D_t = \sqrt{[(x_1 - x_2)^2 + (y_1 - y_2)^2]} \qquad (3.3)$$

where D_t is the distance between inflection points; x_1, y_1 are the coordinates of the earlier time period; and x_2, y_2 are the coordinates of the later time period. The initial values are kept positive to give a magnitude of migration. This method for calculating these pre- and post- reservoir values is displayed in Fig. 3.6.

3.5.3 Geospatial Error

An inherent amount of spatial error occurs within the measures of channel movement using the two methods. If total migration from one temporal period to the next was less than four meters, the measurement was not included in the analysis. Average geospatial error and the number of frames georeferenced are presented in Table 3.2.

Table 3.2. The planform data, including aerial photographs and maps, used in this study. Average geospatial error values for determining migration.

Time Period	# of Frames	Average Spatial Error (m)	Transformation
Texas GLO 1929	10	1.59	2nd order
McLennan 1958	24	3.16	2nd order
McLennan 1972	8	2.62	2nd order
McLennan 1982	30	2.68	2nd order
McLennan 1988	15	2.82	2nd order
McLennan 1993	14	2.82	2nd order
Falls 1955	48	3.18	2nd order
Falls 1960	45	2.88	2nd order
Falls 1968	65	2.96	2nd order
Milam/Robertson 1941	30	2.98	2nd order
Milam/Robertson 1951	28	2.76	2nd order
Milam/Robertson 1958	44	2.95	2nd order
Milam/Robertson 1965	27	2.50	2nd order
Milam/Robertson 1974	18	3.91	2nd order
All counties 1995*	39	2.00	2nd order
All counties 2004*	39	1.00	2nd order
All counties 2008*	39	1.00	2nd order
All counties 2010*	39	1.00	2nd order

* Previously georeferenced by National Agricultural Imagery Program

In addition, data values of meander movement across the floodplain, not rate of migration per year, of less than 12 meters generated from the Texas GLO 1929 and the topographic map data were not considered in this analysis because these values are below the spatial resolution of the maps. This step was undertaken to eliminate error present within those data sources.

3.5.4 Field Surveys

Field sites were selected to observe meander characteristics (Fig. 3.7). Data collected at these sites include bank heights for the outer (cut) bank, photographs of bank conditions and geometry, and tree cores for dating of scroll bar sequences. The inner point bars of the main channel were most readily accessible during field surveys; therefore the outer cut bank heights were measured using a mechanical clinometer and laser range finder. The clinometer measured the angle from the observer to the top of the bank and the range finder measured the ground distance from observer on the point bar to the opposite bank at three to five locations along a specific bend. With angle and distance the outer bank height was computed. The field surveyed bank heights were checked against bank heights measured from a 10-meter resolution digital elevation model (DEM). The difference between field surveyed and DEM heights ranged from 1 to 2 meters.

The tree cores were collected from *Populus deltoides* (eastern cottonwood) along scroll bar topography sequences on point bars in an attempt to correlate tree-ring age with scroll bar position and calculate approximate rates of migration for channel locations prior to the earliest planimetric map data. The method of calculating the rates of channel migration from tree ages and scroll topography has been used with success on

Canadian rivers (Hickin, 1974), but the data are not included in this report because of various problems encountered with poor tree-ring records in the cottonwood tree species along this section of the Brazos River.

The largest and most mature trees, almost always *Populus deltoides* (eastern cottonwood), were selected for coring. Trees were selected in scroll bar sequences older than the GLO maps to obtain dates of channel positions prior to 1929. The data proved unreliable and are not included for a number of reasons noted by Everitt (1968) and include difficulty in reading the rings of a diffuse-porous wood and a low climate stress, or extreme variation, in the Brazos River valley at this location. These factors combine to cause dormancy in tree growth, impeding the ability to determine age, and therefore rates of migration, from tree cores.

Figure 3.7. Large meander bend along middle of study reach looking towards outer bend. Note shear bank wall. Photograph taken by author on June 29, 2010 at UTM Zone 14 694682 E & 3461604 N.

Bank height and bank characteristics were observed to understand mechanisms for bank failure and erosion. The height data for the field sites was compared to the

values obtained from the 10-meter DEM, which was used for calculating deposition and erosion along the entire study reach for the multiple time periods.

3.5.5 Longitudinal Profile – Gradient and Sinuosity Classification

A classification system to segment channel susceptibility to bank failure and movement was developed to segment the rates of migration into different groups based on the physical properties of the channel. This classification system is based on dividing the longitudinal profile of the channel into various segments based on significant changes in gradient. The longitudinal profiles are termed *slope classes*. Ten slope classes were developed from the longitudinal profile. The boundaries of each gradient class are shown in Figure 3.8.

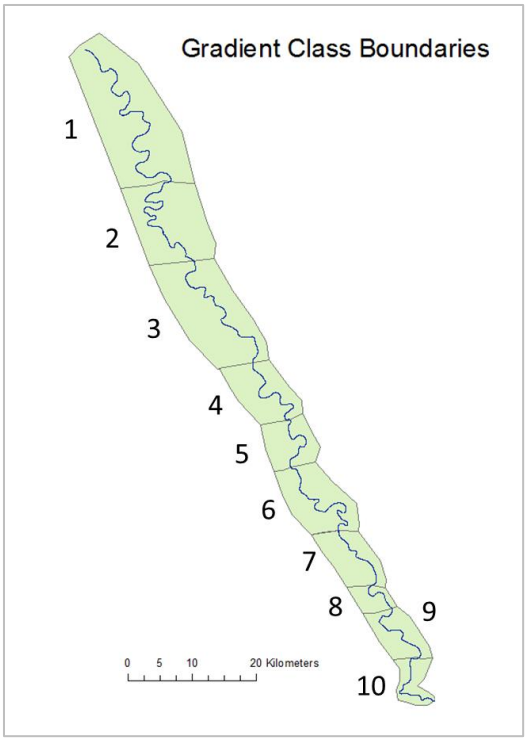

Figure 3.8. Boundaries for ten gradient classes. Division of channel was done through the natural breaks in longitudinal gradient.

The longitudinal profile was generated by extracting point values along the 2004 channel centerline from a U.S. Geological Survey 30-meter DEM. The 2004 channel centerline was used because it corresponds most closely to the date the DEM was generated. Because of the structure of the raster data within the DEM, the resulting points were spatially joined to points spaced every thirty meters along the 2004 channel centerline. This step was used to smooth the profile and reduce duplicate elevation values not immediately positioned along the centerline. The lateral rates of channel migration for all years were then grouped and stratified into the respective gradient classes to gain an understanding of the role gradient and sinuosity serve in impacting rates of migration.

The 2004 channel centerline was corrected for compatibility issues with the 10-meter DEM. The revised channel centerline was used to extract the elevation values from the 10-m DEM. The extracted raster was converted to a point shapefile using the center of the raster cell as the individual point location. The channel centerline was divided into 10 meter segments. The center point of these segments was converted to a point shapefile. The point shapefile was joined to the elevation (raster DEM) shapefile.

Two measures of gradient, or slope, are presented. First, channel gradient whereby the elevation difference between the upstream and downstream channel end points is divided by the channel distance between the two points to give a slope value along the main river channel. Alternately, the change in upper and lower channel bed elevation is divided by the length of the channel to give a channel slope value. The second gradient measure, valley gradient, represents the difference in elevation between upstream and downstream end points divided by the length of the floodplain in the downstream direction.

3.5.6 Estimate of Channel Sediment and Budget

The sediment budget for the Brazos River focused on the sediment deposition and erosion along the main channel. The sediment inputs and outputs along tributaries and overland sources were not accounted.

A budget concerning only freely migrating meanders is calculated. Freely migrating meanders are defined as those meanders that are not immediately adjacent to the upland terraces that bound the valley floor. An exception is made to also include those meanders that while adjacent to the upland terrace are actively migrating in a

direction towards the center of the valley floor for a sufficient amount of time to build an extensive bar complex (Appendix A).

The method used involved creating a series of overlay polygons along specific delineated bends to include all bank line movements within the time series analyzed. The polygon ends were drawn perpendicular to the channel centerline. The total number of freely migrating meanders covered in the sediment budget is thirty three.

A number of assumptions were made to develop this sediment budget. Bends directly adjacent to the valley wall were not measured because the influence of stable geologic formations may influence the style and rate of sediment in the main channel. Those meanders analyzed were freely meandering across the floodplain, specifically as the main channel transitions to and from either side of the river valley. Exceptions to this were made where the river channel is actively migrating away from the valley wall.

Deposition was calculated following a slightly different methodology. The 2004-2008 channel deposition was overlaid atop the 10-meter DEM to provide the most recent significant coverage of meander migration. The deposition amount was calculated by determining the elevation difference between the land surface adjacent to the cut bank and the depositional point bar.

Several assumptions were made. First, the plane of the deposition is held as level. Second, the rate of vertical deposition has remained constant throughout the study time period. Last, all movement of the Brazos River has been lateral, with no vertical change channel depth.

A final sediment budget assessment involved examining several meander bends in the field. These sites are located along the channel section in southern McLennan and northern Falls counties.

A stadia rod and tape measure were used to estimate volumes of bank sediment on the near bank of the channel. The measurements recorded include the height of the bank, height and width of the slumped material. To gather data on the far side of the bank measurements were taken using an inclinometer. Assuming a vertical cutbank, a measurement was taken at the bank top and bottom. Two right triangles can then be used to estimate the total bank height, and, therefore, the slump toe height.

3.6 Results

3.6.1 Hydrology

The hydrologic regime of the Brazos River is highly variable, particularly across the decades (1929-2010) encompassing the study time period. Figure 3.9 displays the total annual and average discharge patterns from 1900 through the summer of 2010.

The trend for individual yearly flows can be seen in figures 3.3 and 3.8. Prior to 1950 yearly channel discharge averaged from 37 m^3/s to 127 m^3/s with a median of 73 m^3/s. After 1950 yearly discharge averaged from 34 m^3/s to 85 m^3/s with a median of 54 m^3/s; representing the change in hydrologic regime impacted by the construction of large reservoirs. Major drought occurred in the 1950s (Reynolds, 1999), accounting for the unusually low discharge values, with a decrease of 294 and 62 m^3/s in total decade discharge in the decades immediately before and after the 1950s. The decrease in overall discharge is observed in the 10-year average total discharge (Fig. 3.3).

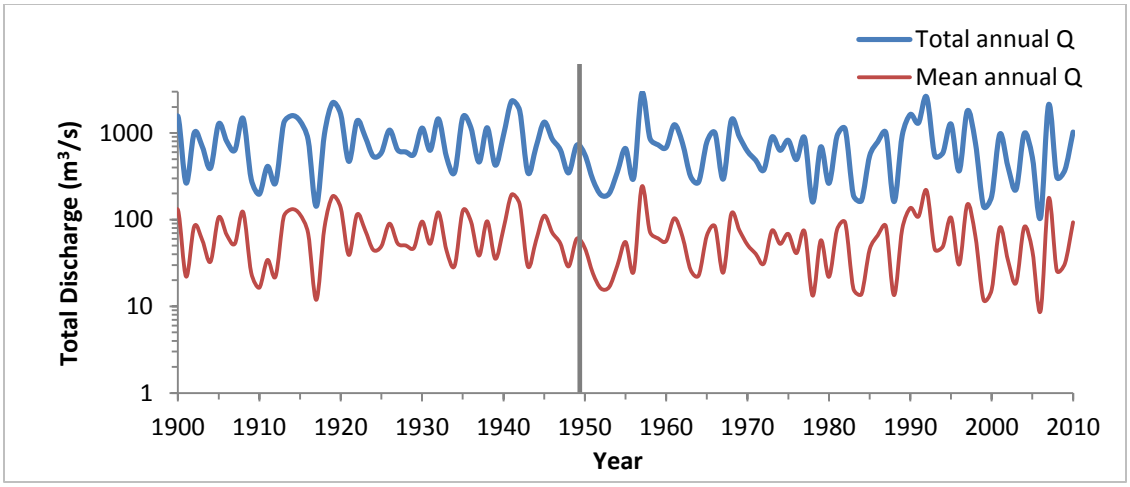

Figure 3.9. Total sum and mean discharge at the Waco gaging station from 1900 through 2010. Notice range of flow values prior to 1949, as compared to subsequent years. The solid vertical line marks the year 1949 when major reservoir construction began on the Brazos River.

3.6.2 Migration

It is hypothesized that positive or negative changes in channel discharge over the decades since major reservoir has affected the rates and magnitudes of lateral channel migration on the Brazos River. At the meter and kilometer scale of this study, the maximum monthly discharge is strongest indicator of the overall rate of migration in a channel segment. The distances of lateral migration and rates of migration were divided by the number of years between sequential migration centerlines, or photograph coverage dates. Table 3.3 displays mean and median rates of migration rates for the 21 time periods measured. The aerial photography data was divided by county boundary based on where and when the photographs were taken. The column for the number of migration points in Table 3.3 is the sample size for each time period. Average rates of lateral migration range from 1.09 to 11.53 m/yr, and median rates of migration range from 0.69 to 12.3 m/yr for the years 1929-2010.

Table 3.3. Time periods and measured values of channel migration. The sample size for each time period is the column of # of migration points (n).

County	Time Period	Channel Length (km)	# of Migration Points (n)	Mean Migration Rate (m/yr)	Median Migration Rate (m/yr)	Standard Deviation
McLennan	1929-1958	34.5	17	6.64	6.14	3.14
	1958-1972	37.1	43	2.05	0.93	2.25
	1972-1982	34.1	35	1.60	1.44	1.25
	1982-1988	35.1	46	2.13	1.61	1.82
	1988-1993	35.9	51	2.58	1.99	2.22
	1993-1995	38.5	46	5.25	3.72	4.26
Falls	1929-1955	77.1	34	7.23	6.4	4.95
	1955-1960	77.3	69	5.18	4.02	4.03
	1960-1968	75.3	70	3.46	2.22	3.67
	1968-1978*	19.0	13	2.82	2.41	1.37
	1978*-1995	26.4	19	1.29	1.23	0.6
	1968-1995	78.42	69	1.09	0.92	0.88
Milam/Robertson**	1929-1941	76.4	29	11.53	10.39	7.12
	1941-1951	54.9	63	3.15	1.45	4.15
	1951-1958	63.6	74	2.47	1.59	2.4
	1958-1965	83.1	89	2.55	1.4	2.67
	1965-1974	55.8	39	3.08	1.85	3.02
	1974-1995	59.8	48	1.55	1.14	1.42
All counties	1995-2004	197.2	229	1.11	0.69	1.01
	2004-2008	185.2	208	2.12	1.51	1.72
	2008-2010	186.4	102	4.6	2.91	4.22

***Migration measurements based on values obtained from topographic maps for the years 1968-1978 and 1978-1995.**

**** Milam & Robertson counties share the Brazos River as an eastern/western border.**

The rates of migration (presented per year) for both pre- and post-dam time periods do not include in the analysis points where meander movement was less than 12 and 4 meters, respectively. This method removed the spatial error of the mapping sources, for both Texas GLO engineering maps and aerial photographs, from the comparison between pre- and post-dam. Values of particular interest in those measured are the pre-dam data from 1929 to 1951 representing rates of migration from 3.15 m/yr +/- 4.5 for the 1941-1951 time period in Milam & Robertson counties to 11.53 m/yr +/- 7.2 for the 1929-1941 time period in Milam & Robertson counties. The rates of

migration for the time period 1929 to 1951 for the river reaches in Falls and McLennan are between these minimum and maximum values in Milam & Robertson counties. The total sample size across the study region for the 1929 to 1951 data is 143, whereas the sample size for the post-dam data is 1250. These data represent channel positions prior to major flow regulation on the Brazos River and show the large variation in rates of migration. Rates of migration were not calculated for meanders moving less than 12 meters in a GLO time period. These values of migration are subsequently higher by an average of 5.7 meters than those of other time periods. Standard deviations are high in some time periods representing great spread among the migration values within those time periods. From this analysis I suggest rates of migration were highest on the Middle Brazos River prior to construction of the major reservoirs upstream.

Rates of lateral channel migration along a 203 km reach of the middle Brazos River (Fig. 3.1) range from 1.09 +/- 0.88 to 11.5 +/- 7.12 m/yr from 1929 to 2010. Taking into account effects of impoundment from several large reservoirs constructed after 1951 (Table 3.1) upstream of the study reach, rates of migration average 1.09 to 5.18 m/yr, with a standard deviation of 2.9 m/yr, since 1955.

Although the migration periods are listed by county, many of the channel lengths overlap into adjacent counties. Also, the migration rate from 1968-1995 is lower than the rates of migration from 1968-1978 and 1978-1995, which represent data from topographic maps. I suggest this discrepancy may be the results of variability in the topographic spatial reference and difficulty in identifying the correct channel boundary on the topographic map. Nevertheless, the data are useful for approximating trends.

A large variation in rates of migration for each county (Fig. 3.9) exists. The ranges observed in the rates of lateral migration are quite large with values ranging from ~ 2 m/yr to 50 m/yr. The range in rates is greatest for early time periods (i.e., 1929-1958) and the 2008-2010 time period for McLennan and Falls Counties. The 2008-2010 maximum includes three meander bends experiencing avulsion (Fig. 3.10).

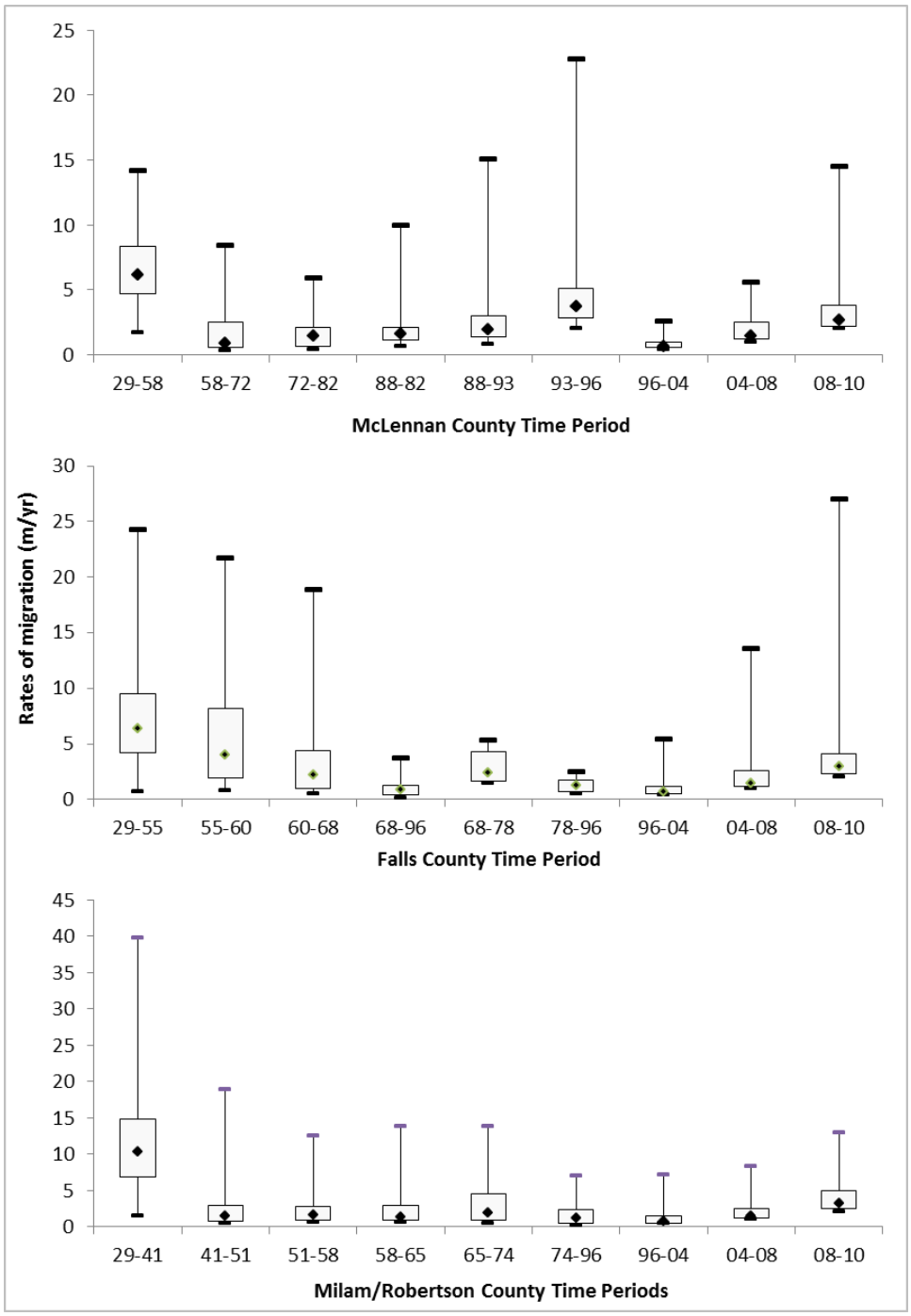

Figure 3.10. Rates of migration for each county.

The values of migration for the individual counties should be compared to the geology presented in Fig. 3.1. The northeast to southwest trend of the bedrock, combined with lithology, may affect the differences in migration occurring among the counties. McLennan and Falls County consist predominantly of clay, conglomerate and mudstone lithologies; whereas Milam/Robertson Counties consists of shales and sandstones. This difference in lithology may explain some of the range in values of migration.

Table 3.4 summarizes the mean, monthly, maximum, total and mean yearly discharge values for each time period, which in turn represents channel migration between sequential digitized channel lines. Monthly discharge values are relatively consistent with values ranging between 28 m^3/s to 100 m^3/s.

Maximum yearly Q represents the maximum discharge experienced by a particular year within the time period (i.e., 1995-2004). A greater range in the values than mean monthly discharge with lows near 283 m^3/s and highs at 1,048 m^3/s is seen in the data. Total discharge for a given time period represents the highest range between any particular flow measures with values ranging from 1,698 m^3/s to greater than 25,470 m^3/s.

Table 3.4. Time periods for discharge values used to characterize surface hydrology for the study reach. Presented are the average monthly, maximum monthly, total sum and average yearly discharges.

County	Time Interval	Mean Monthly Q (m^3/s)	Maximum Monthly Q (m^3/s)	Effective Erosion Q_a	Total Q (m^3/s)	Mean Yearly Q (m^3/s)	Effective Erosion Q_b
McLennan	1929-58	71	1,051	-76	25,684	856	-271
	1958-72	60	434	-693	10,733	716	-411
	1972-82	55	351	-776	7,240	658	-469
	1982-88	47	390	-737	3,964	566	-561
	1988-93	100	807	-320	7,183	1197	70
	1993-95	67	282	-845	2,406	802	-325
Falls	1929-55	67	636	-491	21,631	801	-326
	1955-60	85	1,051	-76	6,127	1021	-106
	1960-68	63	434	-693	6,760	751	-376
	1968-78	58	418	-709	7,654	696	-431
	1978-95	69	807	-320	14,880	827	-300
	1968-95	67	807	-320	22,375	799	-328
Milam/Robertson	1929-41	81	626	-501	12,650	973	-154
	1941-51	75	636	-491	9,905	900	-227
	1951-58	60	1,051	-76	5,750	719	-408
	1958-65	59	434	-693	5,665	708	-419
	1965-74	62	434	-693	7,384	738	-389
	1974-95	67	807	-320	17,704	805	-322
All Counties	1995-04	59	482	-645	7,110	711	-416
	2004-08	67	750	-377	4,041	808	-319
	2008-10	50	239	-888	1,710	570	-557

a: This column represents the effective erosion discharge from the maximum monthly discharge.
b: This column represents the effective erosion discharge from the mean yearly discharge.

The average yearly discharges for a particular time period are presented (Table 3.3). The range for these values is relatively small, considering the difference in the number of years within each time period. Lows range in the low 566 m^3/s with the high in the low 1,132 m^3/s. Thus, the average yearly discharge maintains a relatively constant value, despite differences in the extreme high and low discharges among time periods.

Values for discharge are often correlated with an average rate of migration with discharge as one factor in explaining rates of migration (Winterbottom, 2000; Hooke, 2008). To better understand the effect of different flow values on the range of rates of migration within a particular time period, I utilized boxplots similar to other fluvial studies (O'Connor, 2003; Richardson, 2010). O'Conner (2003) compared rates of channel migration and channel widths for three separate rivers in the Pacific Northwest whereas Richardson (2010) presents a similar approach using width/swath (active channel divided by floodplain distance) and active channel values from 1949-2007 for a New Zealand river. Thus, boxplots are an efficient way to present the range of values of migration for each time period. Figure 3.11 shows the range of rates of migration in relation to increasing average monthly discharge and average yearly discharge.

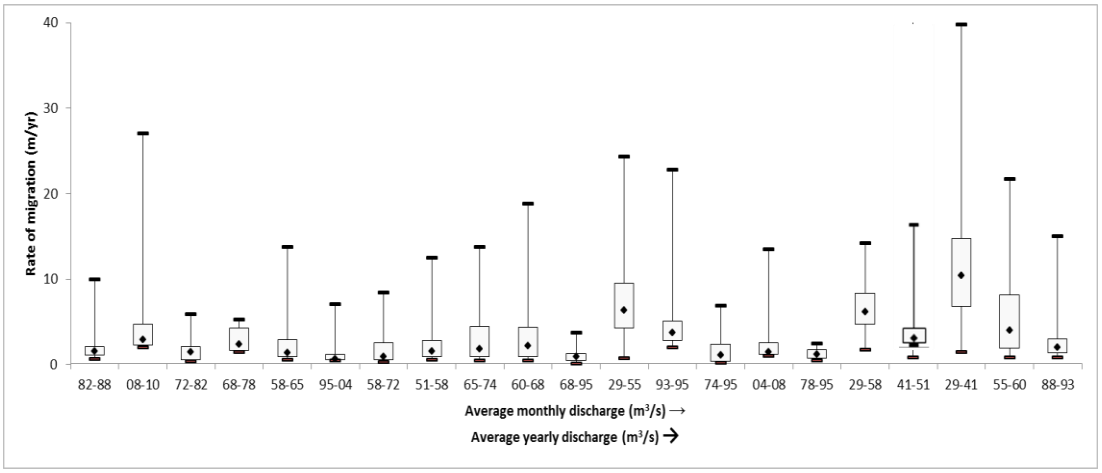

Figure 3.11. Boxplot of rates of migration as average monthly and average yearly discharge increase at the Waco gauging station. Intervals along x-axis represent year time periods, i.e., 1982-1988, etc. The time periods are organized from left to right in increasing order according to the average monthly discharge and average yearly discharge for a particular time period.

Rates of migration in relation to increasing total discharge for the time periods are presented in Fig. 3.12. The rates show moderately large ranges in migration (<5 - >20 m/yr) with lower discharge and very large ranges in rates lateral migration (<5 - >45 m/yr) near the highest total discharges within a time period. The time periods with the largest range in values of migration, which are generally those in the pre-dam period, also have nearly the highest total time-period discharge with values ranging from ~9,905 to ~25,470 total m^3/s. In general, as the number of years increases for a given time period, the range of rates of migration also increases. Thus, the greater total discharge and longer time provide increase the probability the river channel may avulse or erode its banks rapidly.

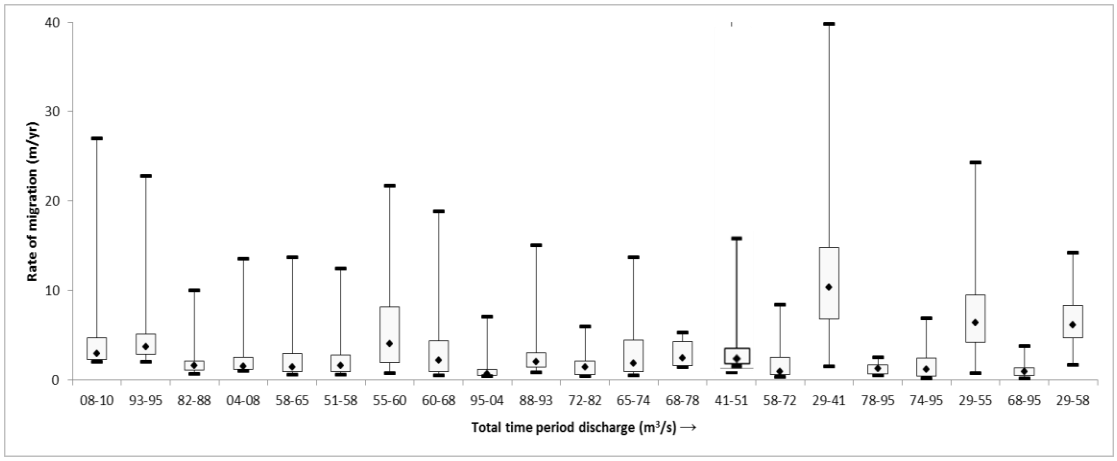

Figure 3.12. Boxplot of rates of migration as the total discharge for a time period increases. Intervals along x-axis represent year time periods, i.e., 2008-2010.

I related the average rates of lateral channel migration to the four discharge variables from Table 3.3, and these are shown in Fig. 3.13 (A-D). Poor correlations of R^2 = 0.1392 and R^2 = 0.0189, exist for Fig. 3.13A and 3.13B, of the influence of average

monthly discharge and average yearly discharge, respectively. Some generalized trends, appropriate to the scale at which the variables were measured, are apparent in Fig. 3.13C and 3.13D. The relationship between rates of migration and maximum monthly discharge (Fig. 3.13C) is correlated at $R^2 = 0.5494$, whereas the rate of migration versus total discharge within a time period is correlated at $R^2 = 0.4397$. These figures omit values of migration obtained from the 1929 datasets. From these values I suggest that the maximum monthly and total discharge have the greatest effect on rates of lateral migration.

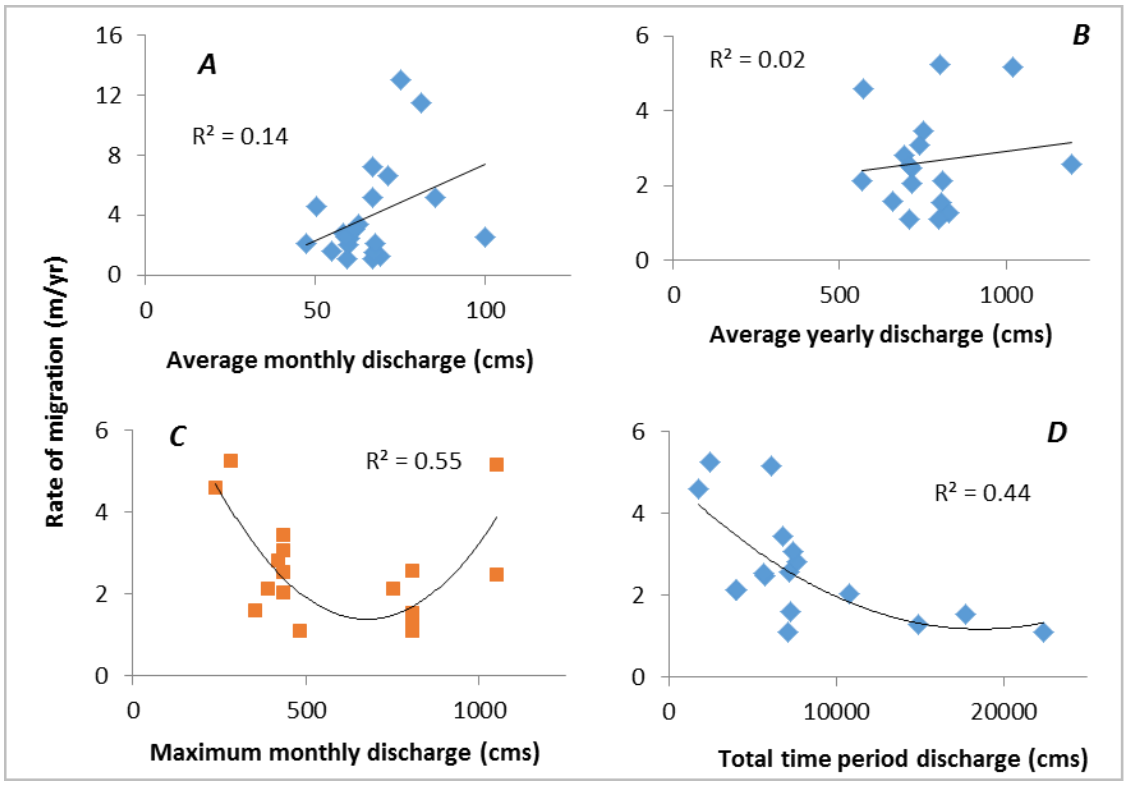

Figure 3.13. Relationships between rates of lateral channel migration and a) average monthly discharge; b) average yearly discharge; c) maximum monthly discharge; and d) total time period discharge.

Figure 3.13b relates the average monthly discharge to average rate of migration. The data cluster towards the middle of the graph with most values falling below 4 m/yr and between 51 and 71 m^3/s.

Figure 3.12b displays average yearly discharge, within a time period, to average rate of migration. More spread is apparent among the data points, but they continue to cluster within the same ranges as the above graph. I suggest that the average yearly discharge has a greater effect on rates of migration versus the variation in average monthly flows.

Figures 3.13c and 3.13d present average rates of migration as a function of maximum monthly discharge and total time period discharge, respectively. In Fig. 3.13c, the values cluster around ~340 - 453 m^3/s and 736-821 m^3/s. As seen in Fig. 3.13d, rates of migration follow a first-order polynomial trend with decreasing rates of migration rate as the total discharge within a time period decreases. The trend has a poor correlation with an $R^2 = 0.4397$. But this explains the variations of channel migration values better than other discharge characteristics.

The maximum monthly discharge and total surface discharge within the channel have the strongest correlation ($R^2 = 0.55$ and $R^2 = 0.4397$, respectively), following a second-order polynomial function. I determined the highest migration rate occurs when the total discharge was lowest; suggesting discharge is one of several factors that need to be considered in determining migration rates. Other factors shown to influence migration along the Brazos River include the presence or absence of established vegetation along the banks and the influence of groundwater, which causes saturation and failure at the

river-aquifer interface and results in bank failure. The nonlinear relationship between high discharge and high rates of migration is supported in the fluvial geomorphic literature. Surface discharge correlates to channel width and slope, which in turn contribute to the radius of curvature. Bankfull discharge is the main contributor to work on channel banks and bottom, with discharges below overbank flooding stage. This is evident in Fig. 3.13a with the highest rates of migration at yearly average discharges of 78 and 80 m^3/s. Time periods with the highest yearly average discharges received overbank flooding which erodes less of the channel bank than bankfull flows.

3.6.3 Longitudinal Profile and Channel Classification

The longitudinal profile of the Brazos River from the southern edge of the City of Waco to the northern Brazos County line is show in Fig. 3.14. The profile is separated into ten slope classes. In addition to joining the DEM values to the centerline, as described previously, the data were not smoothed so as to capture the geometry of the large meanders occurring along the study reach. Examination of the profile shows nine substantial breaks in the profile. Evident in the graph are areas of high sinuosity (i.e., slope classes 6 and 7). The segments of slope classes, the respective channel and valley gradients, and sinuosity values are presented in Table 3.5.

Examination of the data suggests definitive sections occur within the study reach that have distinct gradients. For example, section 2 in Fig. 3.14 has a distinct change in elevation at 43.4 km upstream and at 72.0 km downstream. Because channel slope influences stream power (Bagnold, 1980), changes in slope values along the study reach may translate into changes in rates of lateral channel migration.

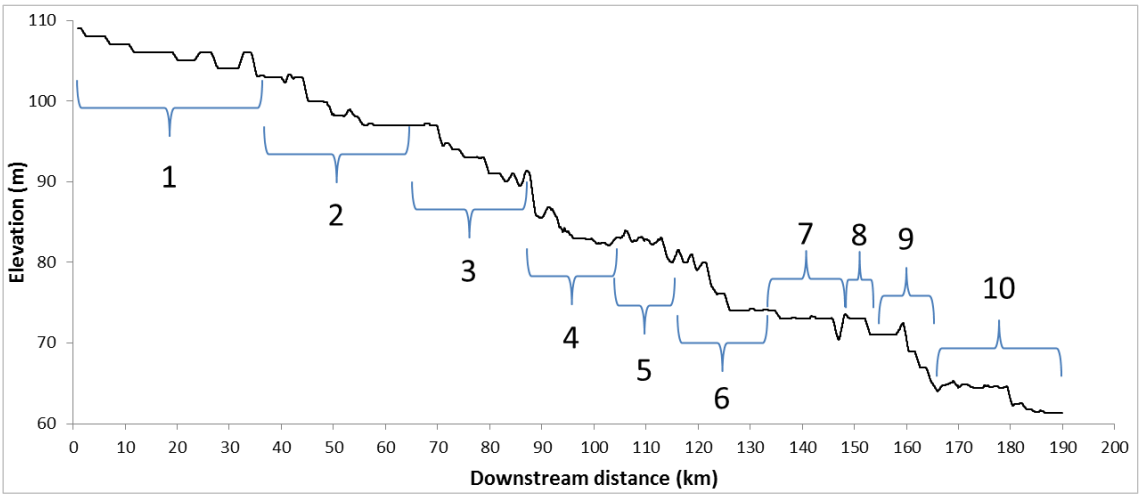

Figure 3.14. Longitudinal profile for the study reach with different slope classes delineated. The distance downstream orginates from the State Highway 77 bridge in southeastern Waco, TX. The line is the moving average of the profile generated using a 10-meter dataset. Vertical exaggeration is 1000.

A trend line, using a moving average with a period of 100, was used to smooth the overall longitudinal trend. The individual classes presented in Fig. 3.14 and Table 3.5 were delineated using the natural breaks in the original raw data from the DEM. Refer to Fig. 3.8 for the location of the individual channel units.

Table 3.5. Channel gradient, valley gradient, and sinuosity for the ten slope classes.

Class	Length (km)	Channel Gradient (m/m)	Valley Gradient (m/m)	Sinuosity
1-A	43.4	0.000138	0.000254	1.839
2-B	28.6	0.000210	0.000455	2.166
3-C	27.0	0.000407	0.000567	1.392
4-D	17.3	-0.000173	-0.000286	1.649
5-E	11.7	0.000684	0.001194	1.746
6-F	23.5	0.000171	0.000313	1.833
7-G	12.0	0.000250	0.000294	1.176
8-H	6.84	0.000439	0.000714	1.629
9-I	14.1	0.000711	0.001124	1.581
10-J	8.57	0.000162	0.000294	1.821

All migration totals, those post reservoir construction and equal to or larger than the four meter error allowance, are stratified by the different slope/gradient classes (Fig. 3.14 and 3.15). The graph does not include measurements collected from topographic maps, i.e., the 1968-1978 or 1978-1995 data from Falls County because of the low number of data points that exist and the overlapping coverage associated with the 1968-1995 data for Falls County.

The values for migration were stratified among the slope classes (Fig. 3.15). Examination of the trend suggests that the rates of migration have a greater range as channel length increases, the slope decreases and the sinuosity increases, though irregularities occur. For example, as sinuosity increases, within a given slope class, the difference between channel and valley gradient increases as well. Irregularities may be explained by additional factors including influence of groundwater and vegetation along the channel banks.

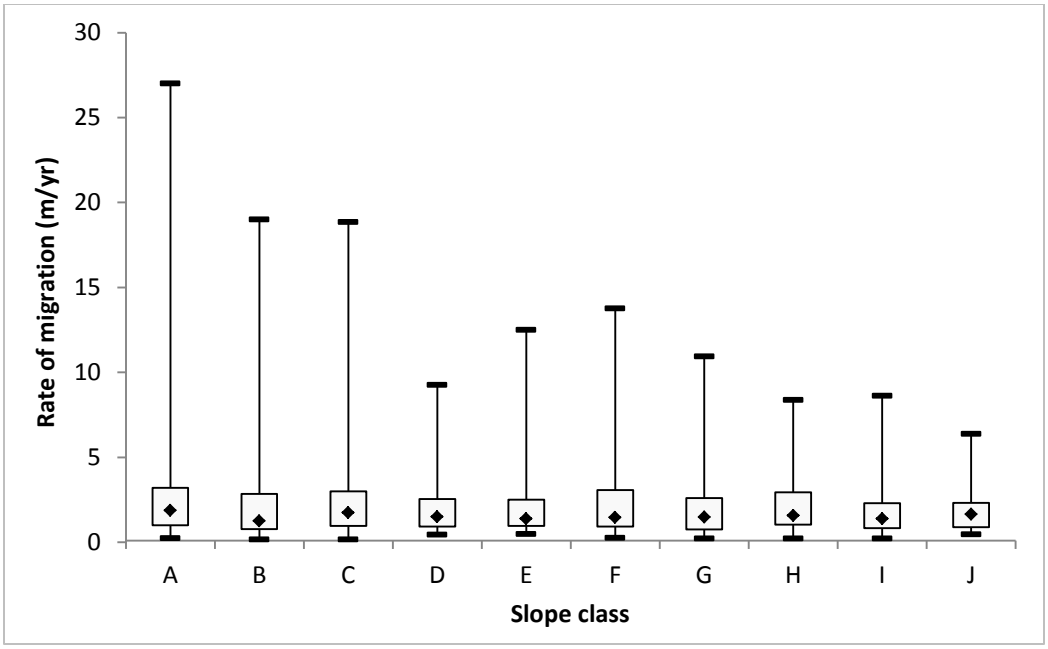

Figure 3.15. Boxplot for total values of migration for each class of slope.

Figure 3.16 displays total rates of migration according to increasing sinuosity. Again, as sinuosity increase, the range of values for lateral rates of migration increases as well. The most sinuous portion of the main channel is located in McLennan County at the upper end of the study reach. This reach also contains the highest rates of migration from 2 to 28 meters.

The range of values for rates of migration is shown in Fig. 3.17 in order of increasing channel gradient. The channel gradient experiences a range of rates of migration from 2-7 m for the 10-J slope class to 2-28m for the 1-A slope class. The largest rate of migration generally occurs around the profile classes having the largest slope and sinuosity, for example slope class B and C (Fig. 3.17).

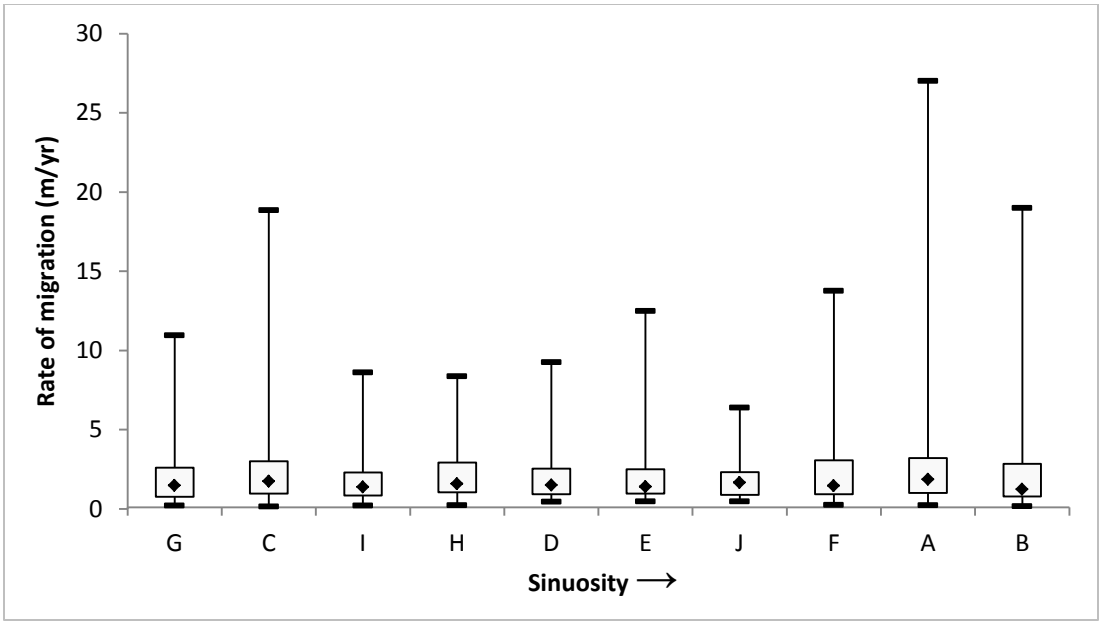

Figure 3.16. Boxplot for migration rates with increasing channel sinuosity. The letters along the x-axis correspond to the slope classes from Table 3.4. Letters were assigned to the different slope classes to more readily differentiate the individual classes.

Examination of the migration values between the Texas GLO images and earliest (1941, 1955 and 1958) aerial photographs shows the highest rates of migration (i.e., ~ 10 meters or greater). High rates of migration for the earliest time periods are expected as major channel impoundments had not been fully constructed yet, allowing greater discharges. These values, however, do not differentiate between lateral channel migrations that occur as the meander bend erodes along the outer bank and any major channel avulsions or cutoffs that may have occurred.

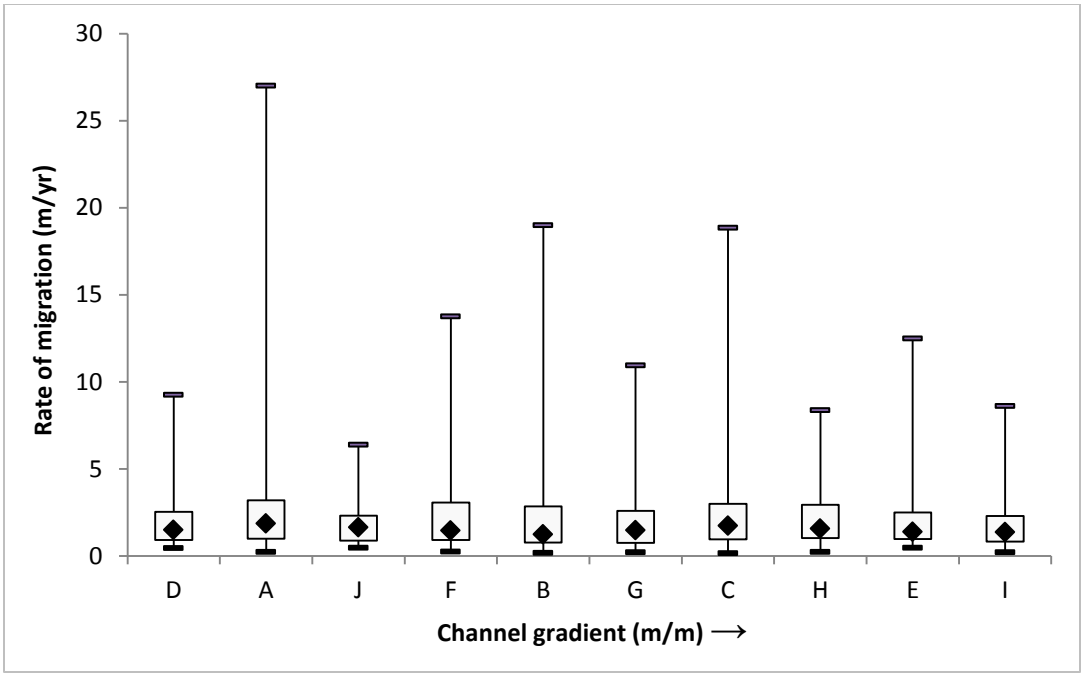

Figure 3.17. Boxplot for migration rates with increasing channel gradient.

Major avulsions or cutoffs may skew the rates of migration towards abnormally high values within the pre-reservoir datasets. The pre-reservoir data consists of engineer drawings of the channel position which lacks the geomorphic detail to determine an avulsion or cutoff. The larger meander bends commonly consist of a long, low point bar with a large sand bar exposed along the inner channel bend. Many of these features are susceptible to avulsions with some supporting isolated stands of vegetation.

3.6.4 Sediment Budget

The values for sediment erosion and deposition for the freely migrating meanders are presented in Table 3.6. The overall net sediment change is a deposition of 5,580,161 m^3. These values are from the thirty-three freely migrating meanders along the study reach.

Appendix A displays the location of the meanders along the entire study reach, along with the location relative to the watershed uplands.

Table 3.6. Sediment budget for selected meanders through study time period. The time period column is arranged that sediment balance for the erosion portion is listed first, with the time period for deposition listed second.

Time Period	County	Total Erosion (m^3)	Total Deposit (m^3)	Sediment Balance
1972-1952/1952-1972	McLennan	13,932,007	19,237,438	-5,305,431
1982-1972/1972-1982	McLennan	4,630,388	16,783,450	-12,153,062
1988-1982/1982-1988	McLennan	3,953,306	6,115,613	-2,162,307
1993-1988/1988-1993	McLennan	10,128,158	2,730,314	7,397,844
1995-1993/1993-1995	McLennan	3,255,091	3,322,823	-67,732
2004-1995/1995-2004	McLennan	382,851	2,551,067	-2,168,216
2008-2004/2004-2008	McLennan	1,869,758	522,258	1,347,500
1960-1955/1955-1960	Falls	24,201,666	4,965,994	19,235,672
1968-1960/1960-1968	Falls	9,755,788	20,095,351	-10,339,563
1995-1968/1968-1995	Falls	9,953,652	15,493,720	-5,540,068
2004-1995/1995/2004	Falls	1,976,270	4,838,540	-2,862,270
2008-2004/2004-2008	Falls	3,056,565	1,674,800	1,381,765
1958-1951/1951-1958	Milam-Rob.	38,355,314	4,471,661	33,883,653
1965-1958/1958-1965	Milam-Rob.	12,530,507	13,682,469	-1,151,962
1974-1965/1965-1974	Milam-Rob.	7,437,067	30,803,595	-23,366,528
1995-1974/1974-1995	Milam-Rob.	14,325,420	7,830,521	6,494,899
2004-1995/1995-2004	Milam-Rob.	4,768,757	6,063,567	-1,294,810
2008-2004/2004-2008	Milam-Rob.	5,442,182	3,191,405	2,250,777
			Total Net Sediment	**5,580,161**

3.6.5 Pre- and Post-Reservoir Changes

The second migration method (Leopold, 1973; Gurnell, 1994) was used to examine rates of migration for pre- and post-reservoir construction periods (Figures 3.18 and 3.19). Analysis of segmented photographs show that impoundment of the upstream reach of the Brazos River has decreased channel migration (Fig. 3.17) by ~ 200-300 meters and the width of the channel by 100-200 meters in some localities (Fig. 3.18). The amount of

migration is based on the period 1929-1950s and the period 1950s-2004, whereas channel width is for the period 1950s and the year 2004.

The largest changes in amount of migration and width of the channel are in the upstream reaches where the channel is most sinuous. The trend line for pre-reservoir migration shows values decreasing in the downstream direction, but still overall higher than those of the post-reservoir period. After completion of the reservoir, the values of migration-distance values range from 50 to ~1,500 meters, whereas channel width ranges from ~30 to 1,200 meters. After several decades of impoundment, migration distances reach 500 meters maximum, and channel width is generally less than 250 meters. These values illustrate the impact that reservoirs have had on the Brazos River.

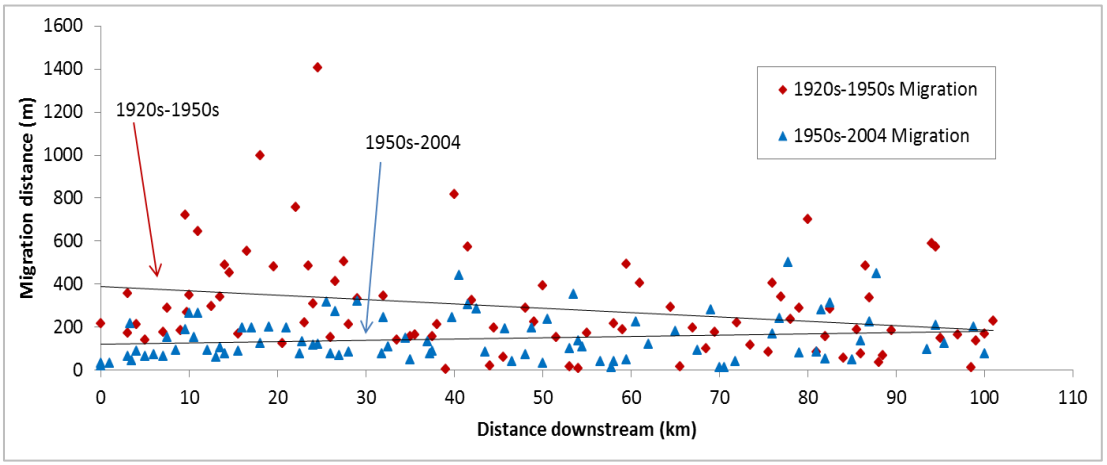

Figure 3.18. Migration amounts for pre (1929-1950s) and post (1950s-2004) reservoir time periods. A marked decrease in migration is observed between the pre and post reservoir time periods. Also, the trend is to decrease in migration distance moving downstream. The linear trend line shows an overall decrease in channel migration for the post reservoir with the values relatively constant. The beginning location is at State Highway 77 in southeastern Waco, Texas.

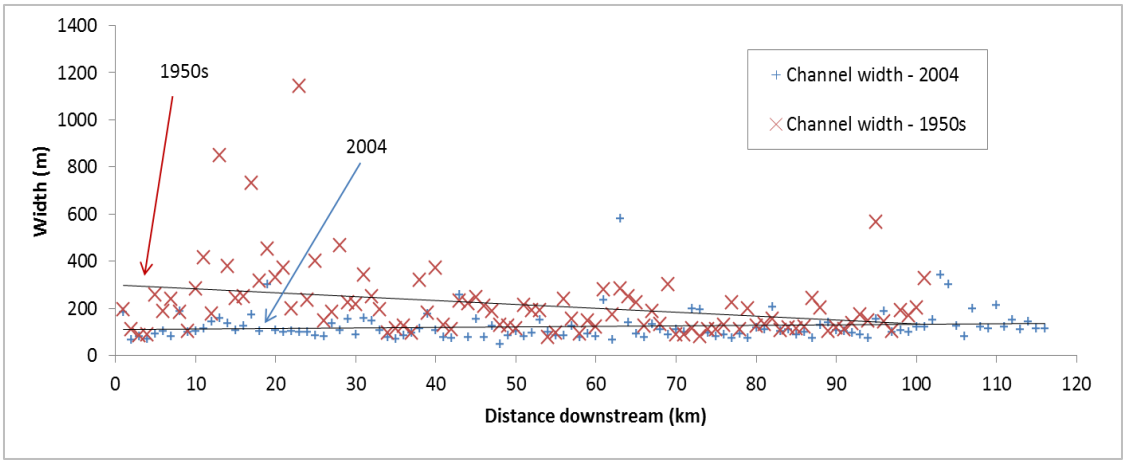

Figure 3.19. Channel width for pre (1929-1950s) and post (1950s-2004) reservoir time periods. A marked decrease in channel width is observed between the pre and post reservoir time periods.

The trend line for the 1950s shows a steady decrease in channel width moving downstream but the overall values are higher than those of the 2004 channel widths, which show a slight increase in channel width moving downstream. The distance downstream is measured from the State Highway 77 Bridge in southeastern Waco, Texas.

3.7 Discussion and Interpretation

The discussion section focuses on 1) channel migration; 2) bank erosion; 3) gaining and losing segments; 4) floodplain position; 5) vegetation. Each section presents the results and a discussion of the impact of the study reach of the Brazos River.

Gillespie and Giardino (1997) showed that the relatively homogenous material of the Brazos floodplain allows one to assume a constant effect of material type on the bank stability. If this variable was neglected, a direct correlation between lateral rate of migration and surface discharge at the scales explored in this study would not exist.

3.7.1 Meander and Bend Migration

Gillespie and Giardino (1997) also looked at migration characteristics along a longer reach and found poor correlations with independent variables affecting rates of migration. Amounts of channel migration, and subsequent rates, decreased markedly after construction of the last major reservoir (Fig. 3.20).

Rates of migration for the study reach are representative of those observed in the middle section of other alluvial rivers (Lawler, 1992). The middle section, termed the sediment transfer zone (Schumm, 1977), has the combination of slope, floodplain material and morphology, and discharge to provide higher stream power relative to upstream or downstream reaches. The concept of high stream power in the middle section helps to explain why rates of migration along this section are greater than those in the deltaic portion of the river (Phillips, 2006).

The clustering of rates of migration (Fig. 3.13c) detailing maximum monthly discharge may represent the "average" flow conditions in those reaches. During months of low discharge the high end values may represent extreme hydrologic events where much geomorphic work takes place.

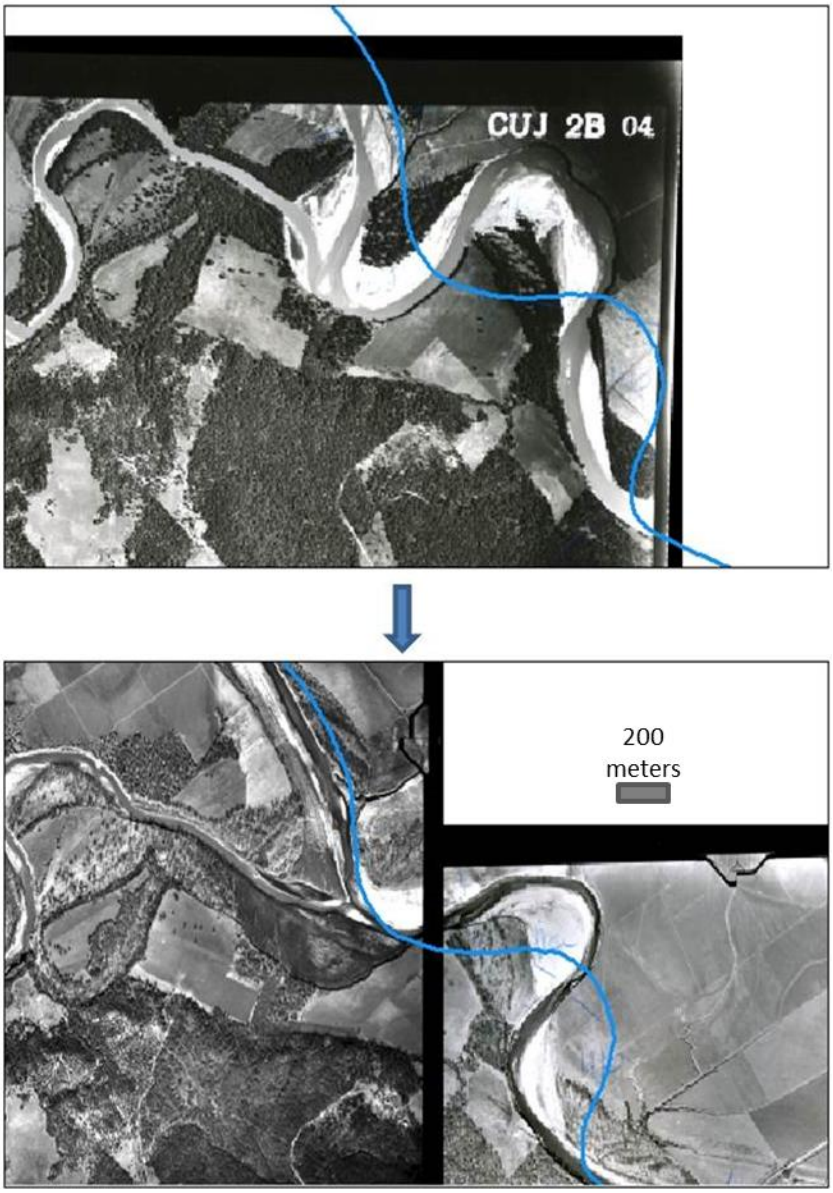

Figure 3.20. Tributary effect on lateral migration with large change in channel position (>20 m) during a ten year period. Top photo is dated 1941 and bottom is 1951. The blue line in both photographs represents the 2004 channel position.

Several tributaries enter the study reach in this area may impact the style and rate of channel migration (Asahi, 2003). These tributaries transport a significant volume of water and sediment to the main Brazos channel and have an impact on the style and

nature of migration in the Brazos Valley. For example (Fig. 3.20), several channel locations in Milam and Robertson counties have experienced significant migration (> 10 meters) during the 1941-1951 time period. Though 1941 had a high discharge (Fig. 3.9), the ten year period does not have an abnormally high rate for the number of years within the time period (Table 3.3). In addition, the tributary seen in Fig. 3.20 may have contributed to the avulsion of the main channel that can be seen in the confluence of the lower photograph.

A comparison of the rates of migration from the Brazos River presented in this study to those of regional areas around the world is presented in Fig. 3.21. The rates of migration and watershed area for the world data points are taken from data compiled by Knighton (1999). The three black X's represent the maximum, mean and minimum rates of migration for the central reach observed in this study. As noted on the graph, a transition appears at watersheds of approximately 90,000 km^2. The Brazos River data points are near this transition, supporting the hypothesis of the unique character of migration along the Brazos River.

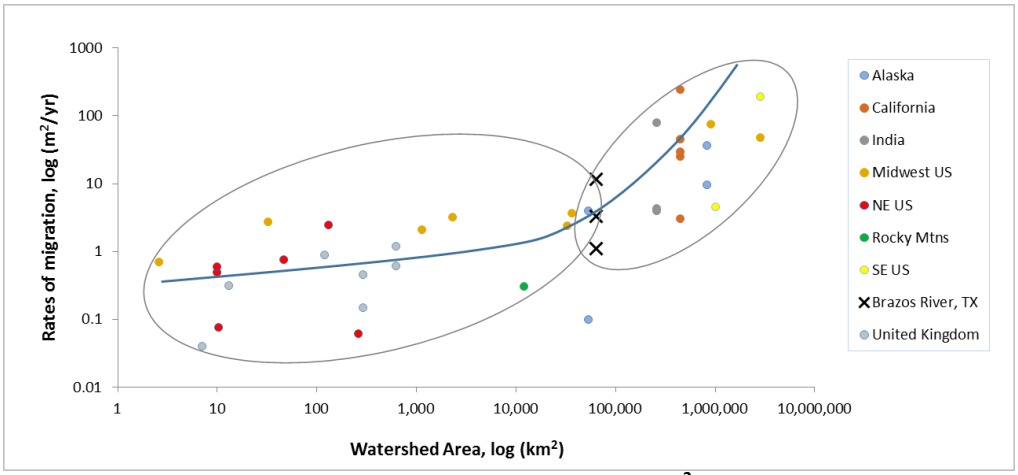

Figure 3.21 Rates of migration compared to total watershed area (km^2) for regions around the world.

The blue line in Fig. 3.21 represents the slope of the transition in rates of migration for drainages of a certain area.

3.7.2 Bank Erosion

Figure 3.22 displays various types of outer cut-bank erosion encountered along the main channel. In the upper portion of a large meander bend, bank morphology is a sloped or slumped bank with vegetative cover (Fig. 3.24). Moving downstream along the meander bend the outer banks transition to a shear or vertical channel wall where the bank toe is more readily eroded away.

Changes in channel geometry along meander bends was observed in field surveys (Fig. 3.22). As the channel migrates laterally across the floodplain, the upper portion of the bank collapses and is deposited along the base of the bend wall. The eroded bank material is then available for further transport downstream with the majority of the material (89-97%) as suspended or dissolved load (Epps, 1973).

Figure 3.23 displays effects of forest clearing on the geometry of banks with a shear bank wall and slump toe. The slump toe is unstable and readily eroded during higher flows. This locality is along the inner bank of a meander bend. As one can see, a marked lack of tree roots results in poor bank stability.

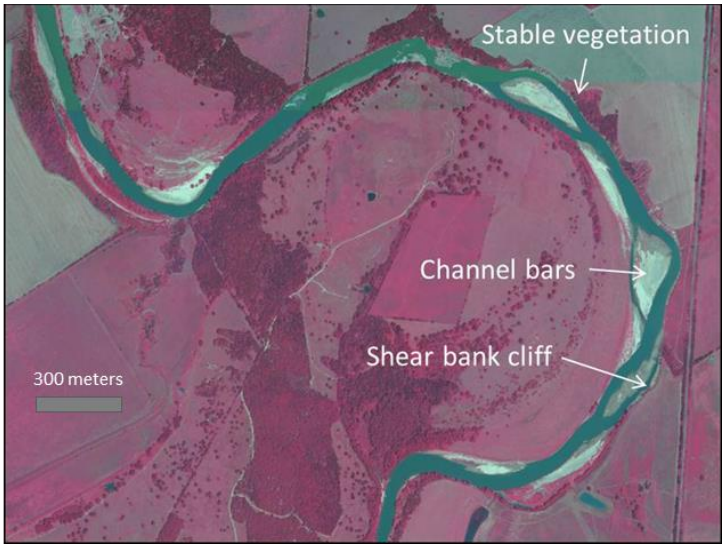

Figure 3.22. Typical large meander bend displaying stable outer banks, with vegetation, in upstream and relatively unstable outer downstream outer banks. Meander bend is migrating away from floodplain valley wall. (Aerial photograph is 2004 NAIP image).

Rates of bank erosion are affected by a variety of other factors. After bankfull discharges begin to recede, the banks are saturated and water begins flows towards the river channel. The pressure change in the channel walls causes slumping and piling of bank material (Fig. 3.24) and is made available for transport during the next high flow (Leopold, 1994).

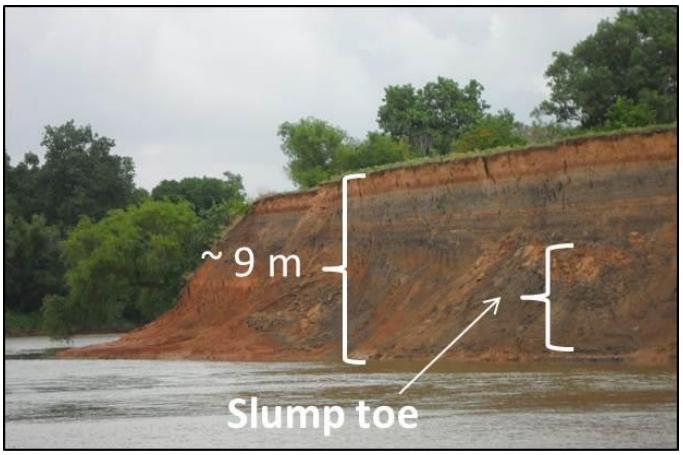

Figure 3.23. Typical outer bank morphology along meanders, including high cliff wall with slump toe at base. Notice high black soil content mixed into the slump toe. Height is approximately 9 meters. Location is central Falls County. Photograph taken by the author on June 30, 2010, at coordinates UTM Zone 14 699734 E & 3453705 N.

Figure 3.24. Inner bank with slump toe. The vegetation is not extensive along the bank and the area has experienced deforestation since the 1995 time frame. Photography taken by the author on June 30, 2010 at coordinates UTM Zone 14 699413 E & 3453984 N.

The longitudinal profile presented earlier (Fig. 3.14) displays the highly sinuous character and large meander bends of the Brazos River. Present in the profile is back-water effects as elevations fluctuate within relatively short distances. The large changes in elevation within the short distance may influence the nature of bank erosion along the

length of a particular meander bend with a lower stream energy along meanders with a radius to width ratio greater than three (Knighton, 1998).

3.7.3 Bedrock Geology and Gaining/Losing Segments

Turco and others (2007) present mapped data for losing and gaining channel sections of the Brazos River based on analysis of hydrograph separation using point data generated along specific sections of the main channel. The mapped reaches of losing or gaining sections are presented in Fig. 3.25.

By comparing the county rates of migration presented in Fig. 3.10 with those reaches experience losing or gaining one can map the effect of surface-groundwater connectivity with rates of lateral migration. Examination of this data shows that stable or losing reaches have greater rates of channel migration, especially southern McLennan County and northern Falls County. Fig. 3.26 compares the rates of migration and radius of curvature for the four major aquifer units underlying the central Brazos River.

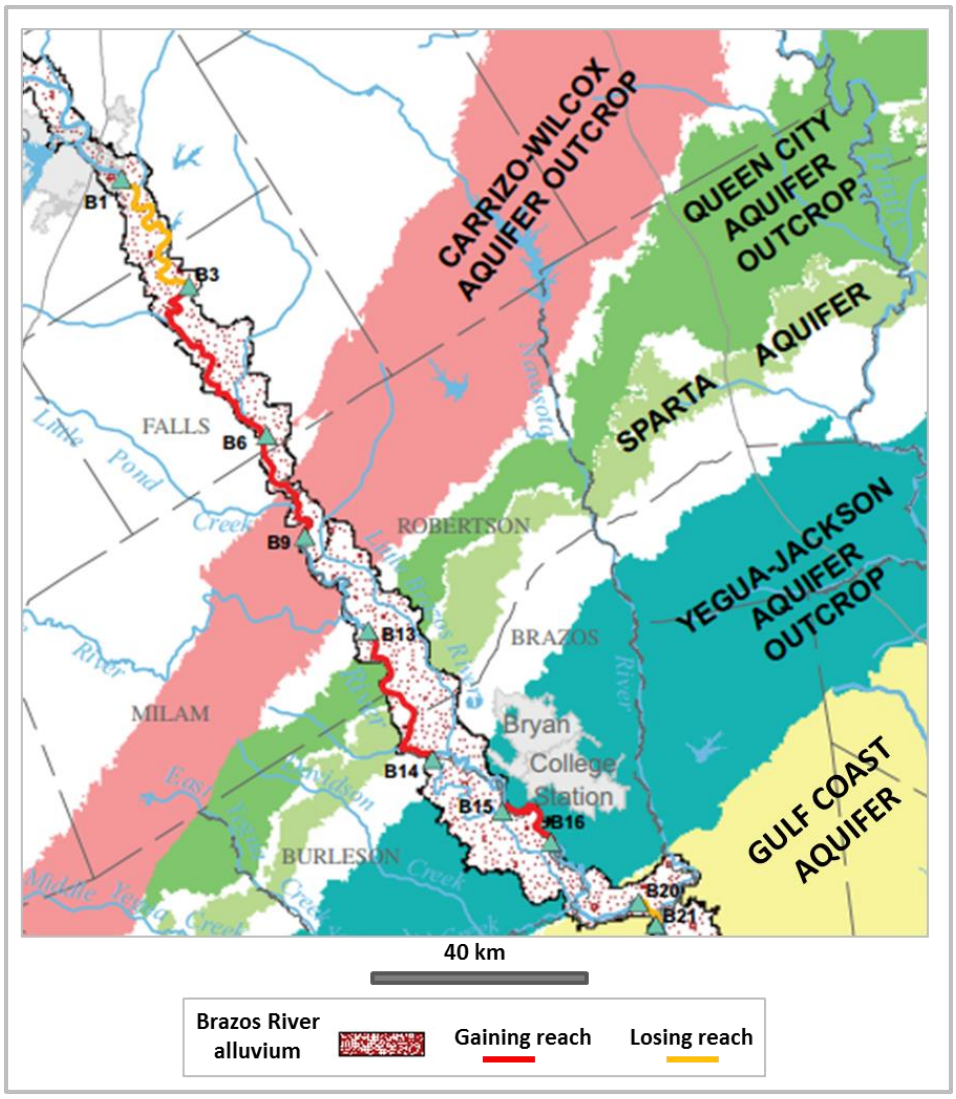

Figure 3.25. Gaining and losing streams along Middle Brazos River (modified after Turco, 2007). The blue box outlines the present study reach.

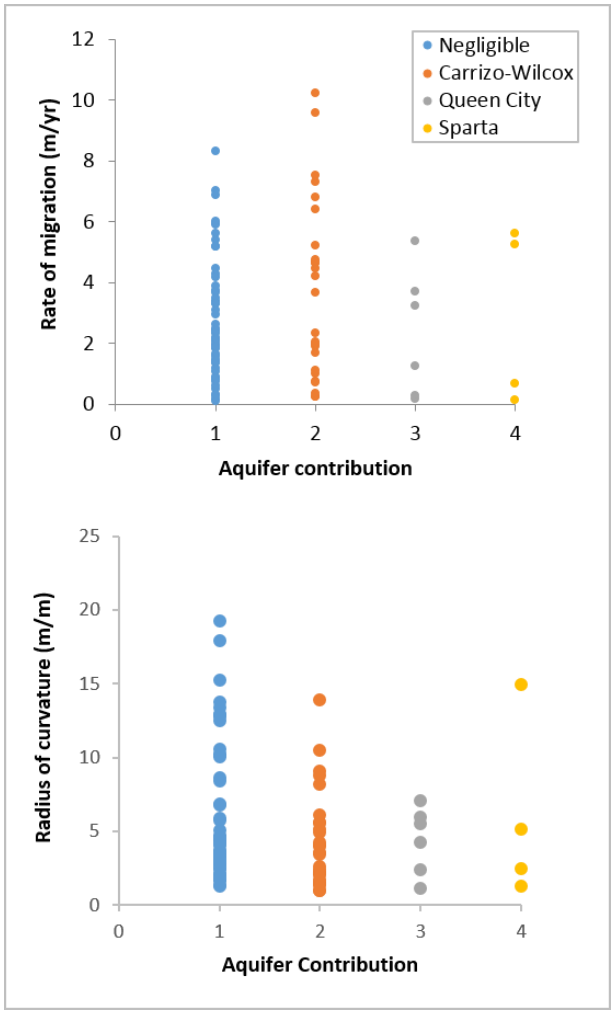

Figure 3.26. Comparison of rates of migration and radius of curvature to the major aquifers underlying the watershed of the Brazos River.

Fig. 3.27 categorizes the rates of migration using the second measurement method (Fig. 3.6) by the five major geologic groups underlying the watershed of the Brazos River. The Gulfian-age Navarro and Taylor groups comprise categories 1 and 2, respectively. Categories 3, 4 and 5 are the Paleocene-age Midway, Eocene-age Wilcox and Eocene-age Clariborne groups, respectively. The overall geology of the region is interbedded siltstones, shales and sandstones with occasional limestone units

interspersed. The geologic formations strike in a northeast-southwest direction while dipping towards the Gulf of Mexico extensional zone. Similar to the graph of aquifer contributions, Fig. 26, no distinct trends emerge between both rates of migration or radius of curvature and the underlying bedrock geology. Localized outcrops in the river channel exert more control on the rate and style of meander migration across the Holocene-age floodplain rather than the overall formation across the drainage basin.

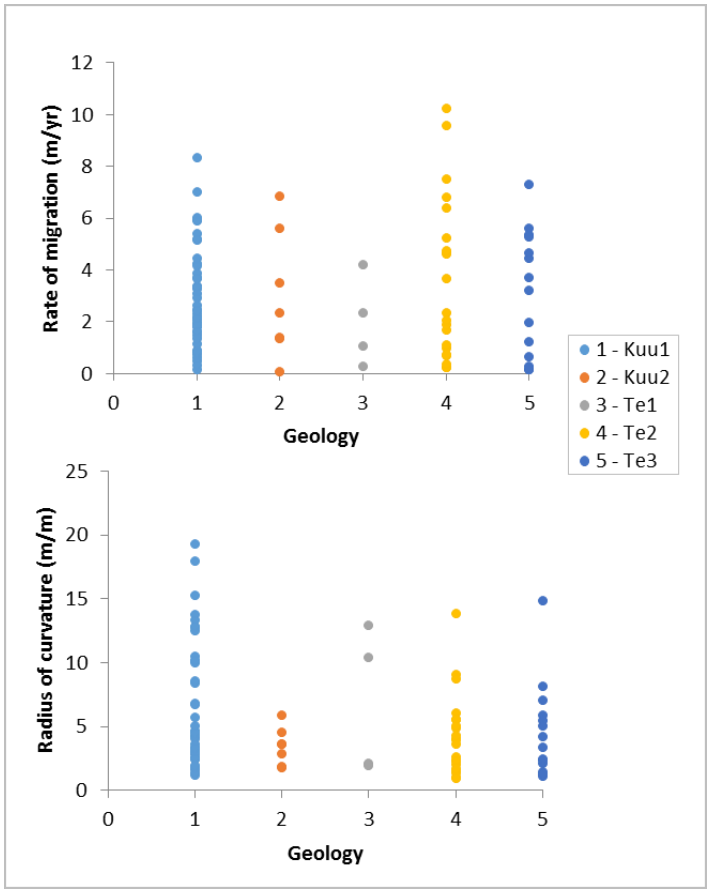

Figure 3.27. Rates of migration and radius of curvature for the five major geologic zones along the central reach of the Brazos River. The various geology types are: 1) Gulfian-age Navarro Group, 2) Gulfian-age Taylor Group, with both groups consisting of interbedded and discontinuous shales and limestones with localized sandstones 3) Paleocene-age Midway Group 4) Eocene-age Wilcox Group and 5) Eocene-age Clariborne Group. The Midway, Wilcox and Clariborne groups consist of interbedded shales, siltstones and sandstones.

Rates of migration are generally highest in losing or stable reaches, whereas reaches experiencing gains are relatively stable. Turco (2007) state small amounts of water are contributed from geologic formations along the channel length between the city of Waco and the norther Falls County line. Conversely, two sections in Falls and the Milam/Robertson county reach receive large contributions to the base flow from the underlying geologic formations. The rate of migration increases as water flows to subsurface areas. The lateral migration of the main channel may occur as water flowing out of the channel bank dislodges sediment and results in bank slumping (Fig. 3.23 and 3.24).

3.7.4 Floodplain Position

The position of the main channel within the floodplain appears to have an effect on the style and magnitude of lateral channel migration. Here I define the floodplain as the relatively level surface with a slope of less than 1.5 degrees. For much of its length through the study area, the main channel flows close to the major watershed terrace, with several large meander loops extending across the middle of the floodplain (Fig. 3.28). Analysis of the proximity of the channel to upland valley walls and the direction of migration I suggest the main channel is attempting to migrate back to the eastern portion of the floodplain (Fig. 3.24).

Nicoll (2010) presents data on confined meanders along the Canadian prairies in which small differences are noted among channel width and bend curvature. Similar to the data on confined channels, I found little correlation between discharge and rates of migration for the Brazos River, with a wide range within the rates of migration, similar

for other rates of freely meandering rivers (Nanson and Hickin, 1986; Williams, 1986). The total volume of water and the maximum monthly discharge for a given time period best explain the variation in channel migration.

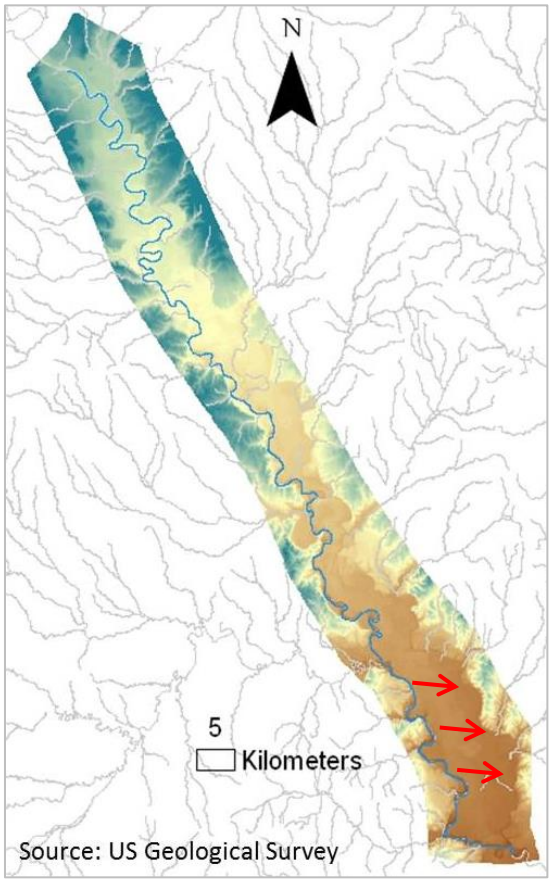

Figure 3.28. Hillshade of Brazos River alluvial valley. The main channel flows along the western valley wall for much of its length through the study reach. Red arrows represent areas of relatively large bank erosion and direction of migration, towards east. The dark blue areas represent higher elevation areas with exposures of Tertiary-age rocks, whereas the light and dark brown color is the active floodplain of the Brazos River.

Insights may be gained by comparing the position of the main channel relative to the topographic boundaries (terraces and watershed uplands) of the floodplain with the rates of migration and radius of curvature for the meander bends measured using the

secondary migration method (Fig. 3.29). The rate of migration is greater for meanders adjacent to the terrace/uplands and lower for meanders migrating into those terraces and uplands. Therefore, the author surmises that as the meander curves back across the downstream axis the energy and material that would go to building point bars and eroding outer banks on the shoreline adjacent to the terrace/upland is redirected towards the opposite bank and increases the rate of migration toward the center of the active floodplain. The channel segments in the central portion of the floodplain, of which there are few, have a more even distribution of erosive and depositional energy and material which works to keep the rates of migration nearer to the overall average of the system.

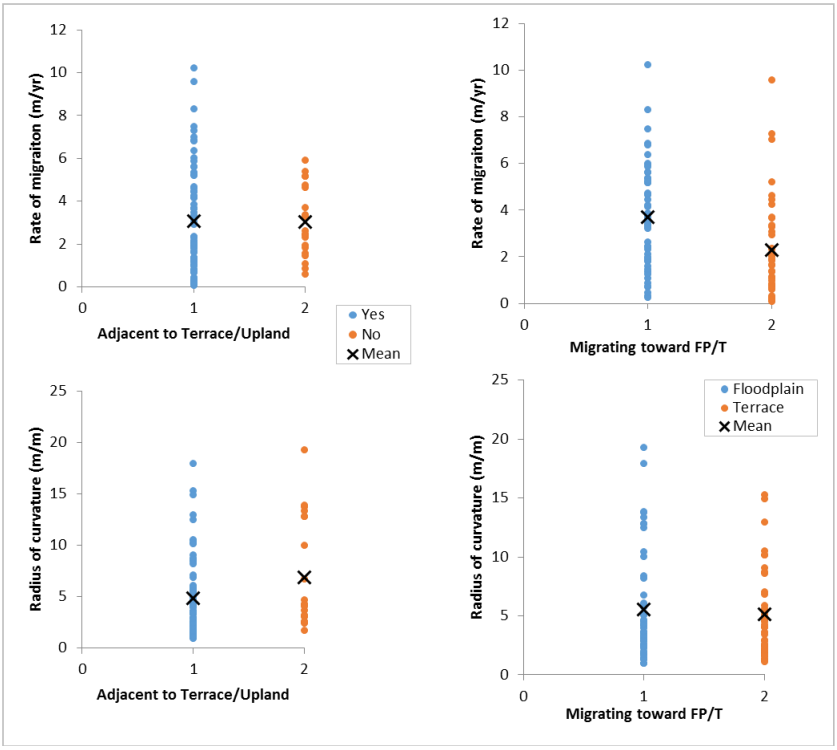

Figure 3.29. Rates of migration and radius of curvature between meander bends adjacent to the terrace and upland boundary of the active floodplain and migrating toward or away from these Tertiary-age terraces adjacent to the floodplain of the Brazos River.

Figure 3.30 is an example of a short segment of the Brazos River displaying the style of channel confinement observed along the majority of both the middle and lower section of the Brazos River. An abandoned channel avulsion occupies the eastern margin of the active floodplain. Two cross sections display the topographic elevations from the western terraces/uplands to the eastern boundary. The Brazos River occupies the western flank of the active floodplain through the majority of the segment from the Falls County line to the Brazos County line.

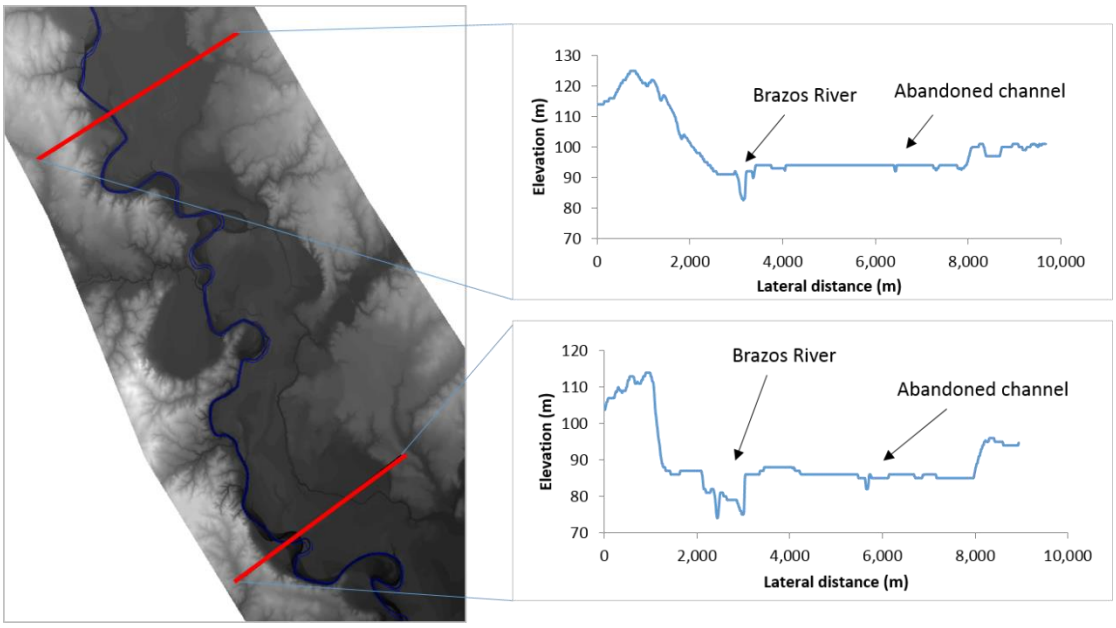

Figure 3.30. Two cross sections of the active floodplain of the Brazos River. The spatial resolution of the digital elevation model is 10 meters.

As stated earlier, Nicoll (2010) studied confined meanders on rivers in central and western Canada, finding the approximate valley to channel width ratio is 2-3; whereas the Brazos River exhibits similar pattern of confinement across the active

floodplain but has a valley to channel width ratio of 57 times. Subtle topographic differences in elevation of several meters impart a confinement pattern on a large lowland river as seen in watersheds with greater relief.

3.7.5 Vegetation

A factor not analyzed, but examined in this work, is the effect of vegetation on bank stability. Many studies have addressed the effect of presence or absence of different types of vegetation on bank stability (Beeson and Doyle, 1995; Micheli, 2004; Esfahani, 2010). Vegetative coverage, whether it consists primarily of grassland or large woody plants, may be an underlying factor in the relationship between hydrologic regime and rates of migration. Observations of numerous bends along the study reach showed areas that have been cleared of vegetation mainly for increased agricultural area (Fig. 3.31).

The meander bends presented in Fig. 3.31 show examples of the effect of cleared vegetation on channel migration. The presence or lack of vegetation, specifically forest or shrub cover, has a strong impact on the magnitude of migration. For example, if one compares (A) to (F) on can see distinct styles of migration, the meanders generally migrate in the direction of areas containing no tree cover. Because of the position of the channel within the valley many of the bends are forced to migrate in one direction and take on an irregular appearance. This channel geometry is exacerbated by the lack of vegetation along many of the outer cut banks.

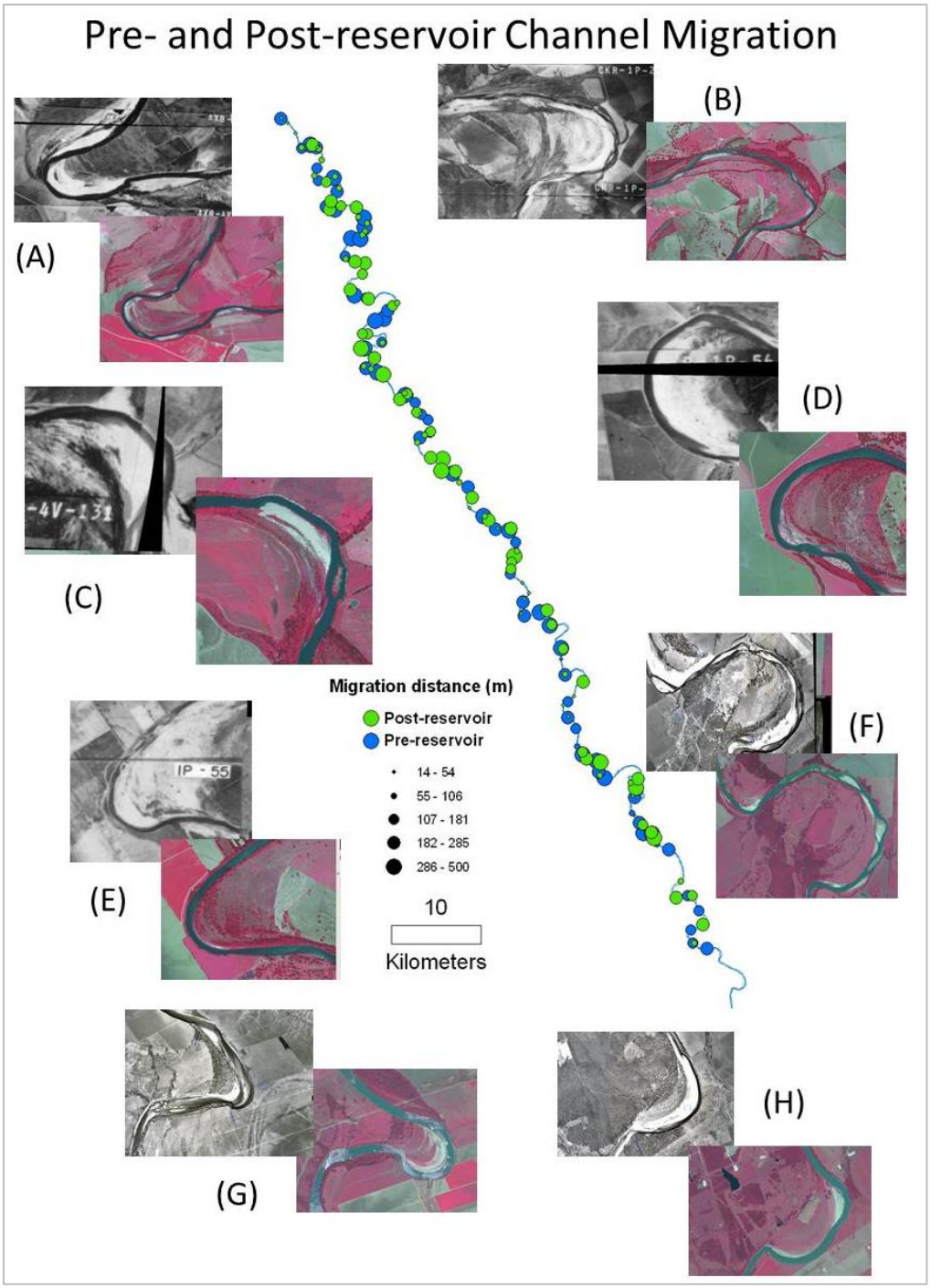

Figure 3.31. Examples of magnitude of migration in locations lacking adequate large woody plants. Proportional symbols display total migration magnitude post- and pre-reservoir construction.

Using the rates of migration generated from the second measurement method, Fig. 3.32 displays the difference observed between meanders with either forest cover or grass/cropland along the outer bend of a meander. To classify as either forest or grass, the riparian area along the outer bend has to contain over fifty percent of either of the two major vegetation types.

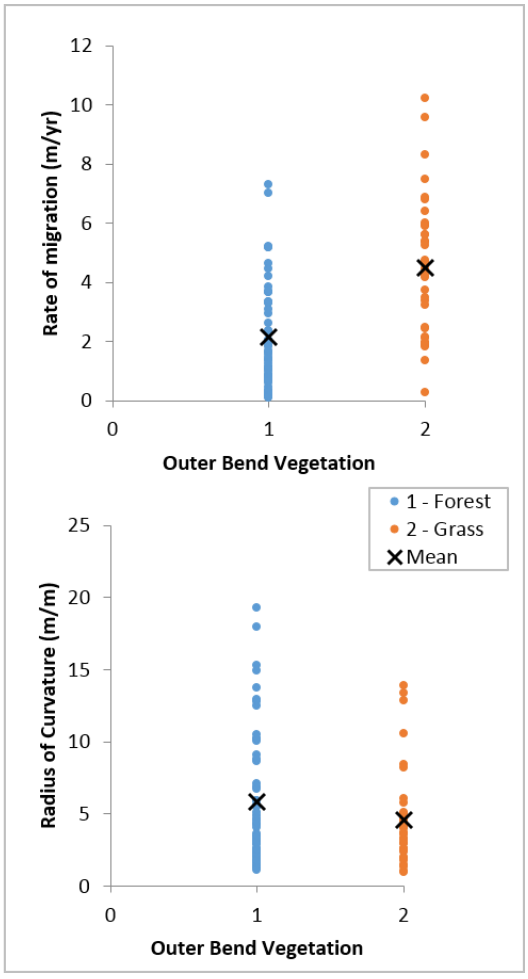

Figure 3.32. Rates of migration and radius of curvature of meander bends with vegetation comprised of predominantly grass or forest on the floodplain adjacent to the outer bend.

Bends were measured from inflection point to inflection point on the upstream and downstream ends of a meander. As seen in the literature, bends with a greater proportion of grass or cropland to riparian forest have on average greater rates of migration. Conversely, the radius of curvature is greater on bends with forested banks as the river is under more stable long term conditions.

3.8 Summary and Conclusions

The main focus of this study was to calculate rates of lateral channel migration along the Middle Brazos River and to understand the effect of surface discharge variations on this migration. Four tasks were established for this project. These tasks were:

1) Calculate rates of meander migration along selected reaches of the Brazos River and correlate values to varying discharges. Determine mechanism of channel migration for temporal intervals (i.e., 1950s, 1960s, etc);

2) Categorize channel banks for erosion occurrence/potential by examining hydrologic shear stress, and associated flow, along banks;

3) Develop sediment budget for selected reaches based on various flow regimes;

4) Determine and classify response of the channel movement within the river valley.

This study found that migration values range from ~1 m/yr to ~50 m/yr from 1929 to 2010. The majority of migration values fall within a range from ~2 m/yr to ~10 m/yr. In generally, as channel gradient and channel sinuosity increased, the range of migration values increased as well, similar to other large alluvial rivers. The ten slope

classes present a framework for classifying the migration potential within this section of the Brazos River.

The Middle Brazos River generally flows along the western side of the floodplain valley. This characteristic affects channel migration in that the channel is migrating towards the eastern side of the valley. This easterly migration direction creates irregular channel meanders with channel erosion concentrated along the outer bank.

After considerable analysis, this study concludes the evidence is inconclusive as the effect of changes in discharge on lateral channel migration along the Middle Brazos River. Discharge does have an impact on migration magnitude, but at the scale measured within this study it is difficult to determine with the volume and timing of water needed to initiate a specific amount of channel migration. This study was unable to determine the exact relationship between surface discharge and channel migration. The two variables quantified in this study, the influence of groundwater and the presence or lack or forest cover, were observed to affect the magnitude of lateral channel migration.

Rates of lateral migration have been calculated for several time periods covering the entire study reach. In general, rates of rates of migration are at the high end for alluvial river migration. Knighton (1998) has shown that generally the larger the drainage basin and the longer the period of measurement, the higher the rate of migration, values generally range from nearly zero to ten meters of lateral migration a year. The Middle Brazos River follows this trend with migration values across the study reach ranging from 1.0 to ~11.0 meters/yr. Overall sediment balance for the freely

migrating meanders is a net positive deposition of 5,580,161 m^3 located predominantly along point bar complexes.

Observed in this dataset is the effect of land use and management on the magnitude of migration. The presence or lack thereof, of large woody plants, namely trees, assists in creating conditions favorable for high rates of bank erosion. Across the study reach areas lacking adequate vegetated cover, especially those areas along large meander bends, experienced the highest rates of bank erosion. Establishment of large woody vegetation along these bends, in particular the outer banks, would be difficult.

In conclusion, the Brazos River is a highly nonlinear system across spatial and temporal scales. At the multiple-reach scale, both basin wide features and channel corridor characteristics affect the rate and style of lateral migration. The author posits the transitional nature of landscapes through the observations along the central reach of the Brazos River; that a large meandering river in a relatively “flat” prairie topography exhibits characteristics of river systems from other landscapes. Nature is not homogeneous.

4 EVOLUTION OF OXBOW LAKES ALONG THE BRAZOS RIVER IN SOUTHEAST TEXAS[2]

4.1 Overview

Oxbow lakes are a major component of the fluvial system in lowland regions. After cutoff, the lake becomes filled with sediment and requires an increasing discharge from the main channel to maintain a hydrologic connection. This connection is necessary for diverse aquatic habitat and to provide storage for sediment. The relationship between the cutoff ratio, diversion angle and rates of sedimentation of twenty eight lakes located on the middle and lower Brazos River, central Texas, were examined.

The time of cutoff was dated using historic maps and aerial photographs. The sediment within the Brazos River system is largely fine sands, silt and clays. The rate of sedimentation was assessed using a digital elevation model to determine the thickness of sediment in the oxbow relative to the main channel. Average rates of sedimentation range from 0.02 to 0.4 meters per year. Field observations of main channel-to-lake connections for five of the lakes were compared to the rates of sedimentation to determine a correlation between discharge events in the main channel and the sediment deposited in the lake. The rates of sedimentation increase as the area of the lake increases. In addition, oxbows with a larger cutoff ratio have a greater number of connections, suggesting sediment is deposited over a wider surface area during flooding.

---

[2] Reprinted with permission from "Evolution of Oxbow Lakes along the Brazos River" by John R. Giardino & Adam A. Lee, 2012. Texas Water Development Board Project Report, 57 p.

4.2 Introduction to Problem

The focus of this work was to determine the processes and rates of oxbow formation in the Brazos River floodplain. Oxbow lakes and similar cutoff channels are ubiquitous features in alluvial rivers in the lowlands and represent one end-member of channel activity (Gagliano and Howard, 1984; Lesack and Marsh, 2010).

The development of oxbows in the Brazos River watershed will be addressed with the following questions: First, what is the rate at which oxbows develop in the active floodplain of the Brazos River? Second, how quickly to oxbows become disconnected hydrologically from the main river (i.e., in-fill with sediments)? Third, are there differences among the morphologic and hydrologic properties of the oxbows of the Brazos River? Fourth, can a chronology of oxbow development from cut-off to remnant lake be established?

Specific attributes investigated include: A) the angle of diversion; B) cutoff ratio; C) main channel-lake connections, and D) flood-connections. As is common in geomorphic systems at this scale, (i.e., channel scale) non-linearity occurs in the various characteristics of oxbows.

The goals of this work are to:

- Quantify rates of planform oxbow development;
- Quantify rates of sediment deposition and meander cutoff in-filling for selected localities along the Brazos River;
- Categorize oxbows and meander scrolls based on the morphologic and hydrologic properties; and
- Develop a chronology of development of an oxbow lake, as it progresses from meandering bend to remnant oxbow lake.

4.3 Literature Review

Tower (1904) presented one of the early studies on the formation of oxbow lakes, and provided many field observations of the various physical components and processes of formation. Oxbow lakes and similar cutoff channels are ubiquitous features in alluvial rivers in the lowlands and represent one end-member of channel activity (Gagliano and Howard, 1984; Lesack and Marsh, 2010). Important to ecology is the rate at which oxbows transition from aquatic to terrestrial habitat, which in turn is controlled by how quickly the cutoff is filled with sediment (Piégay, 2000). Eakhout (2015) demonstrates through observation of a recent cutoff owing from back water effects the three phases between the oxbow and main channel. First, the initial stage leads to cutoff vulnerability, second the process of actual cutoff and third the morphological adjustment, of the main channel in response of the cutoff. Wohl (2015) details the reduction in river connectivity, resulting from human activities, to the adjacent components of the drainage basin, or the critical zone representing the matrix of surface and near-surface chemical and physical processes. This connectivity of river to watershed occurs across longitudinal, lateral and vertical scales (Wohl, 2015), with oxbow development affected by all three ranges.

More recently, Stolum (2006) demonstrated, through modeling, that meandering rivers reach a maximum sinuosity with the limit set by width of the river valley. Once this is reached, sinuosity decreases then oscillates over time. This decrease in sinuosity is often achieved through cutoff of channel segments. Applied to the Brazos River an increase in oxbows per length of valley occurs from the middle to lower river transition south of College Station, Texas.

Utilizing laboratory experiments, Harrison (2015) directly observed the controls on chute formation including river curvature, floodplain gradient, flow resistance to riparian vegetation, magnitude of flood flows, and resistance of adjacent floodplain sediment to erosion. Ishii (2015) describes three components of the facies comprising oxbow infillings. Coarse sediments form the basal units followed by channel fills from main channel deposition. Last, overbank flows deposit fine grain sediments. Of note is the time of preservation of oxbows in the study area, with lakes remaining in the landscape 600-1300 years after initial cutoff.

Determining the age of channel cutoffs is accomplished through historical records and maps (Lewis and Lewin, 1983; Gagliano and Howard, 1984), radiocarbon dating (Holland and Burk, 1982; Brooks and Medioli, 2003), ^{210}Pb and ^{137}Cs dating (Cooper and McHenry; 1989 Gasiorowski, 2005) and optically stimulated luminescence analysis (Rowland, 2005). Using an extensive set of aerial photographs Constantine (2010) calculated dates of cutoff from the midpoint between the aerial photographs taken immediately before and after for a particular cutoff on the main channel. Cutoff ratios and diversion angles are important geometric characteristics controlling the infilling and rates of sedimentation in oxbows lakes (Piégay, 2002; Constantine, 2010). Lowland rivers, similar to the Brazos River, exhibit rates of sedimentation that decrease as the cutoff channel fills over time (Hooke, 1995). Phillips (2006) segments the main channel into a series of river style reaches, which are geomorphically distinct from one another. Constantine (2010) showed that in coarse-grained fluvial systems with high diversion, aggradation rates, or rates of sedimentation, are higher. Work by Hudson (2010)

presents data on several of the oxbows dated in the Brazos River valley concerning the wetted lake area and the distance to the main channel from the abandoned channel entrance. Groundwater levels in the Brazos River watershed fluctuate significantly, and affect the surface water expression in different fluvial environments (Chowdhury, 2010).

Osting et al. (2004) field surveyed six oxbow lakes along the Brazos River to determine the frequency of connections between the active channel and oxbow lakes. The frequency of connections decreased, whereas the magnitude of floods required to connect increased, as oxbows filled with sediment over time. For two oxbow lakes the majority of water remaining in the lakes was sourced from surface connections with the main river, whereas one lake received the majority of water from groundwater via the process of hyperheic upwelling. Concerning sediment infilling, the upstream limb of the oxbow often fills more rapidly with sediment relative to the downstream limb (Hooke, 1995), often closing the oxbow lake to main channel before complete infilling.

Phillips (2011) identified the age or stage of infilling and relative elevation of abandoned channels to the main river as primary controls on the connectivity of cutoffs to the active channel. Lateral distance from the oxbow cutoff to the main channel does not significantly affect the rate of sedimentation in oxbow lakes as the oxbow is still hydrological connected to the main river. River stage is closer in recent oxbows as compared to older oxbows as sediments from the main channel in fill the oxbow within 1 to 5 years from cutoff (Hudson, 2014). The cutoff portion of the river has a greater surface area as compared to the main active channel which allows finer sediments to fall

out of suspension from differences in water velocity between the recent oxbow and main channel.

Tributary input and tie channels (small channels flowing down the center of oxbow cutoff components) affect rates of sedimentation by providing an active pathway for sediment and water to travel between the main channel and oxbow. The development of these tie channels is dependent on the overall substrate of the floodplain with the majority of channels found in lowland, coastal watersheds with a large ratio of silt and fine sand in the sediment load (Rowland, 2005).

Phillips (2011) found the overall geomorphic context of the floodplain, such as adjacent flood basins or abandoned river avulsions (relatively long segments of channel containing multiple meanders) affects the amount of connections and infilling of oxbow lakes. Utilizing field and geospatial data on oxbows from the Sabine River, Phillips (2011) identified six modes of connectivity between the main channel and cutoff segments. The first is flow through whereby a portion of the flow in the main channel regularly passes through the oxbow and returns to the river, representing the initial stage shortly after cutoff. Flood channels and fill-and-spill correspond to high flows in the main channel above normal river stages with fill-and-spill overcoming a physical threshold and spilling into the flood basin represented by a disconnected oxbow. Differences between the flood channel and fill-and-spill are such that a portion of the discharged water returns to the channel during floods in the former whereas the water remains in the flood basin for the latter. The fourth connectivity type is fill-and-drain where high flows at flood stage fill the oxbow with water flowing back into the main

channel when normal flow conditions return. This connectivity type includes a large baseflow component with water flowing back into the main channel through the floodplain substrate. Tributary occupation occurs with a tributary with active discharge flowing through a portion of the oxbow. As the main channel meanders across the floodplain cutoff channel segments may intercept an active tributary channels. The final connectivity type is a total disconnection with the oxbow no longer receiving flood water from the main channel. The properties of the groundwater in the region and whether the main channel is receiving or losing water to the aquifer system also contributes to water volumes in oxbows.

Using one- and three-dimensional modelling Dijk (2014) showed the characteristics; including sediment composition, floodplain elevation and variation in vegetation, of the location just upstream of a bifurcating channel determine in large part the occurrences of chute cutoffs. In addition, the curvature and gradient of the channel is determined at this location, both of which affect the rate of sedimentation in the cutoff (Dijk, 2014). Oxbows with a larger curvature increase rates of sedimentation as the water discharged from the main channel has a longer distance to travel, allowing for more suspended and bedload particles to filter out and settle on the bottom of the oxbow. Conversely, higher channel gradient decreases the rates of sedimentation as water entering the oxbow maintains velocity and continues to entrain a greater portion of the overall sediment load relative to a lower gradient channel.

Most studies of oxbow processes and formations focus on inland alluvial rivers with unidirectional channel flows. Gray et al. (2016) investigated how tidal waves

affected the facies of oxbow sediments, finding higher organic and inorganic carbon, less overall sand content than more terrestrial fluvial-dominated oxbows along the Eel River Estuary in northern California. Despite the facies differences of tidal-dominated as compared to fluvial-dominated oxbows, the bifurcation geometry of the main channel relative to the oxbow is the dominant factor for sedimentation within the plugs of the oxbow limbs adjacent to the main channel. Gray et al. (2015) notes the meandering of the main channel post-cutoff affects sedimentation by construction of point bars or outer cut banks depending on the direction of migration. Migration away from the oxbow develops point bars with lower sedimentation in the oxbow proper as sediment is deposited on the active point bar. Conversely, active migration towards the oxbow, at the point of bifurcation, increases sedimentation as material is transported directly into the oxbow.

During the last several decades, aerial photographs have represented the standard for planimetric data on main channel and oxbow geometries. Despite the advantage of high-resolution of aerial photographs, the temporal scale is often lacking as surveys of large areas are often only repeated every decade. This is especially true in developing nations whom often lack funding for large scale and repeatable aerial surveys. Satellite imagery provides the spatial and temporal scale necessary for repeat surveys, especially along rivers with rapidly migrating meanders (Martha, 2015).

The topographic variations in the geomorphic forms of alluvial rivers, such as channel avulsions, oxbow lakes, crevasse splays and delta fans, are often difficult to detect on digital elevation models (DEM) of 10- or 30-meter resolution. The advent of

high-resolution (~1m) digital elevation data from Light Detection and Ranging (Lidar) surveys increases the observable detail in studies that cover geographic areas that range from hundreds of meters to tens of kilometers in scale (Haugerud, 2003). Lidar, in combination with numerical modeling, can be used to determine the variety of channel flows necessary for reconnecting abandoned channel segments (Hauer, 2014), which has utility in restoring or sustaining biotic habitat. Lidar data on agriculturally-dominated homogenous floodplains often better captures the variation in topography as compared to complex backwater morphologies in heavily forest areas (Džubáková, 2014).

4.4 Physical Setting

The oxbow lakes in the study area are concentrated in the middle and lower reaches of the Brazos River (Figure 4.1). Discharge and sediment are received from the Edwards Plateau and the Texas coastal plain, which comprises the largest part of the middle and lower Brazos watershed. Seasonal discharge pulses dominate floodplain lake hydrology with lake drainage processes and surface evaporation becoming important to lake water levels after lowering of the discharge pulse.

The oxbows studied for this report are located on the Texas Interior Coastal Plains and Coastal Prairies physiographic regions, which exhibits a subtle, yet complex and heterogeneous landscape along with varied land-use histories. The drainage of the Brazos River begins north of the coastal plain in an extra-basinal watershed. Considerable drainage from the High Plains of northwest Texas and the Edwards Plateau enters the Brazos drainage. The coastal plain is comprised of basin-fringe and

intrabasinal drainage systems (Hudson, 2010). The watershed of the river is divided by abandoned Holocene meander belts that occur as raised ridges within the floodplain.

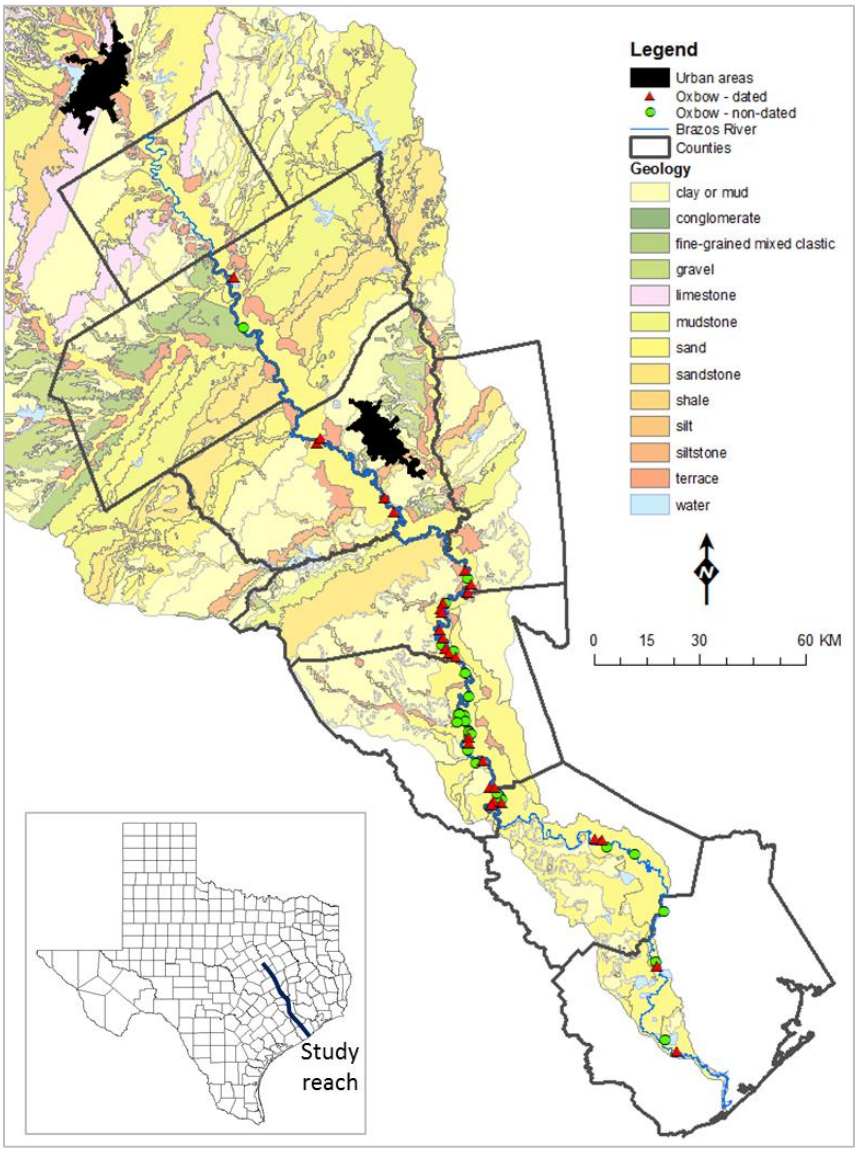

Figure 4.1. Lower Brazos River including locations of oxbow lakes studied and locations of USGS gauging stations.

4.5 Methods

A Geographic Information System (GIS) was used to process a model of specific attributes that were collected for each oxbow locality (Table 4.1); a spreadsheet program (*Excel*®) integrated the data. The specific attributes collected include: 1) the cutoff ratio (C_R); 2) diversion angle (D_A); 3) date of cutoff and 4) rate of sedimentation (S_R).

4.5.1 Cutoff Ratio

The cutoff ratio (equation 1) is derived from the length of the abandoned channel divided by the length of the main active channel:

$$C_R = O_L / M_L \qquad (4.1)$$

where C_R is the cutoff ratio, O_L is the length (m) of the oxbow, and M_L is the length (m) of the main channel, between the upstream and downstream oxbow channel ends (Fig. 4.2).

4.5.2 Diversion Angle and Date Of Cutoff Of Oxbow

Similar, the diversion angle is measured between the upstream portion of the abandoned channel and main channel in the downstream direction (Fig. 4.2). Both characteristics are collected from the most recent aerial photographs of cutoff of the abandoned channel. The dates of cutoff are calculated from the midpoint between the aerial photographs taken immediately before and after for a particular cutoff on the main channel (Constantine, 2010). Typically, the areal coverage covered the span of 20-40 years after establishing date of the cutoff.

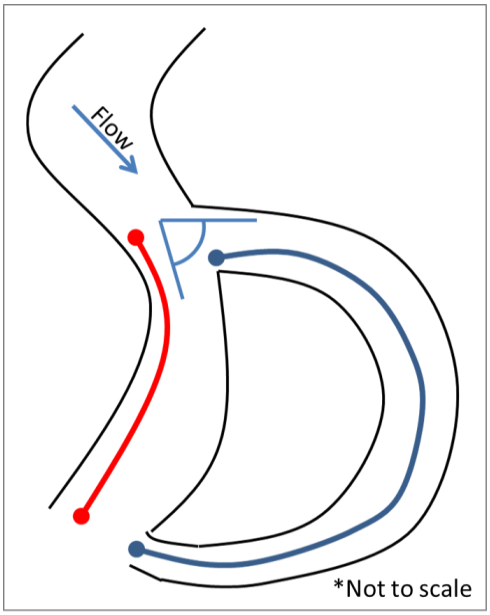

Figure 4.2. Measuring the cutoff ratio and diversion angle along oxbow lakes. The cutoff ratio is calculated by the oxbow length divided by the main channel length. The diversion angle is between the upstream entrance of the cutoff and the main channel.

In a linear geomorphic system, a greater cutoff ratio, for oxbows of equal channel depth and width, results in lower rates of sedimentation as flows connecting the oxbow to the main channel during flood deposit sediment across a larger surface area. Similarly, a larger diversion angle results in an entrance of the abandoned channel further away from parallel flow with the main channel, which reduces rates of sedimentation.

4.5.3 Rates of Sedimentation

Cutoff ratios and diversion angles are important geometric characteristics controlling the infilling and rates of sedimentation in oxbows lakes (Piégay, 2002; Constantine, 2010). The thickness of sediment deposition was obtained by first obtaining the difference between the elevation of the highest point along the upstream arm of the oxbow and the

elevation of the main channel immediately adjacent to the oxbow (Fig. 4.3). The length of cutoff time was calculated by subtracting the cutoff year from the date of the DEM (Appendix B). The sediment thickness was then divided by the number of years since cutoff from the main channel to determine the rate of sedimentation per year, which is expressed in meters per year. Therefore, the rate of sedimentation (Eq. 4.2) is expressed as:

$$S_R = (O_E - M_E) / O_A \quad (4.2)$$

where S_R represents the rate of sedimentation (m/yr), O_E is the elevation of the upstream oxbow surface, M_E is the elevation of the main channel, and O_A is the age of the oxbow in years.

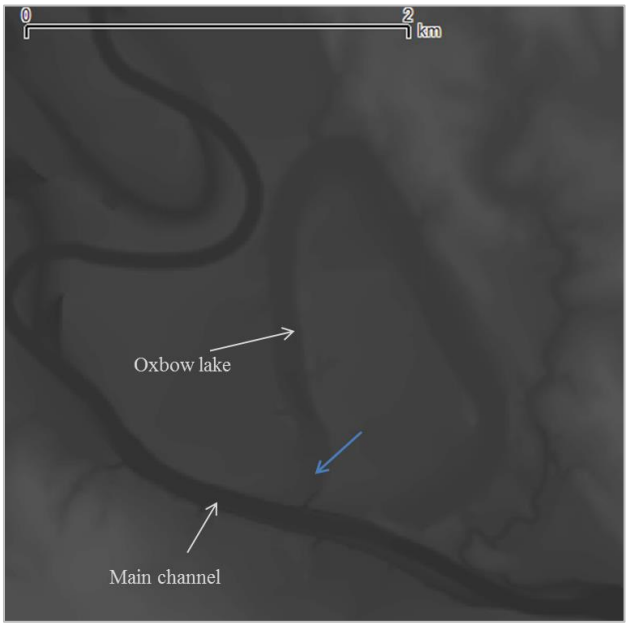

Figure 4.3. Digital elevation model (DEM) of a typical oxbow lake and the main channel. The oxbow lake is the dark black horseshoe form in the center of the image, and the main channel flows along the lower portion of the image. The thin, blue arrow points to highest elevation used in calculation of rates of sedimentation, which is the upstream component of the oxbow lake. Main channel flow is from left to right.

Lowland rivers, similar to the Brazos River, exhibit rates of sedimentation that decrease as the cutoff channel fills over time (Hooke, 1995). This is a result of the oxbow surface bottom elevation rising as sediments are deposited. To calculate extensive changes in the rates of sedimentation over time requires substantial sedimentological and chronological data.

Using the extensive aerial photographs and planimetric maps of the area, an important assumption was made for the rates of sedimentation over the time frame of oxbow cutoff in this study. For the purposes of this work, it is assumed that the oxbow lakes occurring in the Brazos River watershed are in a 'steady-state' condition, whereby rates of sedimentation are assumed constant over time. This assumption can be made because determining changes in the rates of sedimentation over time require either the dating of sedimentary materials using stable isotopes or extensive temporal coverage of aerial photographs (Brooks and Medioli, 2003). In reality, older oxbows are more stable because fewer connections decrease the amount of sediment infill, whereas younger oxbows connect more frequently with the main channel.

Field data, specifically the number of connections to main channel ($C_{\#}$) and the flood-flow [F_F, (Eq. 4.4)] required for connection, for five oxbows from Osting (2004) were the basis for the modeling approach I used to build models (Fig. 4.4 & 4.5) with rates of sedimentation to calculate number of lake to main channel connections and flood flows for the remaining twenty-three oxbows.

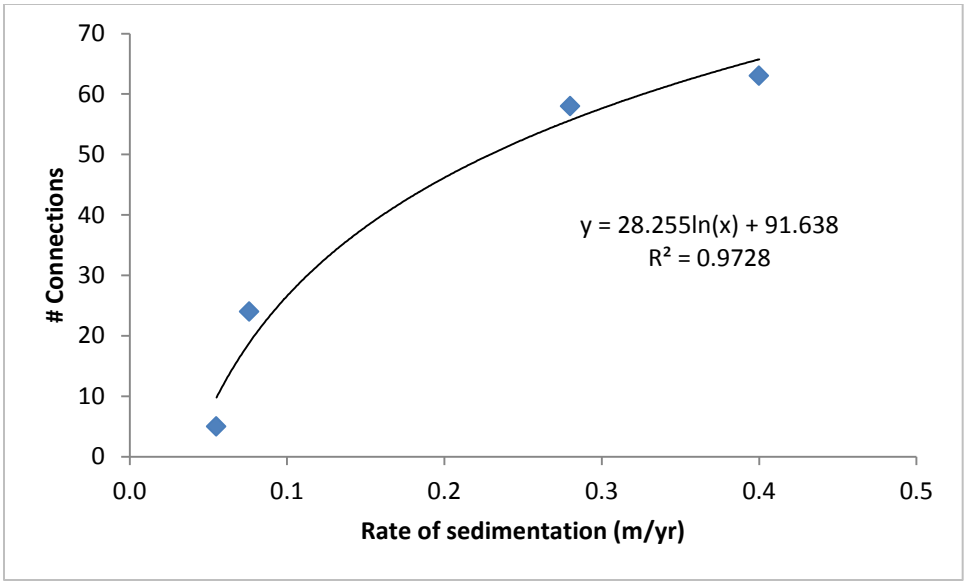

Figure 4.4. Relationship between the number of connections between the oxbow and main channel, and rates of sedimentation. Though rates of sedimentation are controlled by the number of connections, this graph shows the relationship between the two variables.

The number of connections for all dated oxbows using the rate of sedimentation is computed as follows (Eq. 3):

$$C_{\#} = 28.255*\ln(S_R) + 91.638 \qquad (4.3)$$

where, $C_{\#}$ is the number of connections between the main channel and oxbow from the time of cutoff from the main channel to 2011, and S_R is the rate of sedimentation. Figure 4.5 is similar to the previous figure in that it calculates the flood flow (m^3/s) required to connect with the abandoned channel, rather than the rate of sedimentation.

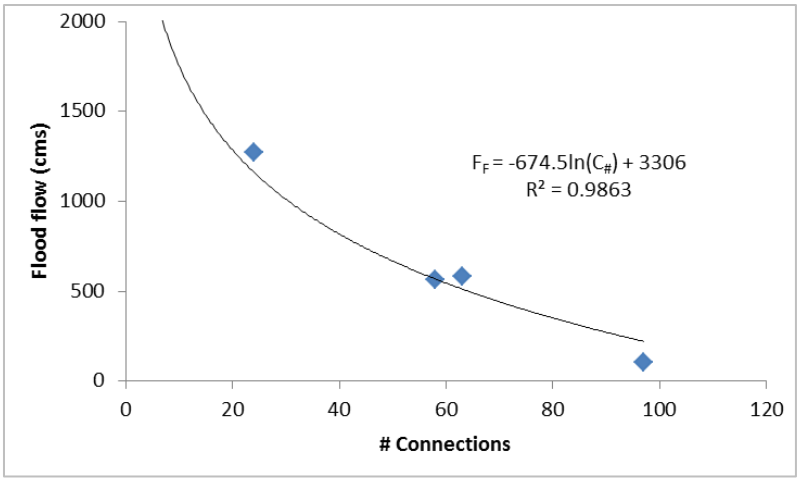

Figure 4.5. Relationship between flood flows and the number of connections for oxbows from Osting (2004).

The calculation of the flow required to maintain connection between the oxbow lake and the main channel is derived from:

$$F_F = -674.5*\ln(C_\#) + 3306 \qquad (4.4)$$

where, F_F is the flood-flow required to connect the main channel to the oxbow lake, and $C_\#$ is the number of connections between the main channel and the oxbow.

To better understand the dynamic characteristics of oxbows in what is often considered a homogenous environment, it is useful to categorize the main channel into distinct reaches. Phillips (2006) segments the main channel into a series of river style reaches, which are geomorphically distinct from one another. Variables from Phillips (2006) used in conjecture with the data collected in this study include the slope of the reach, channel sinuosity, channel/flow patterns, and the channel-floodplain connectivity.

Hydrologic records for five USGS stream gauging stations (Fig. 4.1 & Table 4.1) were compiled for connection flood flows determined by Osting (2004). The daily mean flows were collected for the entire time of record.

Table 4.1. Gauge stations for the middle and lower Brazos River. Year column represents beginning of discharge data collection.

Gauge #	Gauge Name	Year	Location (UTM)
8098290	Highbank	1965	E707398, N3446477
8108700	Bryan - SH 21	1993	E735419, N3390800
8111500	Hempstead	1938	E770962, N3336407
8114000	Richmond	1903	E232885, N3275668
8116650	Rosharon	1967	E249298, N3249472

A model (Fig. 4.5) was created comparing the number of connections and the flood flow required to make that connection. This model was applied to dated oxbows that had cutoff since gauge records began to be recorded for gauge stations directly upstream of the particular oxbows. The number of days containing a flow that equaled or exceeded the modeled flow was obtained for each oxbow to determine the relationship between flood flows and number of connections.

The data points (lakes O2, O4, O14, 027, and 028) used to develop relationships between the number of connections, rates of sedimentation, cutoff ratios, and other factors are a good representation of the variety of oxbow lakes encountered in the Brazos Valley. Oxbow lakes O2, O4, O14, O27 and O28 occur at regular intervals along the main channel, in a range of floodplain valley widths.

4.6 Results and Interpretation

Once cutoff from the main channel the infilling of sediments occurs quickly (Fig. 4.6). The upstream arm infills first with possible development of a tie channel that back drains to the main channel during high flow events. Sediment is deposited primarily in the oxbow because of the larger surface area as compared to the segment of the main channel adjacent to the lake. As sediment is deposited in the oxbow the near river ends fill first, eventually separating the lake from the main channel in all but high flow events.

Field work was done on Big Bend Oxbow to observe the channel and cutoff features and collect sediment samples for sieve analysis (Fig. 4.7). From the aerial photographs the arms of the oxbow were infilled at least partially by 1988. Sediment samples were collected from the downstream arm of the oxbow during the winter months to ensure adequate exposure and access to the bank. A present day tie channel allows water and sediment to reach the back portion of the oxbow during high flow events.

Figure 4.6 Oblique aerial photographs of cutoff of Big Bend Oxbow near College Station, Texas (Aerial photographs provided by C. Matthewson, Texas A&M University). The cutoff occurred approximately in 1974 and by the late 1970s the majority of the arms of the oxbow had infilled with sediments. The main channel is approximately 100 meters wide.

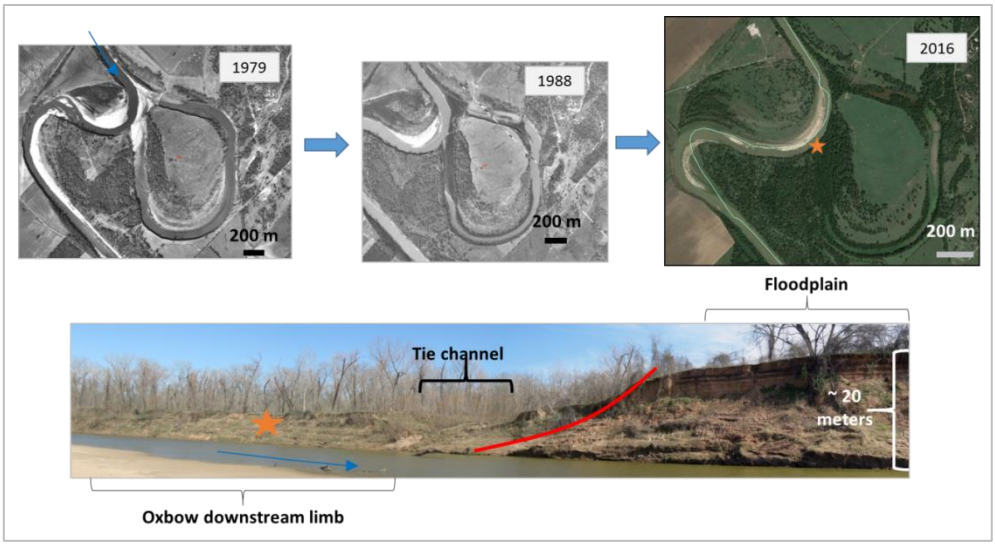

Figure 4.7. Field site along Big Bend Oxbow in western Brazos County. The sediments collected for sieve analysis were taken at the location of the orange star in the bottom photograph.

Sediments were collected at the base and top of the downstream remnant arm of Big Bend Oxbow. A thin layer of organic material is below the top two meters of the oxbow sediments. This layer represents a terrestrial surface in which plant growth established a thin soil and prominent vegetation. Subsequent high flows flooded the surface with additional sediments. The base sediments are larger in grain size and alternate in light and dark colored layers. This alternating deposition represents the back-and-forth flooding and deposition during flows connecting the main channel and oxbow. A grain size difference between the light and dark sediments of the base unit was not performed.

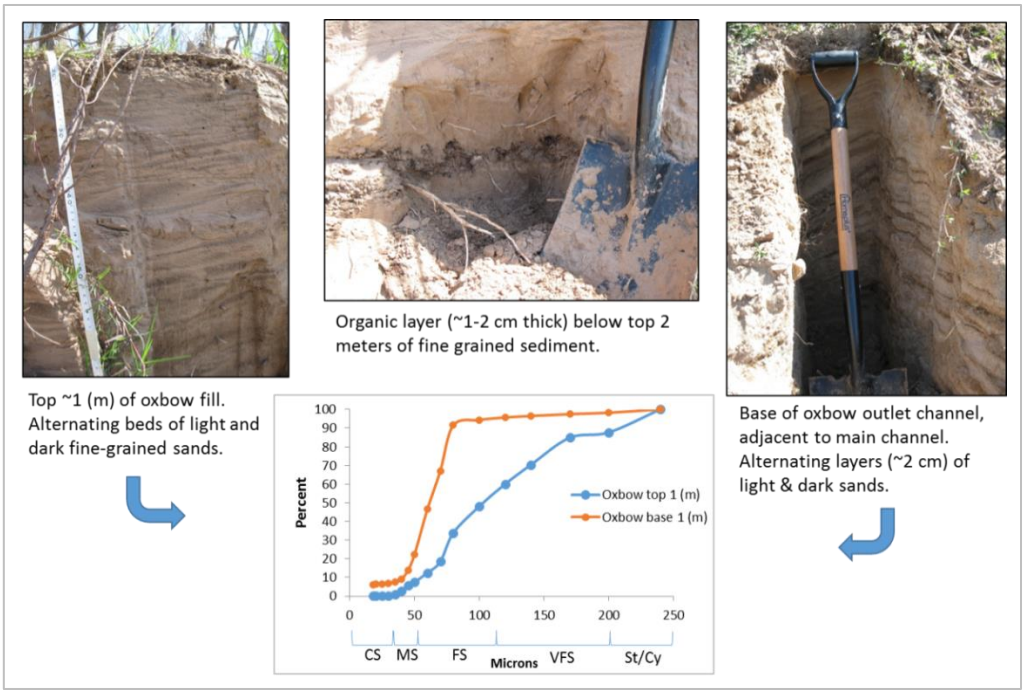

Figure 4.8. Field samples taken on the downstream arm of Big Bend Oxbow. Samples were collected from the top one meter directly below the ground level of the floodplain and approximately one meter above the current water surface of the main channel. The sediment collected at the base may not represent the true basal sediments deposited shortly after formation of the cutoff.

The temporal transition from cutoff channel segment to remnant oxbow lake is relatively quick on the geologic timescale. Fig. 4.9 displays the formation of an oxbow lake in the lower Brazos River floodplain in approximately 1976. Thirty four years later, in 2010, the arms of the oxbow are infilled with sediments. High-resolution Lidar imagery, with a spatial resolution of three meters, provides a detailed map view of the elevation differences, especially in geographic areas of little relief such as the coastal floodplains of the southern United States. Here is this oxbow is visible the subtle elevation highs that prevents river discharge from regularly entering the lake. The elevation high is 65 meters while the low, representing the water surface of the main channel, is 34 meters. The majority of the floodplain adjacent to the main channel is 45-

50 meters. On a global terrestrial scale this is little relief but enough to prevent regular connection between the oxbow and the main channel during low and normal river discharge. A summary of the analyses is presented in Tables 4.2 and 4.3. Rates of sedimentation are examined in relation to cutoff ratio, diversion angles, sinuosity class, slope class, channel/flow pattern class, and channel/floodplain connectivity class.

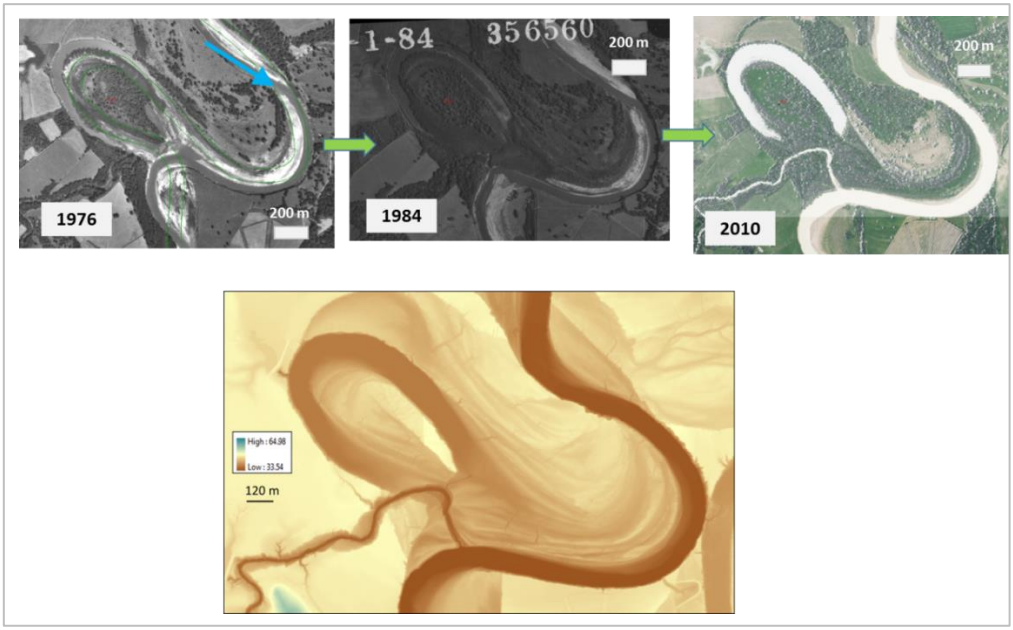

Figure 4.9. Oxbow cutoff in approximately 1976. The cutoff channel has captured a nearby tributary, slowing the rate of sedimentation as water continues to flow into the oxbow during normal flow conditions.

Table 4.2. Oxbow lakes examined in this study. Oxbows were numbered starting from the furthest upstream lake, therefore, lake O27 is closest to the entrance into the Gulf of Mexico.

Oxbow lake	UTM Latitude (m)	UTM Longitude (m)	Cut-off Ratio	Diversion Aangle	Distance to Channel (m)*	Lake Area (km^2)**
O1	713892	3436836	6.10	39.3	100	0.006
O2	737297	3389811	9.98	89.0	220	0.495
O3	738505	3391194	2.52	105.1	-	-
O4	756635	3374278	14.41	77.5	159	0.153
O5	759306	3370459	22.67	129.5	400	0.140
O6	779341	3353993	8.71	50.7	405	0.034
O7	781151	3349800	2.54	56.2	218	0.041
O8	780014	3347769	8.95	133.2	13	0.064
O9	773125	3344514	1.84	109.5	235	0.072
O10	772444	3342875	18.85	98.1	1021	0.110
O11	772825	3342048	11.64	110.9	125	0.204
O12	772114	3337184	11.56	102.5	74	0.144
O13	772956	3334809	12.07	89.8	516	0.088
O14	773721	3331775	5.00	67.2	-	-
O15	774847	3330334	11.22	48.3	337	0.190
O16	776814	3329440	8.29	63.1	59	0.141
O17	780408	3306523	5.11	55.3	774	0.062
O18	780315	3304998	2.98	64.6	113	0.195
O19	784236	3299863	6.85	62.0	-	-
O20	786154	3292235	4.95	128.0	393	0.155
O21	787796	3292221	4.46	84.1	-	0.192
O22	789703	3287926	5.82	66.4	334	0.104
O23	787218	3288256	2.46	132.6	156	0.095
O24	786581	3287503	1.82	99.5	-	-
O25***	234842	3276629	7.10	142.8	210	0.225
O26***	236974	3276175	3.40	141.7	151	0.290
O27***	250403	3239758	25.50	128.8	-	-
O28***	254881	3215198	5.90	143.7	334	0.094

***Values obtained from Hudson (2010). Dashes indicate lake distances not calculated in Hudson (2010), with dashes indicating data not acquired.**

****Values obtained from Hudson (2010), with dashes indicating data not acquired.**

*****The UTM coordinate system for oxbow 25-28 is Zone 15. Oxbows 1-24 occur in UTM Zone 14.**

The numbers of connections, field and modeled, are analyzed against several attributes to determine the planform development and sediment dynamics of 28 dated oxbow lakes. Appendix B contains raw data on the cutoff ratios, Appendix C are the raw values for the diversion angles. Appendix D displays sequential aerial photographs for several dated oxbows.

Oxbow lakes along the Brazos River contain various levels of sedimentation, which is driven primarily by main channel discharge and sediment load. Phillips (2011) used a classification system to assess dominant processes of hydrologic connectivity for cutoff channels along the Sabine River. The six categories include: 1) flow through, whereby high discharge enters and passes through the abandoned channel, 2) flood channels, with high discharges entering the oxbow and then returning to the main channel, 3) fill and spill, where high flows fill the abandoned channel and then spill out into the basin of the surrounding floodplain, 4) fill and drain, with the oxbow filling during high flow and then draining back to the main channel as river discharge decreases, 5) tributary occupied, whereby tributaries of the main channel flow through the cutoff channel, and 6) disconnected, with no flow between the main channel and the cutoff.

Table 4.3. Additional oxbow lake data including the date of cutoff (year), the rate of sedimentation (m/yr), and the type of cutoff channel, according to modified classification scheme.

Oxbow lake	Cutoff Date	Sedimentation Rate (m/yr)	Type*
O1	1933	0.030	Flow through: Tributary occupied
O2	1920	0.076	Fill-and-drain
O3	1974	0.080	Tributary occupied
O4	1974	0.280	Tributary occupied
O5	1920	0.101	Disconnected
O6	1896	0.078	Tributary occupied
O7	1938	0.066	Disconnected
O8	1938	0.033	Tributary occupied
O9	1961	0.211	Flood channel
O10	1913	0.047	Flood channel
O11	1946	0.094	Flood channel
O12	1913	0.093	Fill-and-drain
O13	1913	0.093	Fill-and-drain
O14	1960	0.256	Fill-and-drain
O15	1976	0.400	Flood channel: Tributary occupied
O16	1950	0.143	Disconnected
O17	1960	0.051	Fill-and-drain
O18	1917	0.049	Fill-and-drain
O19	1962	0.027	Fill-and-spill
O20	1948	0.196	Disconnected
O21	1948	0.196	Disconnected
O22	1947	0.231	Disconnected
O23	1947	0.192	Fill-and-drain
O24	1947	0.154	Disconnected
O25	1919	0.075	Flood channel
O26	1919	0.113	Disconnected
O27	1996	0.218	Fill-and-drain
O28	1920	0.055	Disconnected

***Classification type follows Phillips, 2011.**

To compare the accuracy of the rates of sedimentation collected using the Digital Elevation Model, the ground control points from the Osting report (2004) were compared to elevations from the DEM (Table 4.4). The DEM elevations were chosen at the same location using aerial photographs and the DEM. The percent error is low (mean = 4.09%), indicating DEM elevations are comparable to field surveyed points. The major outlier is Cutoff Lake (O28) with a 63.34% error. This error is most likely attributable to the difficulty in establishing an elevation control point. The last lake, Horseshoe Lake,

was not included in this work because a cutoff date could not be determined from historic maps or aerial photographs.

Table 4.4. Difference between elevations (Osting 2004) and DEM elevations concerning control points.

Lake*	Osting Control Points (m)	DEM Control Points (m)	Error (%)
Moehlman Slough (O2)	66.9	67	0.15
Big Bend Oxbow (O4)	58.6	60	2.4
Korthauer Bottom (O14)	38.6	40	3.63
Hog Island Lake (O27)	0.88	0.97	10.2
Cutoff Lake (O28)	13.91	5.1	63.34**

***The lake names are used from Osting (2004), with the label for this work in parenthesis.**

**** The error for 'Cutoff Lake' is very high most likely because of the difficulty of measuring the control point in the original 2004 field survey.**

Figure 4.6 displays the correlation between rates of sedimentation (m/yr) and the cutoff ratio. A very weak correlation ($R^2 = 0.0008$) exists between the two variables, the linear trend slopes downward with many of the rates of sedimentation occurring between 0.0 and 10.0 (m/yr). The majority of the rates of sedimentation greater than 0.1 m/yr occur with oxbows having a cutoff ratio of less than 10.0. As the length of the oxbow increases, relative to the main channel length, the area available for sediment deposition increases; therefore, lowering the rate of sedimentation for an oxbow with a high cutoff ratio. Discounting the four outliers in Fig. 4.10, this relationship is shown in the cluster of points between 0 and ~12 cutoff ratio. A shorter cutoff channel results in less accommodation space at the upstream end of the lake, resulting in increased sediment deposition.

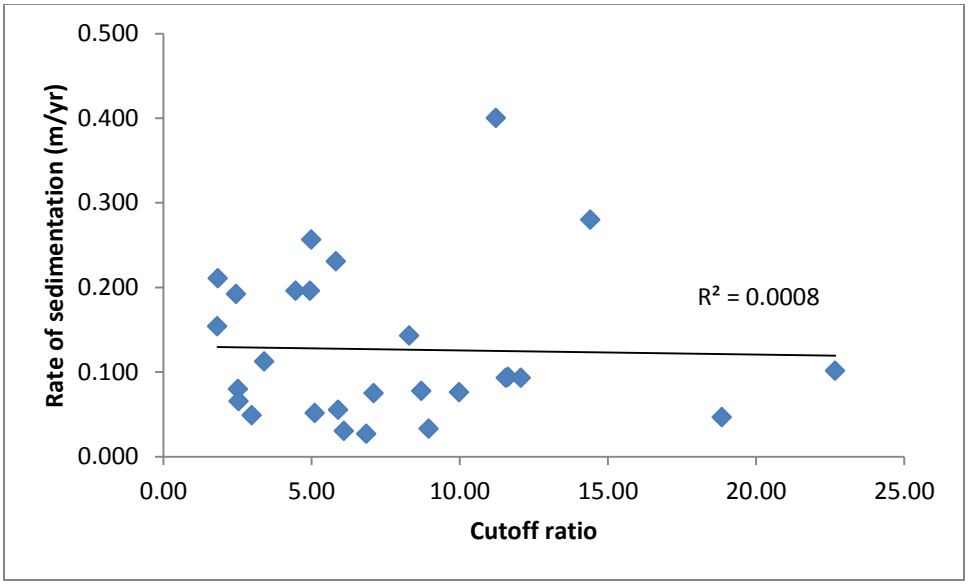

Figure 4.10. Relationship between sedimentation rates and the cutoff ratio.

Figure 4.11 displays a strong correlation (R^2 = 0.84) between rates of sedimentation and the cutoff ratio. As the cutoff ratio increases, the number of connections between the main channel and the oxbow increases. A larger cutoff ratio has a larger lake surface area, allowing for sediment transported into the lake to be deposited in thinner beds throughout the lake area. The flood-flow required to connect the oxbows to the main channel is smaller than oxbows with low cutoff ratios, allowing for lower, more frequent discharges to enter those oxbows.

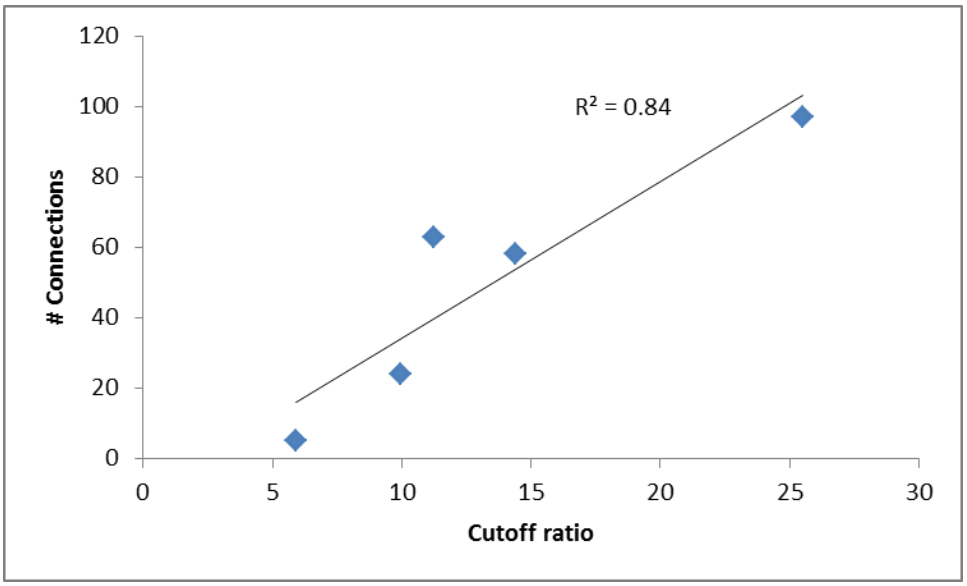

Figure 4.11. Relationship between cutoff ratio and the number of connections from the oxbow lakes studied in Osting (2004).

The relationship between rates of sedimentation and the diversion angle (Fig. 4.12) display a gently sloping downward trend as diversion angles increase. With larger diversion angles the upstream entrance to the oxbow lake approaches a more perpendicular angle to the main channel, which impedes sediment flowing into the abandoned channel during sufficient connection discharges. Sediment is able to enter oxbow lakes with a lower diversion angle because the upstream entrances approach a parallel position with the main channel. Suspended sediment is less susceptible to this general concept of increased sedimentation with a lower diversion angle, which is shown in Fig. 4.12, where rates of sedimentation are generally constant across the range of diversion angles.

The sedimentation in oxbow lakes along the Brazos River is predominantly driven by suspended sediment particles, which are deposited in the abandoned channel at

lower flows relative to those flows for bedload transport. Much of the deposition at these lower flows occurs as water is draining back out of the cutoff lake as the discharge of the main channel decreases. The relationship between rates of sedimentation and the diversion angle (Fig. 4.12) is relatively poor because the majority of deposition required to disconnect from the main channel during normal flow conditions occurs soon after the cutoff. The majority of oxbow lakes in the dataset are twenty to one hundred years old, at these timescales the diversion angle has little influence on overall volume of sediment deposition.

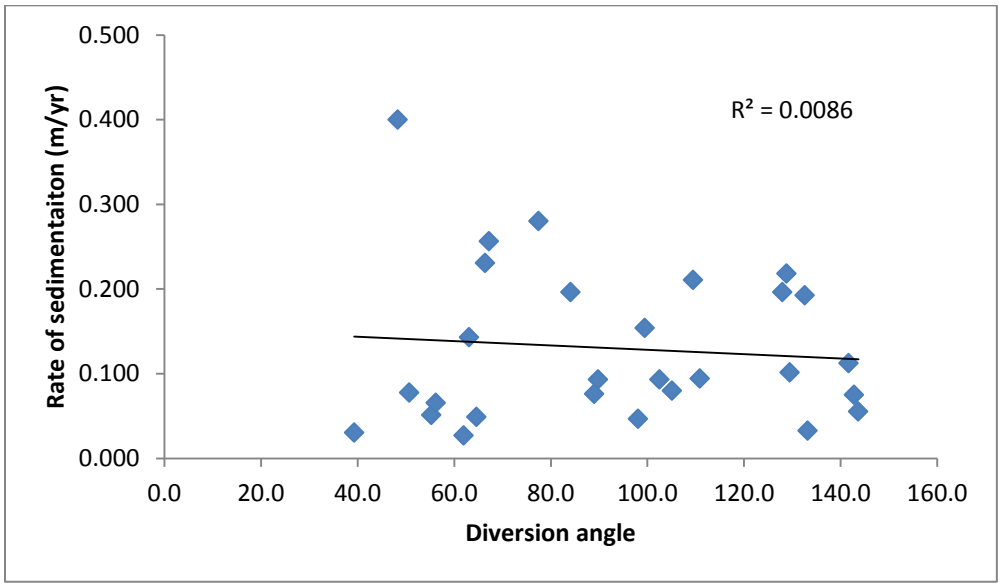

Figure 4.12. Relationship between sedimentation rates and the diversion angle. Main channel flow enters the oxbow more easily when the diversion angle is lower, with higher maximum rates of sedimentation at diversion angles less than 100.

Constantine (2010) showed that in coarse-grained fluvial systems with high diversion, rates of aggradation, or rates of sedimentation, are higher than fluvial systems

with fine-grain sediments. This relationship of high diversion angle-high rate of sedimentation along the coarse-grained channels does not apply to the Brazos River because the Brazos River is a sand-dominated system (Dunn and Raines, 2001), as well as having a high suspended sediment load. Thus, changes in the composition of the sediment load, in addition to the planform characteristics of the oxbow, affect the rate of sedimentation in abandoned channels. These characteristics can be simply stated that as the percentage of suspended particles increases, relative to the total sediment load, the relationship between rates of sedimentation and the diversion angle weakens.

Figure 4.13 displays the relationship between the number of connections, observed (Osting, 2004) and the diversion angle for 5 of the 28 oxbows. A higher diversion angle results in fewer connections between the main channel and the oxbow as the angle of the abandoned channel, is more perpendicular to the direction of water flow in the main channel.

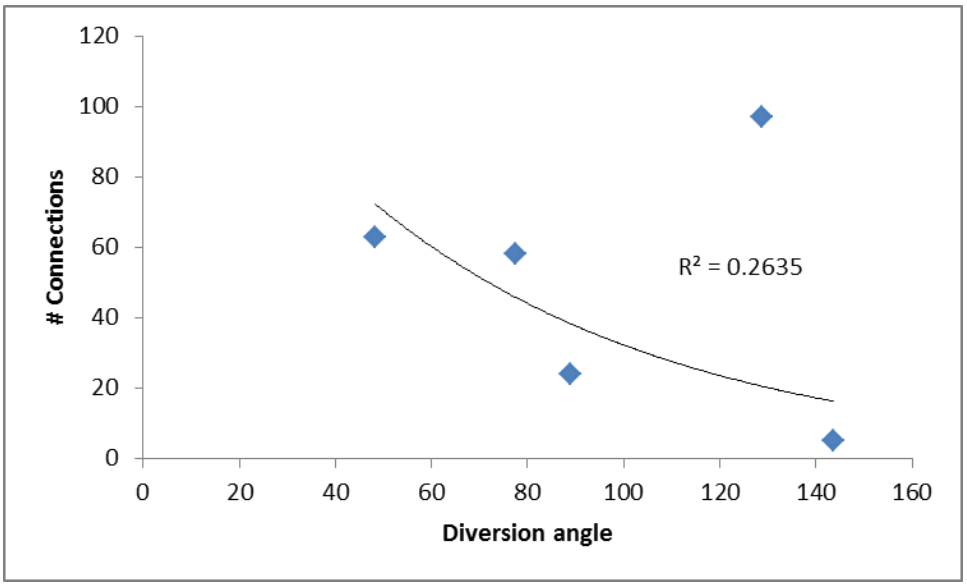

Figure 4.13. Relationship between diversion angle and the number of connections for oxbow lakes studied (Osting 2004). The connections listed are the observed connections in the field. The outlier is O27, a recent oxbow cutoff in the last decade, though number of connections is listed as connecting back to 1983. The correlation improves to R^2 = 0.9241 when the O27 oxbow is not included.

Study of Fig. 4.13 shows an outlier in the upper right corner. This outlier in Fig. 4.13 is a special case. This oxbow is dated to 1996, from Osting (2004) and the use of temporal aerial photographs by the author. The oxbow was cutoff in 1996, yet connections between the oxbow and the main channel have occurred dating to 1983 (Osting, 2004), when the oxbow lake was not yet separated from the main channel. If this data point is removed from the population, which though cutoff only since 1996 is nevertheless listed as reconnecting since the 1980s, a strong correlation of R^2 = 0.9241 occurs. This supports the assumption that oxbow lakes with greater diversion angles reconnect less with the main channel inferred from Fig. 4.12, whereby oxbows with higher diversion angles, in the upstream abandoned channel arm, have lower rates of sedimentation.

The oxbow lake data in relation to the geomorphically determined river style classes (Phillips 2006) is presented in Figures 4.14-4.17. Examination of these data suggests that several of the classes across the different characteristics include a low number of data points. Overall, several characteristics of the development of oxbows are presented.

Boxplots of rates of sedimentation according to sinuosity classes from river reach styles (Appendix D) are shown in Figure 4.10. Sinuosity is classified as: low sinuosity, 1.25–1.49; meandering, 1.50-1.99; strongly meandering, 2.0-3.0, and tortuous, >3.0. The median rate increases as sinuosity of the channel increases. The greatest range in sedimentation occurs with strongly meandering (the dimensionless ratio of the main channel length to valley length is 2.0-3.0) channel segments.

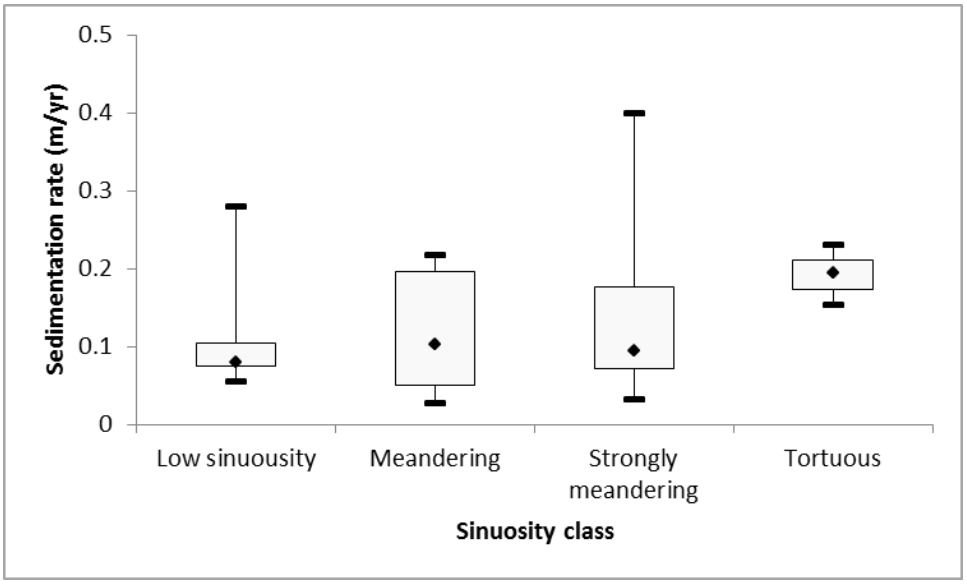

Figure 4.14. Relationship between sedimentation rates and sinuosity classes after Phillips (2006).

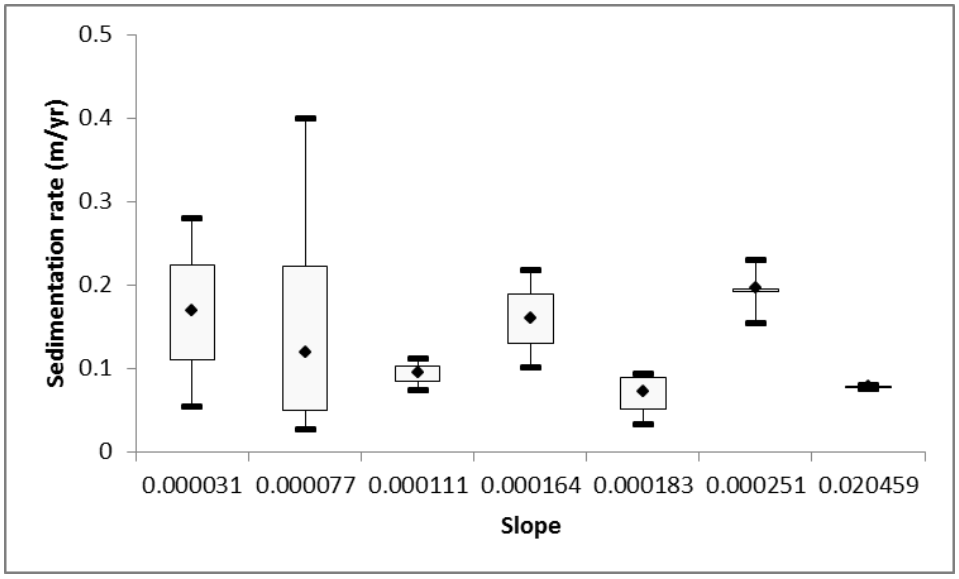

Figure 4.15. Relationship between sedimentation rates and channel slopes presented after Phillips (2006).

Boxplots for rates of sedimentation in six slope gradients classes for the main channel are shown in Figure 4.15. The largest range occurs in the lower two slope classes. Examination of these data suggests that increasing slope results in greater rates of sedimentation.

Boxplots for the two major channel/flow patterns in the study area as shown in Fig. 4.16. All oxbows dated and observed in the study area occur in a class of either a main single thread channel or a single thread channel with tributaries acting as avulsion channels along the river floodplain. The tributaries flow parallel along the main channel through the floodplain. Rates of sedimentation have a greater range in the single thread channel, with the median and 3rd quartile greater in the second channel/flow class. Thus, it can be extrapolated that greater variability occurs in the sediment dynamics between the main channel and the oxbow lake where avulsion channels do not occupy the river

floodplain. Here, the definition of the floodplain includes recent Quaternary sediments deposited between major Tertiary terraces (Waters and Nordt, 1995).

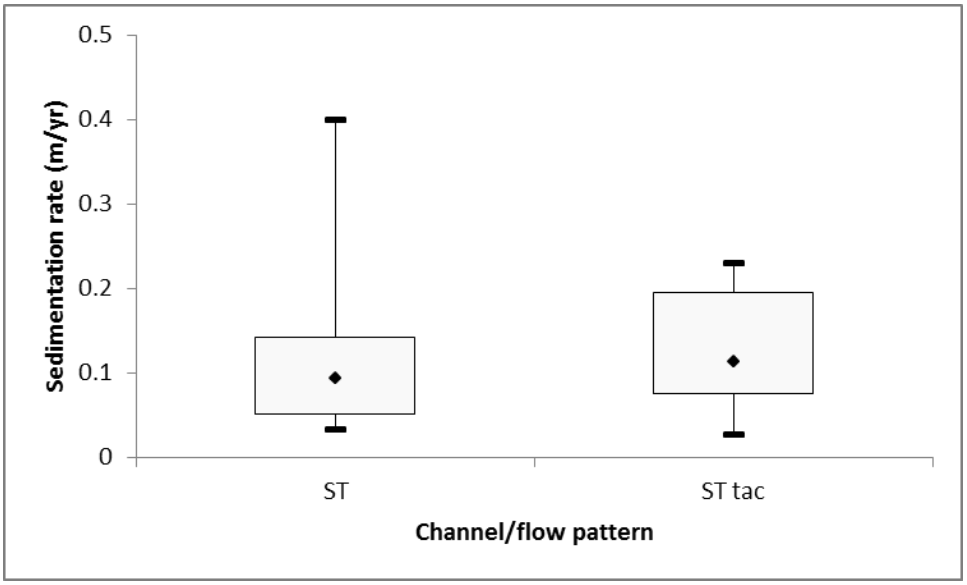

Figure 4.16. Boxplot of sedimentation rates for single thread and single thread with tributaries occupying avulsion channel and flow pattern. Sedimentation rates between the channel types are approximately equal for the majority of data points; ST = single thread channel, ST tac = tributaries occupying avulsion channels.

Of the four classes developed by Phillip (2006), the channel-floodplain connectivity is perhaps most relevant to the evolution of oxbows in the Brazos River watershed, specifically rates of sedimentation contributing to the infilling of abandoned channels. I hypothesized that different connectivity classes would have a marked influence on the rates of sedimentation (Fig. 4.17). The first quartile, median and third quartile rates of sedimentation are relatively close in value, ranging from 0.05 m/yr to 0.2 m/yr. The 'low' connectivity class has the greatest range, but also contains the most oxbow data points. Overall, because I assumed a steady-state nature of the observed

sedimentation rates for the lower Brazos River oxbows (i.e., sedimentation is assumed constant every year in an oxbow) the flood flows required for connection are skewed towards lower values.

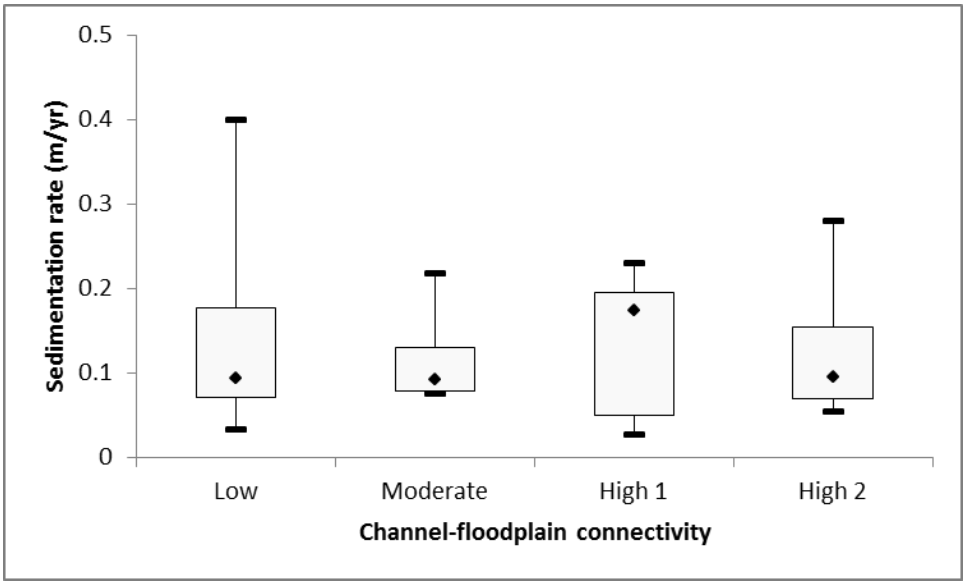

Figure 4.17. Boxplot of sedimentation rates for channel-floodplain connectivity. High 1 is primarily from flooding of oxbows, sloughs, and flood basins; High 2 is from cross-floodplain flow.

Many of the oxbow lakes occur near the boundary between different river reaches outlined by Phillips (2006). The upstream or downstream proximity may influence the geomorphology of many of the oxbows studied in this study.

A strong correlation $R^2 = 0.92$ between the number of connections and the age (i.e., years since cutoff from main channel) of an oxbow lake is shown in Figure 4.18. The number of connections on the horizontal axis for these data points, with each point representing an oxbow lake, is from the field surveys from Osting (2004), whereas the

age of the oxbow is from the analysis of historical maps and aerial photographs. The number of connections is a point-in-time measurement rather than the connection history over the life of the oxbow from disconnect to the main river until final in-filling. This correlation of decreasing connections with increasing age occurs as the abandoned channel slowly fills with sediment.

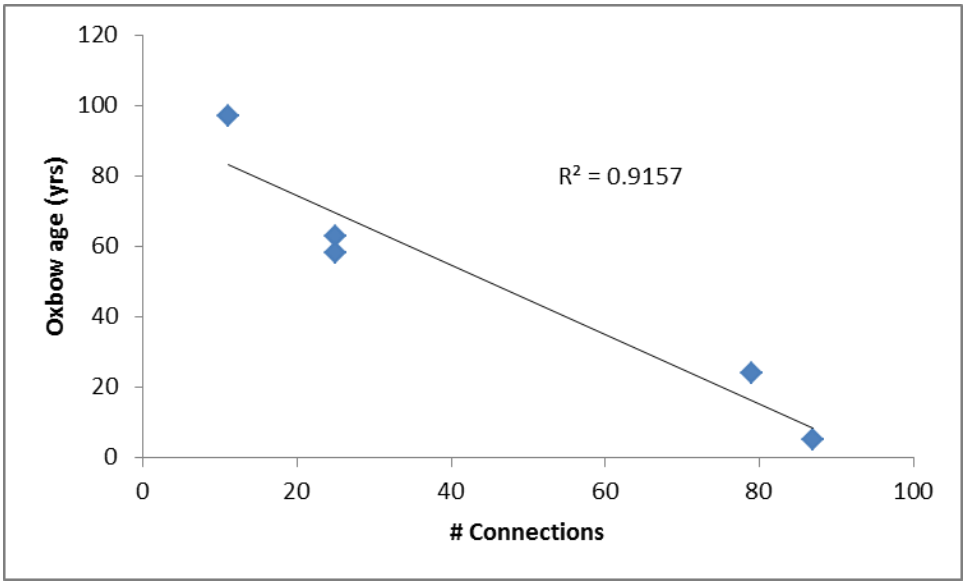

Figure 4.18. Relationship between the number of connections and the age in years of the oxbow. The values for the number of connections is from field surveys taken during one calendar year (Osting, 2004).

The number of connections for each oxbow and the main channel, and the flood-flow or discharge required for those numbers of connection is determined using Equations (3) and (4) (Table 4.5). Because a small number of sites were field surveyed to observe and record the number of oxbow-main channel connections and required discharge, the values in Table 4.5 allow one to investigate the number of actual days,

using the stream discharge data from the gauges in Table 4.1, which the main channel did connect to oxbow lakes, versus the number of connections the between main channel and oxbow. The duration of the reconnection is important, beyond just the absolute number of connections, because connections of longer duration should result in increased sediment deposition.

The relationship between the modeled number of connections, calculated with Equation (4.1), and the age of dated oxbows is displayed in Figure 4.19. Though a weak correlation exists, $R^2 = 0.33$, nonetheless, the general trend is apparent that younger oxbow cutoffs have a greater number of connections with the main channel during high discharge periods.

Table 4.5 Modeled number of connections and modeled flood-flow (m^3/s) needed to reconnect the main channel to oxbow lakes along the Brazos River. This data were used to compare the number of days of a given flood to the modeled number of connections between the main channel and oxbow. The location of oxbow lakes is presented in Figure 4.1 and Table 4.1.

Oxbow Lake	Modeled # Connections	Modeled Flood Flow (m^3/s)
O1	7	1952
O3	19	1327
O4	20	1276
O5	56	595
O6	27	1084
O7	19	1304
O8	15	1495
O9	7	1952
O10	48	700
O11	5	2227
O12	25	1136
O13	25	1147
O14	25	1147
O15	53	625
O16	66	482
O17	37	876
O18	8	1928
O19	6	2064
O20	10	1727
O20	46	729
O21	46	729
O22	50	664
O23	45	737
O24	39	839
O25	18	1339
O26	30	1014
O27	49	686
O28	10	1768

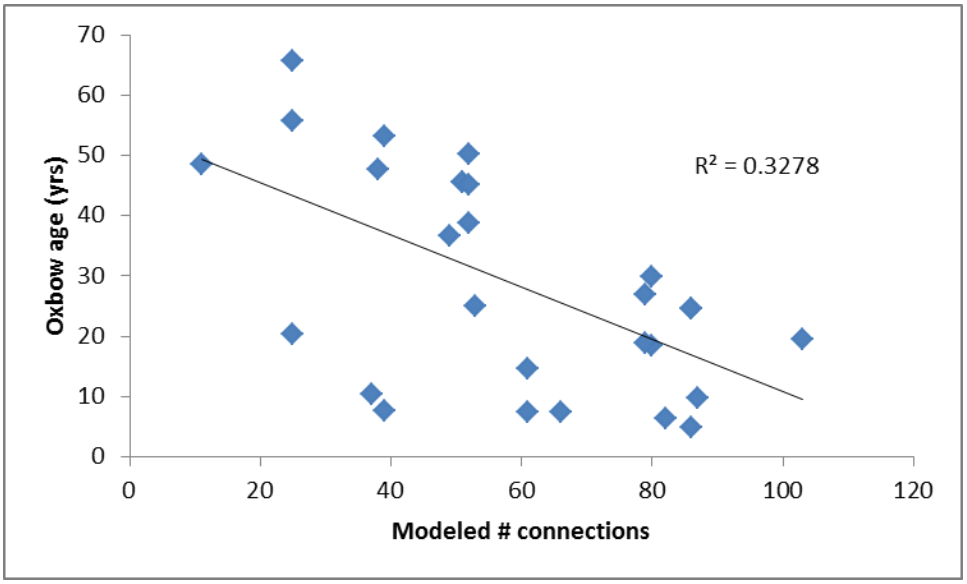

Figure 4.19. Relationship between modeled connections and oxbow cutoff age for entire dataset. The number of connections presented here is dependent on the values obtained in Equation 3.

The correlation shown in Fig. 4.20 is the modeled number of connections compared to the number of days in which the required flood flow for reconnection occurred, as recorded from nearby USGS gauging stations. Only 13 of the 28 dated oxbows are incorporated in the relationship between modeled connections because the cutoff dates for the excluded oxbows were within the period of discharge for the gauging station associated with a particular oxbow. Using historic stream discharges and the relationship between connections and rates of sedimentation, one can estimate the number of days a particular discharge will cause connection between the main channel and the abandoned oxbow lake.

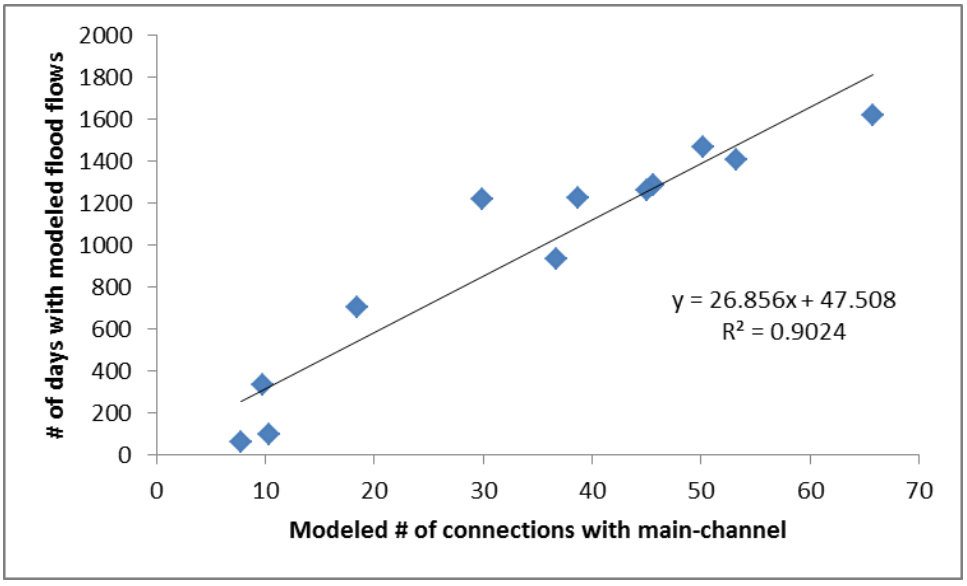

Figure 4.20. Relationship between the number of days with a modeled flood flow and the modeled number of connections with the main channel.

Using the following equation:

$$y = 28.95x - 4.3218 \quad (4.5)$$

where, y is the number of days for a given flood-flow, sufficient to reconnect, and x is the modeled number of connections between the main-channel and oxbow lake. An estimate of the number of days, from the date of channel cutoff to 1999, an oxbow will connect based on the modeled number of connections with the main channel can be accomplished using Equation (4.5). With predicted discharge values, it is possible, in combination with the rates of sedimentation, to estimate when oxbows become relatively disconnected from the main channel and at what point they may sufficiently fill with sediment to disconnect.

The third goal in this study is to categorize the oxbows based in part on the hydrologic properties. Table 4.4 includes the application of an abandoned channel water

body scheme (Phillips, 2011) to the Brazos River oxbow dataset in this work. The determination for each oxbow class was accomplished using the historic discharge records at selected gauging stations, Table 4.1, historic aerial photographs, and a ten-meter resolution digital elevation model (DEM). The before and after aerial photographs of a cutoff were examined to note changes in ratio of vegetation to open channel sands, changes in channel width, presence of tributary streams, and presence of any splay or over bank deposits adjacent to the oxbows. The digital elevation model displays the elevation of the lake relative to the surrounding floodplain, which can determine the pattern of sediment deposition during high discharge events.

Few cutoffs occur as 'fill-and-spill' type, with the majority as 'fill-and-drain'. An interesting result was the large number of 'disconnected' cutoffs, despite the relatively recent date of cutoff. This suggests a rapid infilling of sediment with a rapid tapering off in subsequent decades following channel abandonment. Secondly, note the relatively numerous cutoff lakes categorized as 'tributary occupied'. Of the 28 oxbows, 6 (21%) having tributary streams routing through either the up or downstream of the oxbow ends. This flow pattern affects the sedimentation of the lake and discharge required to connect between the main channel and oxbow. Four of the six 'tributary occupied' oxbows have low rates of sedimentation, with these lakes having been abandoned from the 1890s to 1930s. Thus, the tributaries are effective at routing sediment back towards the main channel. The scheme is appropriate for the oxbows along the middle and lower Brazos River. Additional field research could produce a refinement.

In addition to the flood-flow data shown, work by Hudson (2010) presents data on several of the oxbows dated in this work concerning the wetted lake area and the distance to the main channel from the abandoned channel entrance (Fig. 4.21 & 4.22). As the distance from the main channel decreases, the rates of sedimentation rate generally increases in magnitude, with the highest rates in oxbow lakes that are 0.4 km or less from the main channel is shown in Figure 4.21. 'Distance to main channel' varies over time as the main channel migrates across the floodplain.

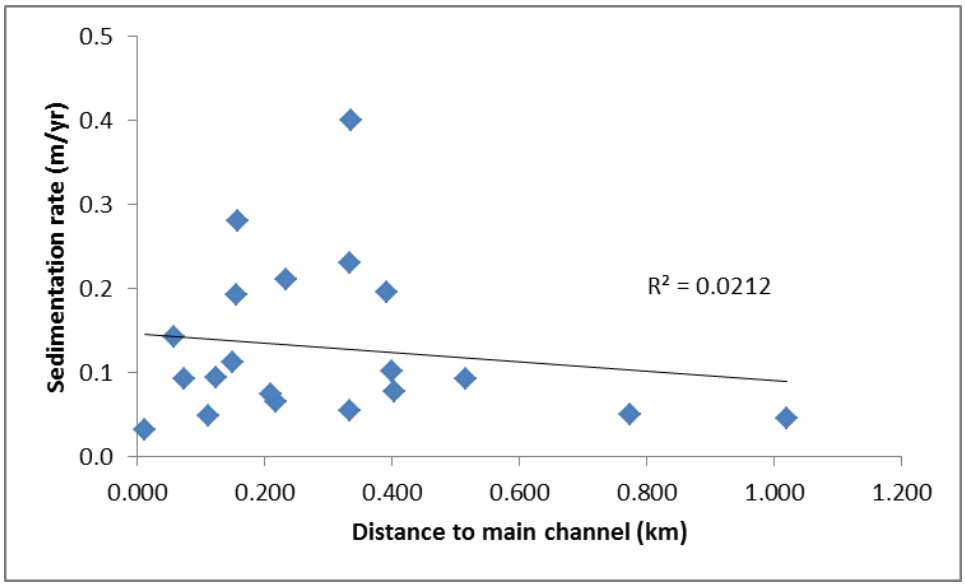

Figure 4.21. Relationship between sedimentation rates and distance to main channel after Hudson (2010).

A weak correlation between the wetted-lake area and rates of sedimentation was found (Fig. 4.22). Though a similar relationship should exist as that between rates of sedimentation and cutoff ratios, the opposite appears to be true, with a more pronounced upward trend. As lake area increases, the rates of sedimentation also increase. This

relationship is opposite of what was shown in Fig. 4.10, whereas the cutoff ratio increases, the lake lengthens relative to the main channel, and the rates of sedimentation decrease. Thus, changes in the width of the abandoned channel between oxbows may explain why rates of sedimentation increase with larger wetted lake area, but decrease with larger cutoff ratios.

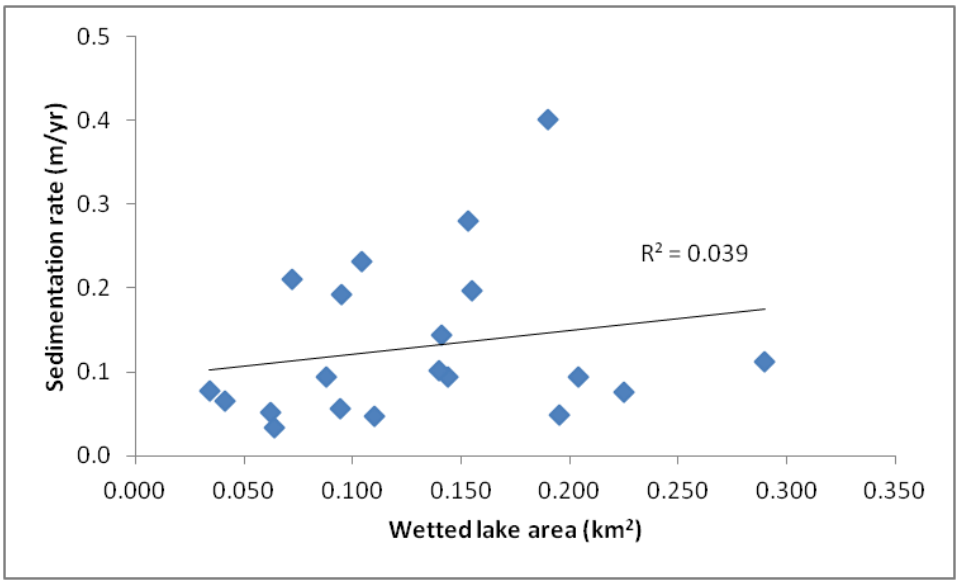

Figure 4.22. Relationships between sedimentation rates and the wetted lake area presented after Hudson (2010).

The highest ratios of sedimentation are found in lakes between 0.15 and 0.20 km^2 in area. Several factors may affect lake area; thus this analysis is tentative. First, groundwater levels in the Brazos River watershed fluctuate significantly, affecting the surface water expression in different fluvial environments (Chowdhury, 2004). Second, evaporation can affect lake levels, and, therefore, area changes over the course of a season. Third, it is difficult to determine the origin of water in the lake, whether it is

remnant water from separation to the main channel or flood water from recent reconnections.

The fourth goal developed a chronology of oxbow lake development from channel meander to cutoff to fully abandoned channel. Morken and Kondolf (2003) developed a model of oxbow lake evolution based on the Sacramento River (Fig. 4.23). From observations on the oxbows in the middle and lower Brazos River floodplain, lakes may reconnect with the main channel during especially high magnitude discharge events.

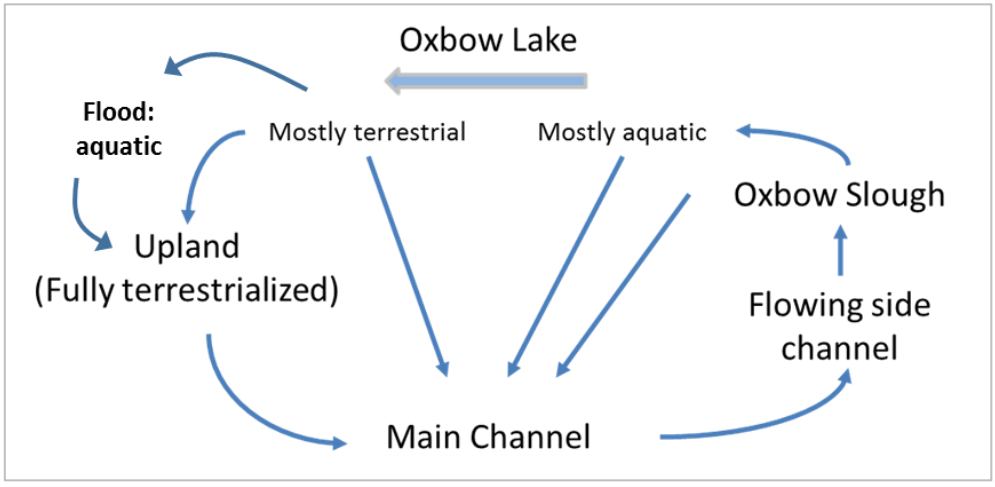

Figure 4.23. Conceptual model of oxbow lake evolution (after Morken and Kondolf, 2003). The addition of a flooding phase where the oxbow is reconnected hydraulically to the main channel may occur during high discharge events in the river.

The Sacramento and Brazos rivers differ in geomorphic properties, including the composition and percentages of suspended and bed load sediments. Despite these differences, the Sacramento model is applicable to the Brazos River oxbows. Dominant influences are the land use within the floodplain and main channel discharge regime.

Unlike the Sacramento River, for which the model was developed on chute cutoffs, the oxbow lakes along the Brazos River are mainly the result of meander cutoff with a narrowing of the meander belt. Therefore, the model may need modification for use in the Brazos River environment, but it does have a good potential for application.

4.7 Summary and Conclusions

This work addresses four components associated with the evolution of oxbows in the middle and lower Brazos River watershed: 1) quantifying the rate of planform oxbow development, or cutoff; 2) quantifying the rates of sediment deposition; 3) categorizing oxbow lakes based upon their morphologic and hydrologic characteristics; and 4) developing a chronology of development of an oxbow lake as it progresses from meandering bend to remnant oxbow lake.

Summarizing the first task, quantifying rates of oxbow development, 28 of the 54 (52%) total oxbow lakes occurring in the middle and lower reaches of the Brazos River are dated as having cutoff on or after 1896, with a cutoff occurring on average every 4.2 years. The oldest cutoff occurred in 1886, whereas the youngest cutoff occurred in 1995.

Summarizing the second task, rates of sedimentation, (m/yr), the average rate ranges from 0.02 to 0.4. From this analysis, the study suggests that the cutoff ratio slightly decreases rates of sedimentation; whereas an increase in diversion angle lowers the rates of sedimentation.

From this study of the various river style reaches it is suggested that many different characteristics result in similar rates of sedimentation. The most marked classes are low slopes and tortuous sinuosity, both which result in higher rates of sedimentation.

Ongoing channel migration removes the depositional sedimentary units of the oxbows. Thus, oxbow dynamics in the middle and lower Brazos watershed are subject to a number of fairly rapid environmental changes.

As supported through the literature, this work provides geomorphic context for channel remnants and the myriad of ecological benefits from these major components of the floodplain. The oxbows in the work are shown to be highly active and large scale features that transition to dormant, i.e., disconnected from the main channel, on human lifespan timescales. As observed, an oxbow lake in the watershed of the Brazos River can go from active erosion and deposition of sediments to a relatively stable, i.e., reconnections only during large discharge or flood events, terrestrial surfaces in one to two decades. The oxbow lakes are highly active in both a spatial and temporal aspect. In the context of the theory of geomorphology pertaining to dynamic equilibrium; these landscapes features are catastrophic, on a local scale, events on a steady time scale represented by the consistent meander of a river across its active floodplain.

The results of this study suggest that a future project should focus on determining how the rate of sedimentation changes as an oxbow fills over time. This important research would negate the steady state assumption, made in this work, concerning the number of oxbow-main channel connections and flood flows required to make the connection. Flood flows and rates of sedimentation will change over time as an oxbow fills with sediments.

5 SUMMARY

This work sought to examine the meandering dynamics of fluvial channels in both the vertical and horizontal space, with an added temporal component. From the three studies; namely step-pool streams along Grand Mesa, and the meandering Brazos River with its adjacent oxbow channel remnants in east-central Texas, one observes the forces of erosion, deposition and landscape formation. Both landscapes, the alpine and the lowland, have undergone substantially changes in the overall composition of their respective watersheds in the last few hundred years. Change is always a constant in surficial geology but the rapid advancement of European settlement altered the magnitude of these changes. Both landscapes contain impoundment surface water, with subsequent changes in energy dissipation over the landscape, and both have land cover and land use changes driven largely by agricultural activities.

Concerning the alpine step-pool streams of Grand Mesa; the reservoir releases down the step-pool streams do not alter the overall channel morphology. Comparing the mesa and mountain-peak topographies; channel widths and wavelength are different, which is attributable to the larger discharge and drainage area of the mountain-peak studies. The particle sizes comprises the steps are similar but height of the steps exhibits little difference between the topographies. Finally, organization and adjustment of sediment and channel forms is continuing along Grand Mesa with the streams along the early evolutionary stage of energy dissipation across the system. Overall, the general variables of the drainage basin such as slope, hydro-cycle, drainage area, etc., explain

the morphologies of channels, as compared to the specific characteristics of individual physiographic provinces.

Meandering along the central portion of the Brazos River shows rates of migration increasing as the average monthly discharge and average yearly discharge increase. The pre-reservoir migration distance is greater (50 to 1,500 m) than the post-reservoir migration distance (10 to 500 m). Overall, the river has decreased in the rates of migration and channel width. Despite this decrease, bank erosion, especially along river reaches with a substantial riparian corridor of large woody plants, continues to be a focus of land and water management strategies, and concern for those living and working in the Brazos River Valley. From this study, one observes the highly non-linear nature of river systems across spatial and temporal scales. It is difficult to pin any one major variable as the driving factor of lateral channel movement. At the multiple-reach scale, both basin-wide features and channel-corridor characteristics affect the rate and form of lateral migration. A notable observation: this large, meandering river in a relatively "flat" prairie topography exhibits characteristics of river systems from other landscapes, namely the major influence of channel confinement by high valley boundaries impeding channel movement. This finding further underlies the evolving nature of the coastal and near-coastal Texas landscape as adjustment continues subsequent to the last major glacial episodes.

The final component of this study of meandering channels is the remnant river segments in the form of oxbow lakes adjacent to the Brazos River. High initial rates of sediment infilling, immediately after cutoff, are examples of a local catastrophic event

on steady time-static equilibrium intervals. From the data gathered in this analysis, combined with previous work by others in the Brazos River floodplain, there is a strong relationship between the age and channel-lake connectivity of these cutoff segments. Under the steady-state conditions established for this study, older oxbows have fewer connections over time, presenting land and resource managers and conservators a tool in understanding the hydrologic relationship, vital to functioning ecosystems, between active and inactive channel components. These floodplain features are highly active, both spatially and temporally, in the river corridor.

REFERENCES

Abrahams, A.D., Li, G., and Atkinson, J.F., 1995. Step-pool streams: adjustment to maximum flow resistance. Water Resources Research 31, 2593-2602.

Allen, J.R., 1982. Sedimentary Structures: Their character and physical basis, Vol. 1. Elsevier Science: Amsterdam, 593 pp.

Asahi, K., Kato, K., and Shimizu, Y., 2003. Estimation of sediment discharge taking into account tributaries to the Ishikari River. Journal of Natural Disaster Science 25, 17-22.

Bagnold, R.A., 1980. An empirical correlation of bedload transport rates in flumes and natural rivers. Proceedings of the Royal Society, London 372, 452-473.

Baker, F., Rundell, J., Hasebi, K., Cole, R., and Aslan, A., 2002. Geomorphic evolution of Grand Mesa, western Colorado. Geological Society of America, paper No. 207-1.

Beeson, C.E., and Doyle, P.F., 1995. Comparison of bank erosion at vegetated and non-vegetated channel bends. Journal of American Water Resources Association 31, 983-990.

Bellmore, R.J., Duda, J. J., Craig, L. S., Greene, S. L., Torgersen, C. E., Collins, M. J. and Vittum, K., 2016. Status and trends of dam removal research in the United States. WIREs Water. doi:10.1002/wat2.1164

Billi, P., D'Agostino, V., Lenzi, M.A., and Marchi, L., 1998. Bedload, slope and channel processes in a high-altitude torrent. In: Klingemann, P.C., Beschta, R.L., Komar P.D. and Bradley, J.B. (Eds.) Gravel-bed rivers in the environment. Highlands Ranch, CO: Water Resources Publications, pp. 15-38.

Billi, P., Preciso, E., and Salemi, E., 2014. Field investigation on step-pool morphology and processes in steep mountain streams. Agriculture and Forestry 60, 7-29.

Briaud, J.L., and Chen, H.C., 2001. Predicting meander migration: evaluation of some existing techniques. Texas Transportation Institute, Report 2105-1, 50 pp.

Briaud, J.L., Chen, H.C., Park, S., and Shah, A., 2002. Meander migration rate: evaluation of some existing methods. Texas Transportation Institute, Report 2105-S, 4 pp.

Briaud, J.L., Chen, H.C., Chang, K.A., Chung, Y.A., Park, N. Wang, W. and Yeh, P.H., 2007. Establish guidance for soil properties-based prediction of meander migration

rate. Texas Department of Transportation, Report FHWA/TX-07/0-4378-1, 334 pp.

Brooks, G.R., and Medioli, B.E., 2003. Deposits and cutoff ages of Horseshoe and Marion oxbow lakes, Red River, Manitoba. Géographie physique et Quaternaire 57, 151-158.

Buckingham, S.E. and Whitney, J.W., 2007. GIS methodology for quantifying channel change in Las Vegas, Neveda. Journal of American Water Resources Association 43, 888-898.

Buraas, E.M., Renshaw, C.E., Magilligan, F.J. and Dade, W.B., 2014. Impact of reach geometry on stream channel sensitivity to extremem floods. Earth Surface Processes and Landforms 39, 1778-1789, doi: 10.1002/esp.3562.

Canovaro, F., Paris, E., and Solari, L., 2004. Influence of macro-roughness arrangement on flow resistance. In: Morte, D., Greco, M., Carravetta. A. (Eds.). River flow 2004. Taylor and Francis Group, London, pp. 287-293.

Chartrand, S.M., and Whiting, P.J., 2000. Alluvial architecture in headwater streams with special emphasis on step-pool topography. Earth Surface Processes and Landforms 25, 583-600.

Chin, A., 1989. Step-pools in stream channels. Progress in Physical Geography 13, 391-407.

Chin, A., 1998. On the stability of step-pool mountain streams. Journal of Geology 106, 56-69.

Chin, A., 1999. The morphologic structure of step-pools in mountain streams, Geomorphology 27, 191-204.

Chin, A., 2002. The periodic nature of step-pool mountain streams. American Journal of Sciences 302, 144-67.

Chin, A., and Wohl, E., 2005. Toward a theory for step pols in stream channels. Progress in Physical Geography 29, 275-296.

Chin, A., Phillips, J.D., 2007. The self-organization of step-pools in mountain streams. Geomorphology 83, 346-358.

Chin, A., Anderson, S., Collison, A., Ellis-Sugai, B.J., Haltiner, J.P., Hogervorst, J.B., Kondolf, G.M., O'Hirok, L.S., Purcell, A.H., Riley, A.L., and Wohl, E.E., 2008.

Linking theory and practice for restoration of step-pool streams. Environmental Management 43, 645-660.

Chowdhury, A.H., 2010. Hydraulic interaction between groundwater, Brazos River and oxbow lakes: evidences from chemical and isotopic compositions, Brazos River Basin, Texas. Texas Water Development Board, Report 375, 69 pp.

Church, M., and Zimmerman, A., 2007. Form and stability of step-pool channels: research progress. Water Resources Research 43, W03415, doi:10.1029/2006WR005037.

Church, M., and Ferguson, R.I., 2015. Morphodynamics: Rivers beyond steady state. Water Resources Research 51, 1883-1897.

Clifford, N., Cope, M., Gillespie, T., and French, S., 2016. Key methods in Geography. Sage Publications, London. 752 pp.

Cole, R.D., and Sexton, J.L., 1981. Pleistocene surficial deposits of the Grand Mesa area, Colorado. New Mexico Geological Society Guidebook, 32nd Field Conference, Western Slope Colorado, pp. 121-126.

Cole, R.D., 2001. Late Cenozoic erosional history of Grand Mesa, Western Colorado. Geology Society of America, Joint Annual Meeting, Rocky Mountain and South-Central Sections, Session No. 13.

Cole, R.D., 2007. The Grand Mesa basalt field, western Colorado. Geological Society of America Annual Meeting Abstracts with Programs, 39, 307.

Comiti, F., Mao, L. (2012) Recent Advances in the Dynamics of Steep Channels. In: Church, M., Biron, P.M., and Roy, A.G. (Eds), Gravel-Bed Rivers: Processes, Tools, Environments. John Wiley & Sons, Ltd, Chichester, UK, pp. 353-374. doi: 10.1002/9781119952497.ch26

Constantine, J.A., Dunne, T., Piégay, H. and Kondolf, G.M., 2010. Controls on the alluviation of oxbow lakes by bed-material load along the Sacramento River, California. Sedimentology 57, 389-407.

Cooper, C.M. and McHenry, J.R., 1989. Sediment accumulation and its effects on a Mississippi River oxbow lake. Environmental Geology and Water Science 13, 33-37.

Curran, J.H., and Wohl, E.E., 2003. Large woody debris and flow resistance in step-pool channels, Cascade Range, Washington. Geomorphology 51, 141-157.

Darling, A., Rider, K., Gloyd, J., and Cole, R.D., 2007. Sedimentologic characteristics of late Cenozoic gravel-armored surfaces on the southwestern flank of Grand Mesa, western Colorado. Geological Society of America Annual Meeting Annual Meeting Abstracts with Programs 39, 307.

David, S. R., Edmonds, D. A., and Letsinger, S. L., 2016. Controls on the occurrence and prevalence of floodplain channels in meandering rivers. Earth Surf. Process. Landforms. doi: 10.1002/esp.4002.

Dijk, W.M., Schuurman, F., van de Lageweg, W.I., and Kleinhans, M.G., 2014. Bifurcation instability and chute cutoff development in meandering gravel-bed rivers. Geomorphology 213, 277-291.

Doyle, M.W., Stanley, E.H., and Harbor, J.M., 2002. Geomorphic analogies for assessing probably channel response to dam removal. Journal of the American water Resources Association 38, 1567-1579.

Duckson, D.W., and Duckson, L.J., 1995. Morphology of bedrock step-pool systems. Water Resources Bulletin, Vol. 31, 43-51.

Duckson, Jr., D.W., and Duckson, L.J., 2001. Channel bed steps and pool shapes along Soda Creek, Three Sisters Wilderness, Oregon. Geomorphology 38, 267-279.

Dunn, D.D., and Raines, T.H., 2001. Indications and potential sources of change in sand transport in the Brazos River, Texas. U.S. Geological Survey Water-Resources Investigations Report 01-4057, 38 pp.

Dunne, T., and Leopold, L.B., 1978. Water in Environmental Planning. San Francisco, W.H. Freeman Co., 818 pp.

Džubáková, K., Piégay, H., Riquier, J., and Trizna, M., 2015. Multi-scale assessment of overflow-driven lateral connectivity in floodplain and backwater channels using LiDAR imagery. Hydrological Processes 29, 2315-2330.

Eakhout, J.P.C., and Hoitink, A.J.F., 2015. Chute cutoff as a morphological response to stream reconstruction: The possible role of backwater. Water Resources Research 51, 3339-3352.

Ellis, M.S., and Gabaldo, V., 1989. Geologic map and cross sections of parts of the Grand Junction and Delta 30'x 60' quadrangles, west-central Colorado: U.S. Geological Survey Coal Investigations Map C-124, scale 1:100,000.

Epps. L.W., 1973. A geologic history of the Brazos River. Baylor Geological Studies, Bulletin 24, 44 p.

Esfahani, F.S., and Keshavarzi, A.R., 2010. How far must trees be cultivated from the edge of the flood plain to provide best river bank protection? International Journal of River Basin Management 8, 109-116.

Everitt, B.L., 1968. Use of the cottonwood in an investigation of the recent history of a flood plain. American Journal of Science 266, 417-439.

Ferguson, R.I., 1984. Kinematic model of meander migration. In: Elliott, C.M. (Eds.), River meandering. American Society of Civil Engineers, New Orleans, pp. 942-951.

Finnegan, N.J., Roe, G., Montgomery, D.R., and Hallet, B., 2005. Controls on the channel width of rivers: Implications for modeling fluvial incision of bedrock. Geological Society of America 33, 229-232. Doi:10.1130/G21171.1.

Gagliano, S.M., and P.C. Howard, 1984. The neck cutoff oxbow lake cycle along the Lower Mississippi River. In: Elliott, C., (Editor), River Meandering. ASCE, New York, pp. 147-158.

Gasiorowski, M., and Hercman, H., 2005. Recent changes of sedimentation rate in three Vistula oxbow lakes determined by 210Pb dating. Geochronometria 24, 33–39.

Gillespie, B.M., 1992. The nature of channel planform change: Brazos River, Texas. PhD thesis, Texas A&M University, 338 p.

Gillespie, B.M., and Giardino, J.R., 1997. The nature of channel planform change: Brazos River, Texas. Texas Journal of Science 49, 109-142.

Gordon, N.D., McMahon, T.A., Finlayson, B.L., Gippel C.J., and Nathan, R.J., 2004. Stream Hydrology: An Introduction for Ecologists. 2nd edition. John Wiley & Sons, New York. 444 pp.

Gordon, E., and Meentemeyer, R.K., 2006. Effects of dam operation and land use on stream channel morphology and riparian vegetation. Geomorphology 82, 412-429.

Graf W.L., 2006. Downstream hydrologic and geomorphic effects of large dams on American rivers. Geomorphology 79, 336-360.

Grant, G.E., Swanson F.J., and Wolman, M.G., 1990. Pattern and origin of stepped-bed morphology in high gradient streams, western Cascades, Oregon. Geological Society of America Bulletin 102, pp. 340-352.

Gray, A.B., Pasternack, G.B., Watson, E.B., and Goñi, M.A., 2016. Abandoned channel fill sequences in the tidal estuary of a small mountainous, dry-summer river. Sedimentology, 63. doi: 10.1111/sed.12223.

Gregory, K.J., 1985. The Nature of Physical Geography. Edward Arnold, London, 262 pp.

Guneralp, I., and Rhoads, B.L., 2010. Spatial autoregressive structure of meander evolution revisited. Geomorphology 120, 91-106.

Gurnell, A.M., Downward, S.R., and Jones, R., 1994. Channel planform change on the River Dee meanders, 1876-1992. Regulated Rivers: Research and Management 9, 187-204.

Hail, Jr., W.J., 1972. Reconnaissance geologic map of the Cedaredge Area, Delta County, Colorado. U.S. Geological Survey, Miscellaneous Geologic Investigations Map 1-697.

Halwas, K.L., and Church, M., 2002. Channel units in small, high gradient streams on Vancouver Island, British Columbia. Geomorphology 43, 243-256.

Harrison, L.R., Dunne, T., and Fisher, G.B., 2015. Hydraulic and geomorphic processes in an overbank flood along a meandering, gravel-bed river: implications for chute formation. Earth Surface Processes and Landforms 40, 1239-1253. doi: 10.1002/esp.3717.

Hauer, C., Mandlburger, G., Schober, B., and Habersack, H., 2014. Morphologically related integrative management concept for reconnecting abandoned channels based on airborne Lidar data and habitat modeling. River Research and Applications 30, 537-556.

Haugerud, R.A., Harding, D.J., Johnson, S.Y., Harless, J.L., Weaver, C.S., and Sherrod, B.L., 2003. High-resolution Lidar topography of the Puget Lowland, Washington-A bonanza for Earth Science. GSA Today 13, 4-10.

Heitmuller, F.T., 2014. Channel adjustments to historical disturbances along the lower Brazos and Sabine Rivers, south-central USA. Geomorphology 204, 382-398.

Hickin, J.M., 1974. The development of river meanders in natural river channels. American Journal of Science 274, 414-42.

Hickin, E.J. and Nanson, G.C., 1975. The character of channel migration on the Beatton River, north-east British Columbia, Canada. Bulletin of the Geological Society of America 86, 487-94.

Hickin, E.J. and Nanson, G.C., 1984. Lateral migration rates of rivers bends. Journal of Hydraulic Engineering 110, 1557-67.

Heede, B.H., 1984. Changes in river meanders: a review of techniques and results of analyses. Progress in Physical Geography 8, 473-508.

Holland, M.M. and Burk, C.J., 1982. Relative ages of western Massachusetts oxbow lakes. Northeastern Geology 4, 23-32.

Hooke, J.M., 1995. River channel adjustment to meander cutoffs on the River Bollin and River Dane, northwest England. Geomorphology 14, 235-253.

Hooke, S.J., 2008. Temporal variations in fluvial processes on an active meandering river over a 20-year period. Geomorphology 100, 3-13.

Hudson, P., 2010. Floodplain lake formation and dynamics in the lower reaches of the large Texas coastal plain rivers: Brazos, Guadalupe, and San Antonio rivers. Texas Water Development Board, Contract Report No. 0600010583, 100 p.

Hughes, M.L., McDowell, P.F., and Marcus, W.A., 2006. Accuracy assessment of georectified aerial photographs: Implications for measuring lateral channel movement in a GIS. Geomorphology 74, 1-16.

Ishii, Y. and K. Hori, 2015. Formation and infilling of oxbow lakes in the Ishikari lowland, northern Japan. Quaternary International 397, 136-146. doi: 10.1016/j.quaint.2015.06.016.

Jiménez, M.A., and Wohl, E., 2013. Solute transport modeling using morphological parameters of step-pool reaches. Water Resources Research 49, 1345-1359.

Johnson, K.N. and Finnegan, N.J., 2015. A lithologic control on active meandering in bedrock channels. Bulletin of the Geological Society of America 127, 9-10. doi: 10.1130/B31184.

Judd, H.E., 1964. A study of bed characteristics in relation to flow in rough, high-gradient natural channels. Ph.D. Thesis, Utah State University, 182 p.

Keller, E.A., and Melhorn, W.M., 1978. Rhythmic spacing and origin of pools and riffles. Geological Society of America Bulletin 89, 723-730.

Kinoshita, R., 1961. Investigation of channel deformation in Ishikari River. Report for the Bureau of Resources No. 36, Department of Science and Technology, Japan.

Knighton, D., 1998: Fluvial forms & processes: a new perspective. Hodder Education, London. 383 pp.

Kondolf, G.M., 1997. Hungry Water: Effects of dams and gravel mining on river channels. Environmental Management 21, pp. 533-551.

Kondolf, G.M., and Podolak, K., 2014. Space and time scales in human-landscape systems. Environmental Management 53, 76-87.

Konsoer, K.M., Rhoads, B.L., Langendoen, E.J., Best, J.L., Ursic, M.E., Abad, J.D., and Garcia, M.H., 2016. Spatial variability in bank resistance to erosion on a large meandering, mixed bedrock-alluvial river. Geomorphology 252, 80-97.

Lagasse, P.F., Zevenbergen, L.W., Sptiz, W.J., and Thorne, C.R., 2004. Methodology for predicting channel migration. National Cooperative Highway Research Program, Transportation Research Board, NCHRP doc-67, 214 pp.

Lancaster, S.T., and Bras, R.L., 2002. A simple model of river meandering and its comparison to natural channels. Hydrological Processes 16, 1-26.

Lauer, J.W., and Parker, G., 2008. Net local removal of floodplain sediment by river meander migration. Geomorphology 96, 123-149.

Lawler, D.M., 1992. Process dominance in bank erosion systems. In Carling, P.A. and Petts, G.E. (Eds), Lowland floodplain rivers. Wiley, Chichester, pp. 117-43.

Lazarus, E.D., and Constantine, J.A., 2012. Generic theory for channel sinuosity. Proceedings of the National Academy of Sciences 110, 8447-8452. doi: 10.1073/pnas.124074110.

Lenzi, M.A., 2001. Step-pool evolution in the Rio Cordon, Northeastern Italy. Earth Surface Processes and Landforms 26, 991-1008. doi: 10.1002/esp.239.

Lenzi, M.A., 2002. Stream bed stabilization using boulder check dams that mimic step-pool morphology features in Northern Italy. Geomorphology 45, 243-260.

Leopold, L.B., Wolman, M.G., and Miller, J.P., 1964. Fluvial Processes in Geomorphology. Freeman, San Francisco. 522 pp.

Leopold, L.B., and Maddock, T.J., 1953. Hydraulic geometry of stream channels and some physiographic implications. U.S. Geological Survey Professional Paper 252, 55 p.

Leopold, L.B., 1970. An improved method for size distribution of stream-bed gravel. Water Resources Research 6, 1357-1366.

Leopold, L.B., 1973. River channel change with time – an example. Geological Society of America Bulletin. 84, 1845-1860.

Leopold, L.B., 1994. A view of the river. Harvard University Press, London. 320 pp.

Lesack, L.F.W., and Marsh, P., 2010. River-to-lake connectivities, water renewal, and aquatic habitat diversity in the Mackenzie River Delta. Water Resources Research 46, W12504. doi: 10.1029/2010WR009607.

Lewis, G. W. and Lewin, J., 1983. Alluvial Cutoffs in Wales and the Borderlands. In: Collinson, J.D., and Lewin, J. (Eds.), Modern and Ancient Fluvial Systems, Special Publications of the International Association of Sedimentologists 6. Blackwell Publishing Ltd., Oxford, UK, pp 145-154. doi: 10.1002/9781444303773.ch11.

MacFarlane, W.A., and Wohl, E.E., 2003. Influence of step composition on step geometry and flow resistance in step-pool streams of the Washington Cascades. Water Resources Research 39, 1037.

Magiligan, F.J., Nislow, K.H., Kynard, B.E., and Hackman, A.M., 2016. Immediate changes in stream channel geomorphology, aquatic habitat, and fish assemblages following dam removal in a small upland catchment. Geomorphology 252, 158-170.

Marren, P.M., Grove, J.R., Webb, A., and Stewardson, M.J., 2014. The potential for dams to impact lowland meandering river floodplain geomorphology. The Scientific World Journal, 24 pp. doi: 10.1155/2014/309673.

Martha, T.R., Sharma A., and Kumar, K.V., 2015. Development of meander cutoffs-a multi-temporal satellite-based observation in parts of Sindh River, Madhya Pradesh, India. Arabian Journal of Geosciences 8, 5663-5668.

Massong, D.A., and Montgomery, D.R., 2000. Influence of sediment supply, lithology and wood debris on the distribution of bedrock and alluvial channels. Geological Society of America Bulletin 112, 591-599.

Mathewson, C.C., and Minter, L.L., 1981. Impact of water resource development on the hydrology and sedimentology of the Brazos River, Texas with implications on shoreline erosion. Association of Environmental & Engineering Geologists 18, 39-53. doi: https://doi.org/10.2113/gseegeosci.xviii.1.39.

McBoom, M., Ringer M., and Zhang, Y., 2014. Instream woody debris and riparian forest characteristics in the Sabine River, Texas. Southeastern Naturalist 13, 1-14.

McDowell, P.F., 2013. Geomorphology in the late twentieth century. In: Shroder, J. (Editor in Chief), Orme, A.R., Sack, D. (Eds.), Treatise on Geomorphology. Academic Press, San Diego, CA, vol. 1, The Foundations of Geomorphology, pp. 108–123.

Micheli, E.R., Kirchner, J.W., and Larsen, E.W., 2004. Quantifying the effect of riparian forest versus agricultural vegetation on river meander migration rates, Central Sacramento River, California, USA. River Research Applications 20, 537-548.

Milzow C., Molnar, P., McArdell, B.W., and Burlando, P., 2006. Spatial organization in the step-pool structure of a steep mountain stream (Vogelbach, Switzerland). Water Resources Research 42, WO4418.

Molnar, P., Densmore, A.L., McArdell, B.W., Turowski, J.M., and Burlando, P., 2010. Analysis of changes in the step-pool morphology and channel profile of a steep mountain stream following a large flood. Geomorphology 124, 85-94.

Montgomery, D.R., Buffington, J.M., Smith, R.D., Schmidt, K.M., and Press, G., 1995. Pool spacing in forest channels. Water Resources Research 31, 1097-1105.

Montgomery, D.R., and Buffington, J.M., 1997. Channel reach morphology in mountain drainage basins. Geological Society of American Bulletin 109, 596-611.

Moody, L. F., 1944. Friction factors for pipe flow. Transactions of the ASME 66, 671–684.

Morais, E.S., Rocha, P.C., and Hooke, J. 2016. Spatiotemporal variations in channel changes caused by cumulative factors in a meandering river: The lower Peixe River, Brazil. Geomorphology 273, 348-360.

Morken, I., and Kondolf, G.M., 2003. Evolution assessment and conservation strategies for Sacramento River oxbow habitats. The Nature Conservancy, Sacramento River Project, 50 p.

Nanson, G.C., and Hickin, E.J., 1986. Statistical analysis of bank erosion and channel migration in western Canada. Geological Society of America Bulletin 97, 497-504.

Nicoll, T.J., and Hickin, E.J., 2010. Planform geometry and channel migration of confined meandering rivers on the Canadian prairies. Geomorphology 116, 37-47.

O'Connor, J.E., Jones, M.A., and Haluska, T.L., 2003. Flood plain and channel dynamics of the Quinault and Queets Rivers, Washington, USA. Geomorphology 51, 31-59.

Osting, T., Furnans, J., and Mathews, R., 2004. Surface connectivity between six oxbow lakes and the Brazos River, Texas. Texas Water Development Board Report, 152 p.

Phillips, J.D., 1999. Divergence, convergence, and self-organization in landscapes. Annals of the Association of American Geographers 89, 466-488.

Phillips, J.D., 2006. Field data collection in support of geomorphic classification of the lower Brazos and Navasota Rivers. Texas Water Development Board Report, 100 p.

Phillips, J.D., 2011. Hydrological connectivity of abandoned channel water bodies on a coastal plain river. River Res. Applications, p. 12. doi: 10.1002/rra.1586.

Piégay, H., Bornette, G., Citterio, A., Hérouin, Moulin, B., and Statiotis, C., 2000. Channel instability as a control on silting dynamics and vegetation patterns within perifluvial aquatic zones. Hydrological Processes 14, 3011-3029.

Piégay, H., Bornette, G., and Grante, P., 2002. Assessment of silting-up dynamics of eleven cut-off channel plugs on a free-meandering river (Ain River, France). In: Allison, R.J. (Eds.) Applied Geomorphology. John Wiley & Sons. New York. pp. 227-247.

Pierce, K.L., 2003. Pleistocene glaciations of the Rocky Mountains. Development in Quaternary Science 1, ISSN 1571-0866. doi: 10.1016/S1571-0866(03)01004-2.

Recking, A., Leduc, P., Liébault, F., and Church, M., 2012. A field investigation of the influence of sediment supply on step-pool morphology and stability. Geomorphology 139, 53-66, doi:10.1016/j.geomorph.2011.09.024.

Reid, H.E., and Brierley, G.J., 2015. Assessing geomorphic sensitivity in relation to river capacity for adjustment. Geomorphology 251, 108-121.

Reynolds, R.L., Rosenbaum, J.G., van Metre, P., Tuttle, M., Callender, E., and Goldin, A., 1999. Greigite (Fe_3S_4) as an indicator of drought – the 1912-1994 sediment magnetic record from White Rock Lake, Dallas, Texas, USA. Journal of Paleolimonology 21, 193-206.

Rhoads, E.L., M.A. O'Neal, and Pizzuto, J.E., 2009. Quantifying bank erosion on the South River from 1937 to 2005, and its importance in assessing Hg contamination. Applied Geography 29, 125-134.

Rhoads, B.L., Lewis, Q.W., and Andresen, W., 2016. Historical changes in channel network extent and channel planform in an intensively managed landscape: Natural versus human-induced effects. Geomorphology 252, 17-31.

Richard, G.A., Julien, P.Y., and Baird, D.C., 2005. Statistical analysis of lateral migration of the Rio Grande, New Mexico. Geomorphology 71, 139-155.

Richardson, J.M. and Fuller, I.C., 2010. Quantification of channel planform change on the lower Rngitikei River, New Zealand, 1949-2007: response to management? Palmerston North. N.Z.: Massey University. School of People, Environment and Planning, 27 p.

Ritter, D.F., Kochel, R.C., and Miller, J.R., 2006. Process Geomorphology, 4th edition. Waveland Press, Inc, Long Grove, IL. 560 pp.

Rowland, J.C., Lepper, K., Dietrich, W.E., Wilson, C.J., and Sheldon, R., 2005. Tie channel sedimentation rates, oxbow formation age and channel migration rate from optically stimulated luminescence (OSL) analysis of floodplain deposits. Earth Surface Processes and Landforms 30, 1161-1179.

Schmidt, J., and Wilcock, P.R., 2008. Metrics for assessing the downstream effects of dams. Water Resources Research 44, 19 p.

Schumm, S.A. 1977. The fluvial system. Wiley-Interscience, New York. 338 pp.

Schuurman, F., Shimizu, Y., Iwasaki, T., Kleinhans, M.G., 2016. Dynamic meandering in response to upstream perturbations and floodplain formation. Geomorphology 253, 94-109.

Schwendel, A.C., Nicholas, A.P., Aalto, R.E., Sambrook Smith, G.H., and Buckley, S., 2015. Interaction between meander dynamics and floodplain heterogeneity in a large tropical sand-bed river: the Rio Beni, Bolivian Amazon. Earth Surface Processes and Landforms, 40. doi: 10.1002/esp.3777.

Shah, S.D., Houston, N.A., and Braun, C.L., 2007. Hydrogeologic characterization of the Brazos River alluvium aquifer, Bosque County to Fort Bend County, Texas. U.S. Geological Survey, Scientific Investigations Map 2989, 5 sheets.

Shields, F.D., Simon, A., and Steffen, L.J., 2000. Reservoir effects on downstream river channel migration. Environmental Conservation 27, 54-66.

Stolum, H.H., 1996. River meandering as a self-organisation process. Science 271, 1710-1713.

Texas Board of Water Engineers, 1960. Channel gain and loss investigations, Texas streams, 1918-1958. Texas Board of Water Engineers Bulletin 5807D, 270 p.

Texas Instream Flow Program, 2009. Middle & Lower Brazos Study Design Workgroup. February 9, 2009.

Texas Water Development Board, 2008. Texas Instream Flow Studies: Technical Overview. Report 369, 147 pp.

Tower, W.S., 1904. The development of cut-off meanders. Bulletin of the American Geographical Society 36, 589-599.

Turco, M.J., East, J.W., and Milburn, M.S., 2007. Base flow (1966-2005) and streamflow gain and loss (2006) of the Brazos River, McLennan County to Fort Bend County, Texas: U.S. Geological Survey Scientific Investigations Report 2007-5286, 27 p.

Urban, M.A., and Rhoads, B.L., 2004. Catastrophic human-induced change in stream-channel planform and geometry in an agricultural watershed, Illinois, USA. Annals of the Association of American Geographers 93, 783-796.

Waters, M.R., and Nordt, L.C., 1995. Late Quaternary floodplain history of the Brazos River in East-Central Texas. Quaternary Research 43, 311-319.

Wertz, J.B., 1966. The flood cycle of ephemeral streams in the south-western United States. Association of American Geographers 56, 598-633.

Whittaker, J.G., and Jaeggi, M.N.R., 1982. Origin of step-pool systems in mountain streams. Proceedings of the American Society of Civil Engineers, Journal of the Hydraulics Division 108, 758-73.

Whittaker, J.G., 1987. Sediment transport in step-pool streams. In: Thorne, C.R., J.C. Bathurst, R.D. Hey (Eds.), Sediment Transport in Gravel-bed Rivers. Wiley, Chichester, pp. 545-579.

Wilcox, A.C., and Wohl, E.E., 2007. Field measurements of three-dimensional hydraulics in a step-pool channel. Geomorphology 83, 215-231.

Wilcox, A.C., Wohl, E.E., Comiti, F., and Mao, L., 2011. Hydraulics, morphology, and energy dissipation in an alpine step-pool channel. Water Resources Research, Vol. 47, W07514, doi: 10.1029/2010WR010192.

Williams, G.P., 1986. River meanders and channel size. Journal of Hydrology 88, 147-164.

Williams, F., and Chronic, H., 2014. Roadside geology of Colorado, Third Edition. Mountain Press Publishing Company, Montana. 416 pp.

Winterbottom, S.J., and Gilvear, D.J., 2000. A GIS-based approach to mapping probabilities of river bank erosion: regulated River Tummel, Scotland. Regulated Rivers-Research and Management 16, 127-140.

Winterbottom, S.J., 2000. Medium and short-term channel planform changes on the Rivers Tay and Tummel, Scotland. Geomorphology 34, 195-208.

Wittmann, H., von Blanckenburg, F., Kruesmann, T., Norton, K.P., and Kubik, P.W., 2007. Relation between rock uplift and denudation from cosmogenic nuclides in river sediment in the Central Alps of Switzerland. Journal of Geophysical Research 112, 1-20. doi: 10.1029/2006JF000729.

Wohl, E.E., and Grodek, T., 1994. Channel bed-steps along Nahal Yael, Negev desert, Israel. Geomorphology 9, 117-126.

Wohl, E.E., 2000. Substrate influences on step-pool sequences in the Christopher Creek Drainage, Arizona. Journal of Geology 108, 121-129.

Wohl, E.E., Kuzma, J.N., and Brown, N.E., 2004. Reach-scale channel geometry of a mountain river. Earth Surface Processes and Landforms 29, 969-981.

Wohl, E.E., and Wilcox, A., 2005. Channel geometry of mountain streams in New Zealand. Journal of Hydrology 300, 252-266.

Wohl, E.E., 2015. River in the Critical Zone. Developments in the Critical Zone 19, 267-293.

Wolman, M.G., 1954. A method of sampling coarse river-bed material. Transactions American Geophysical Union 35, 951-956.

Wolman, M.G., and Leopold, L.B., 1957. River flood plains: some observations on their formation. U.S Geological Survey Professional Paper 282-C. 30 p.

Wooldridge, C.L., and Hickin, E.J., 2002. Step-pool and cascade morphology, Mosquito Creek, British Columbia: a test of four analytical techniques. Canadian Journal of Earth Sciences 39, 493-503.

Yeend, W.E., 1969. Quaternary geology of the Grand and Battlement Mesas area, Colorado: U.S. Geological Survey Professional Paper 617, 50 p.

Zimmermann, A., and Church, M., 2001. Channel morphology, gradient profiles and bed stresses during flood in a step-pool channel. Geomorphology 40, 311-327.

Zimmermann, A., Church, M., and Hassan, M.A., 2008. Identification of steps and pools from stream longitudinal profile data. Geomorphology 102, 395-406.

Zimmermann, A., 2009. Experimental investigations of step-pool channel formation and stability. Ph.D. Thesis, University of British, Vancouver, .

Zimmermann, A.E., 2013. Step-pool channel features. In: Shroder, J. (Editor in Chief), Wohl, E. (Ed.), Treatise on Geomorphology. Academic Press, San Diego, CA, vol. 9, Fluvial Geomorphology, pp. 346-363.

APPENDIX A

Sediment Budget – Meander Maps

The following maps depict areas of erosion and deposition along the thirty three freely migrating meanders. Each image denotes the areal extent for a particular time period. The polygon enclosing each meander is shown only to delineate the boundaries of an individual meander. The deposition values show the data as the older year *minus* the younger year, while the erosion is shown as the younger year *minus* the older year.

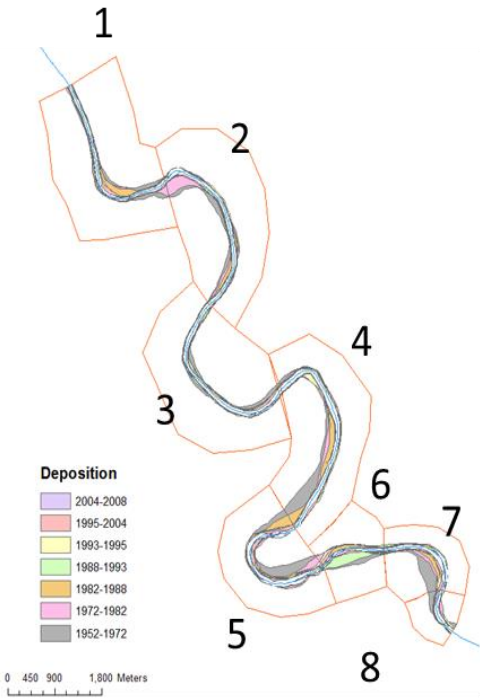
1
2
3
4
5
6
7
8
Deposition
2004-2008
1995-2004
1993-1995
1988-1993
1982-1988
1972-1982
1952-1972
0 450 900 1,800 Meters

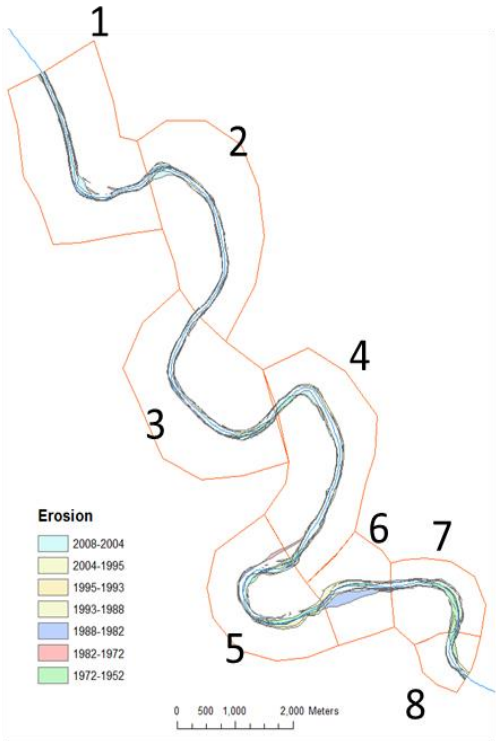
1
2
3
4
5
6
7
8
Erosion
2008-2004
2004-1995
1995-1993
1993-1988
1988-1982
1982-1972
1972-1952
0 500 1,000 2,000 Meters

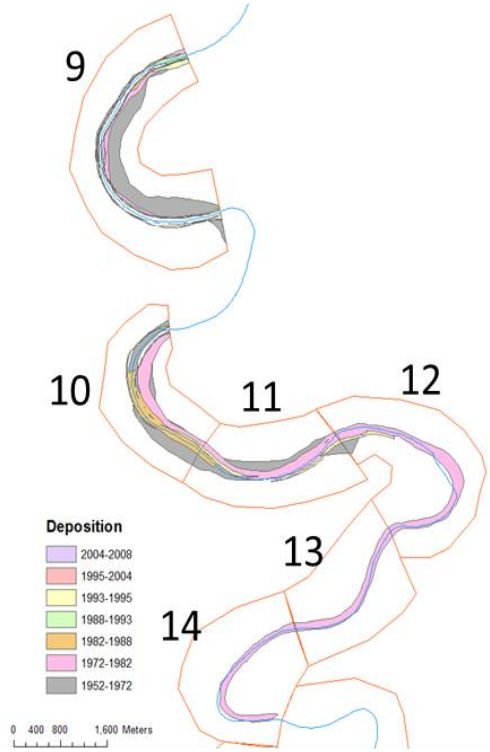
9
10
11
12
13
14
Deposition
2004-2008
1995-2004
1993-1995
1988-1993
1982-1988
1972-1982
1952-1972
0 400 800 1,600 Meters

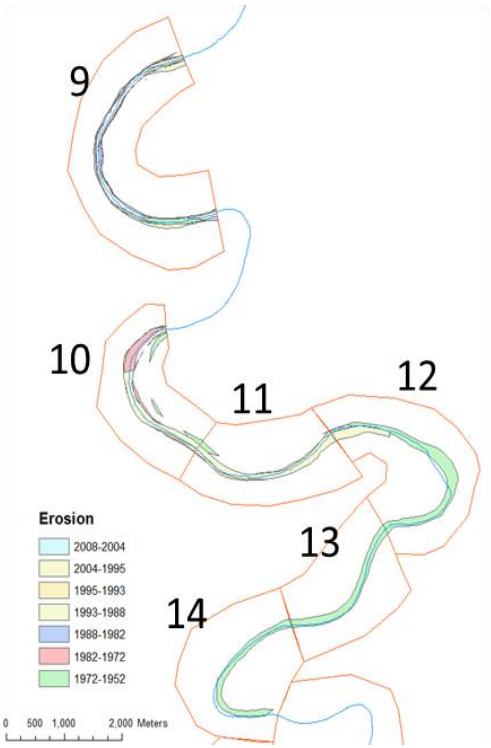
9
10
11
12
13
14
Erosion
2008-2004
2004-1995
1995-1993
1993-1988
1988-1982
1982-1972
1972-1952
0 500 1,000 2,000 Meters

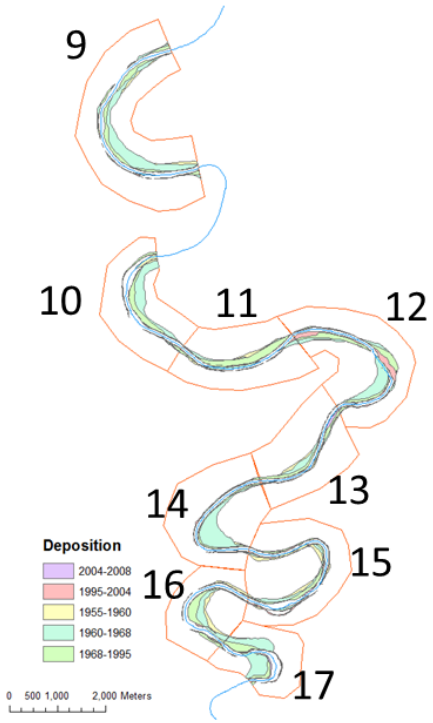
9
10
11
12
13
14
15
16
17
Deposition
2004-2008
1995-2004
1955-1960
1960-1968
1968-1995
0 500 1,000 2,000 Meters

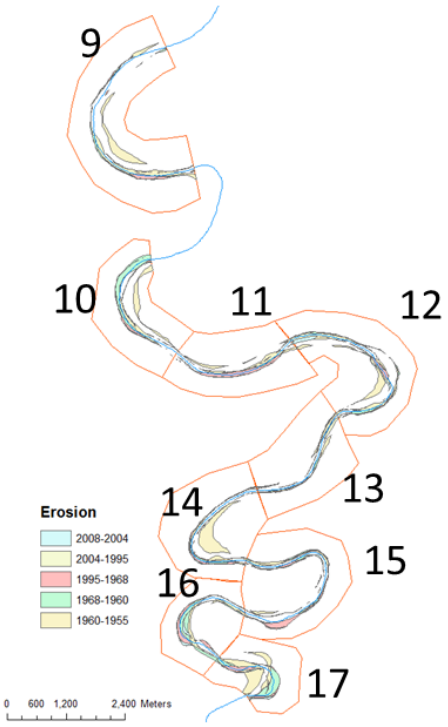
9
10
11
12
13
14
15
16
17
Erosion
2008-2004
2004-1995
1995-1968
1968-1960
1960-1955
0 600 1,200 2,400 Meters

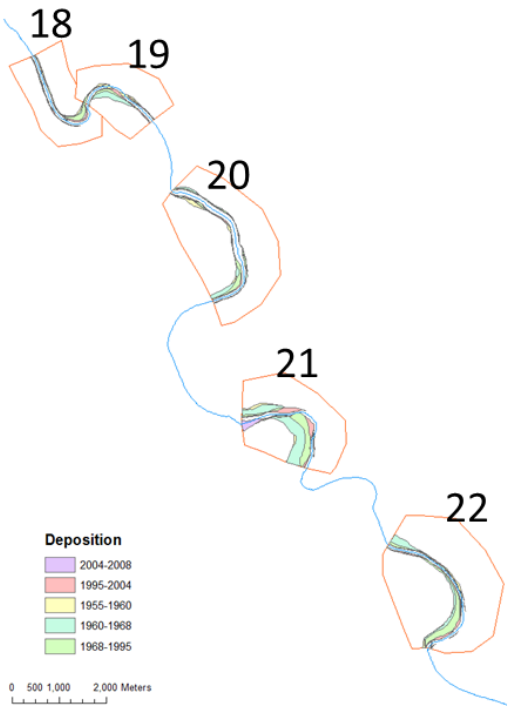
18
19
20
21
22
Deposition
2004-2008
1995-2004
1955-1960
1960-1968
1968-1995
0 500 1,000 2,000 Meters

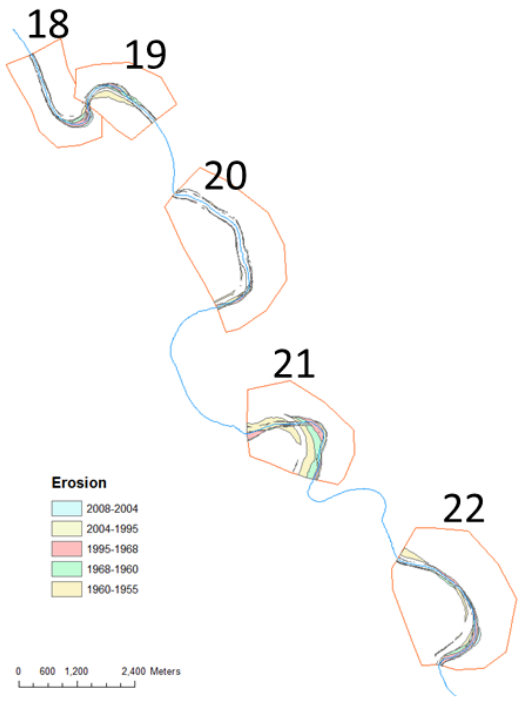
18
19
20
21
22
Erosion
2008-2004
2004-1995
1995-1968
1968-1960
1960-1955
0 600 1,200 2,400 Meters

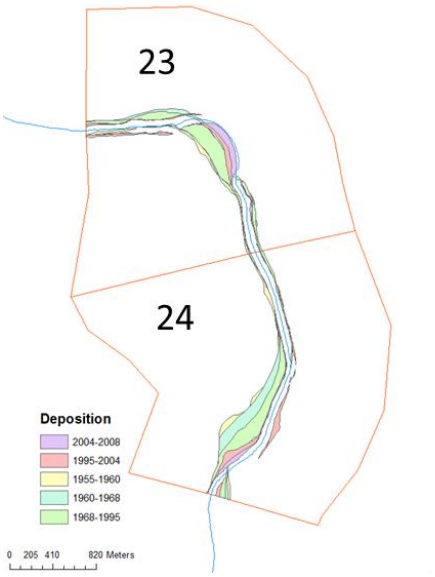
23
24
Deposition
2004-2008
1995-2004
1955-1960
1960-1968
1968-1995
0 205 410 820 Meters

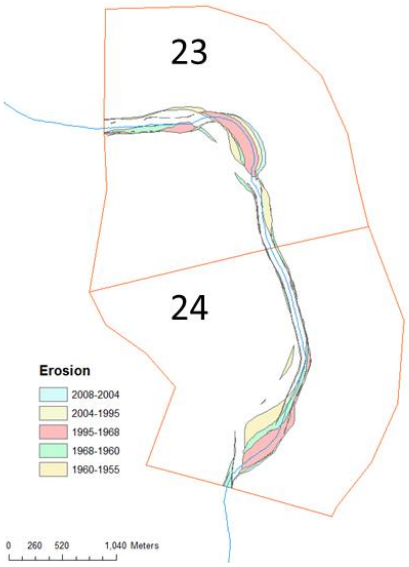
23
24
Erosion
2008-2004
2004-1995
1995-1968
1968-1960
1960-1955
0 260 520 1,040 Meters

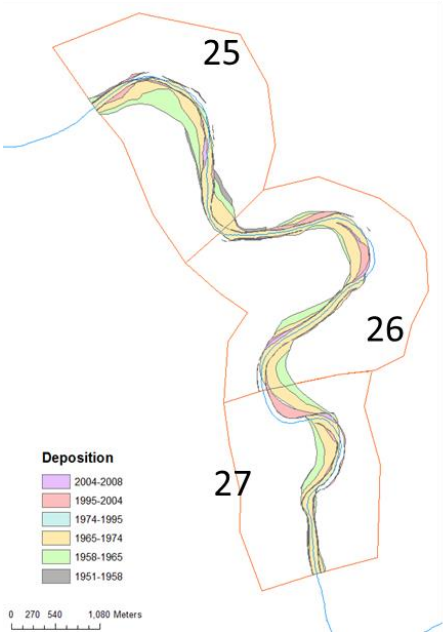
25
26
27
Deposition
2004-2008
1995-2004
1974-1995
1965-1974
1958-1965
1951-1958
0 270 540 1,080 Meters

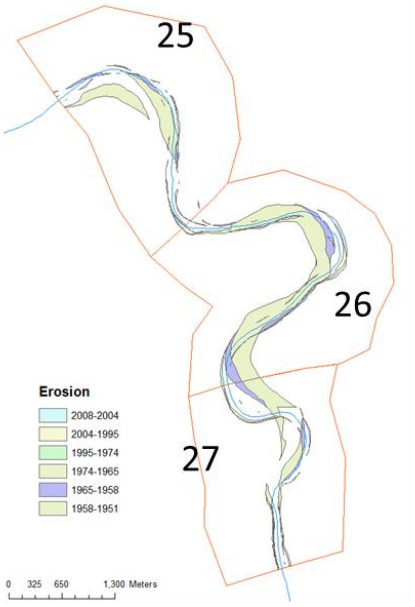
25
26
27
Erosion
2008-2004
2004-1995
1995-1974
1974-1965
1965-1958
1958-1951
0 325 650 1,300 Meters

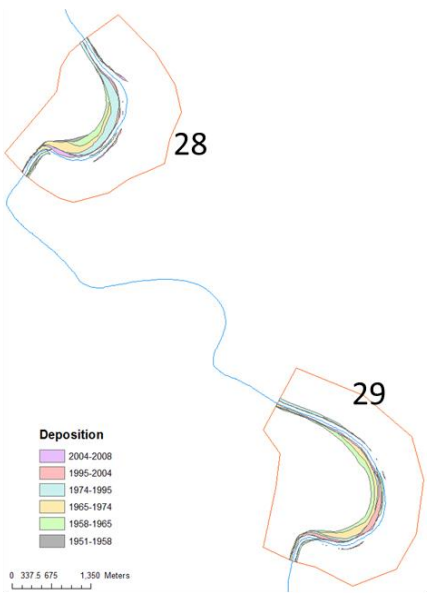
28
29
Deposition
2004-2008
1995-2004
1974-1995
1965-1974
1958-1965
1951-1958
0 337.5 675 1,350 Meters

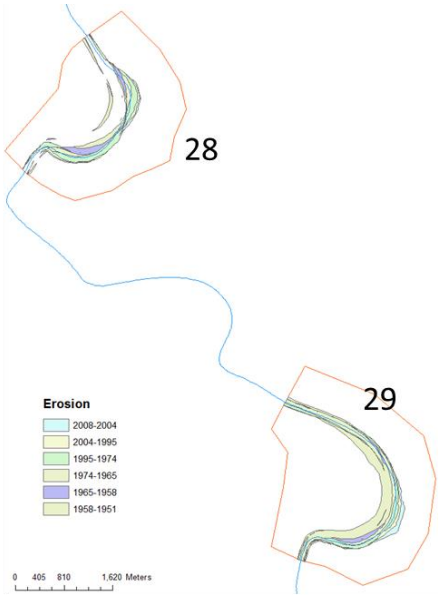
28
29
Erosion
2008-2004
2004-1995
1995-1974
1974-1965
1965-1958
1958-1951
0 405 810 1,620 Meters

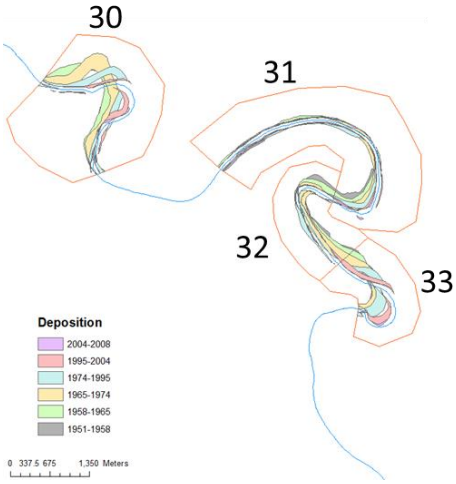
30
31
32
33
Deposition
2004-2008
1995-2004
1974-1995
1965-1974
1958-1965
1951-1958
0 337.5 675 1,350 Meters

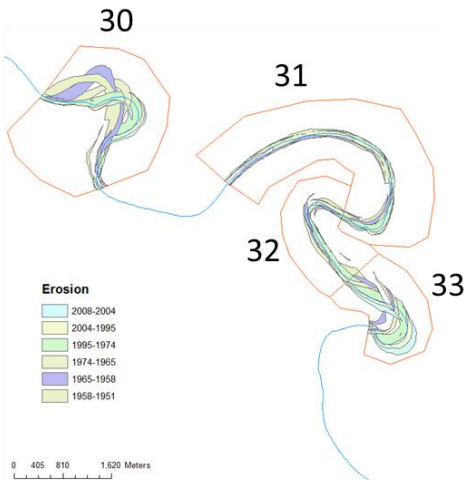
30
31
32
33
Erosion
2008-2004
2004-1995
1995-1974
1974-1965
1965-1958
1958-1951
0 405 810 1,620 Meters

APPENDIX B

The lake, and associated channel, segments for each oxbow used to calculate the cutoff ratio. The ratio is calculated by dividing the length of the lake segment by the channel segment. A higher ratio equates to a longer lake segment relative to the corresponding channel segment. The channel segment is the portion of the main channel between the upstream and downstream entrances of the oxbow lake.

Oxbow ID	Channel Segment	Lake Segment	Length (m)	Ratio
O1	y		572.6	6.10
		y	3490.8	
O2	y		415.7	9.98
		y	4147.6	
O3	y		278.9	2.52
		y	702.5	
O4		y	3423.0	14.41
	y		237.5	
O5		y	2710.0	22.67
	y		119.5	
O6	y		299.7	8.71
		y	2609.9	
O7		y	1660.1	2.54
	y		652.4	
O8	y		220.8	8.95
		y	1977.1	
O9	y		984.9	1.84
		y	1809.9	
O10	y		159.5	18.85
		y	3006.4	
O11	y		368.7	11.64
		y	4290.6	
O12	y		402.2	11.56
		y	4650.8	
O13	y		187.9	12.07
		y	2267.5	
O14	y		375.2	5.00
		y	1874.9	
O15		y	2304.8	11.22
	y		205.4	
O16		y	4505.3	8.29
	y		543.1	
O17		y	2172.8	5.11
	y		425.4	
O18	y		676.2	2.98
		y	2013.9	
O19		y	2163.5	6.85
	y		315.8	
O20		y	1687.5	4.95

	y		341.1	
O21		y	2515.2	4.46
	y		563.9	
O22	y		470.6	5.82
		y	2738.5	
O23		y	1601.7	3.70
	y		432.9	
O24		y	1491.8	1.82
	y		819.0	
O25		y	2582.9	7.08
	y		364.7	
O26	y		475.6	3.40
		y	1615.7	
O27		y	2826.2	25.49
	y		110.9	
O28		y	1268.6	5.86
	y		216.5	
O25		y	2582.9	7.08
	y		364.7	
O26	y		475.6	3.40
		y	1615.7	

APPENDIX C

The diversion angle is calculated by drawing a triangle between the upstream lake end and the main channel. By knowing the lengths of the three sides of the triangle the three angles can be determined. The *a* and *b* sides correspond to the oxbow and main channel, respectively, with the *c* side connecting the two.

Oxbow ID	Side	Length (m)	Angle
O1	a	406.9	
	b	215.0	
	c	276.3	39.3
O2	a	286.4	
	b	214.9	
	c	355.1	89.0
O3	a	261.0	
	b	175.2	
	c	350.1	105.1
O4	a	343.2	
	b	173.7	
	c	349.4	77.5
O5	a	403.4	
	b	129.2	
	c	495.7	129.5
O6	a	354.5	
	b	260.3	
	c	276.8	50.7
O7	a	355.4	
	b	313.1	
	c	317.2	56.2
O8	a	333.7	
	b	206.9	
	c	498.6	133.2
O9	a	183.9	
	b	145.2	
	c	269.7	109.5
O10	a	196.4	
	b	127.6	
	c	248.9	98.1
O11	a	359.6	
	b	158.6	
	c	441.8	110.9
O12	a	376.4	
	b	166.5	
	c	443.3	102.5
O13	a	320.5	
	b	86.0	
	c	331.5	89.8
O14	a	284.6	

	b	141.1	
	c	264.2	67.2
O15	a	320.4	
	b	93.8	
	c	267.3	48.3
O16	a	245.5	
	b	209.7	
	c	240.0	63.1
O17	a	409.1	
	b	300.9	
	c	343.2	55.3
O18	a	441.8	
	b	332.3	
	c	424.2	64.6
O19	a	853.1	
	b	215.9	
	c	775.5	62.0
O20	a	579.3	
	b	264.6	
	c	770.8	128.0
O21	a	356.5	
	b	402.2	
	c	508.9	84.1
O22	a	509.9	
	b	284.9	
	c	474.2	66.4
O23	a	317.6	
	b	195.5	
	c	472.4	132.6
O24	a	263.9	
	b	235.1	
	c	381.2	99.5
O25	a	427.3	
	b	224.6	
	c	621.3	142.8
O26	a	524.6	
	b	294.9	
	c	777.8	141.7
O27	a	223.8	
	b	94.8	
	c	292.7	128.8
O28	a	410.2	
	b	219.9	
	c	601.6	143.7

APPENDIX D

Listed below are the important attributes for each lake using the river reach styles classification. The main channel was partitioned into a number of distinct reaches, based in part on the categories listed below, such as underlying geology, channel slope, etc. The oxbows observed in this study categorized according to which river reach style they occurred in. Under the sinuosity column, the values are as follows: low sin = 1.25 – 1.49; mean = 1.50 – 1.99; str mean = 2.0 – 3.0; and tort = >3.0. In the Channel/flow pattern column, the ST tac represents single thread main channel with tributaries occupying the avulsion channels, and the ST represents single thread main channel. In the channel-floodplain connectivity column, which describes the frequency of connections between the main channel and the adjacent floodplain, the abbreviations represent as follows: low = low connectivity; mod = moderate connectivity; high 1 = high connectivity primarily from flooding of oxbows, sloughs, and flood basins; and high 2 = high connectivity primarily from cross-floodplain flow.

Oxbow	RR*	Geology	Slope	Sinuosity	Channel/flow Pattern	Channel-floodplain Connectivity
O1	-	-	-	-	-	-
O2	1	Eocene	0.020459	low sin	ST tac	mod
O3	1	Eocene	0.020459	low sin	ST tac	mod
O4	3	Eocene	0.000164	mean	ST tac	mod
O5	3	Eocene	0.000164	mean	ST tac	mod
O6	8	Miocene	0.000183	str mean	ST	low
O7	8	Miocene	0.000183	str mean	ST	low
O8	8	Miocene	0.000183	str mean	ST	low
O9	10	Miocene	0.000077	str mean	ST	low
O10	8	Miocene	0.000183	str mean	ST	low
O11	8	Miocene	0.000183	str mean	ST	low
O12	8	Miocene	0.000183	str mean	ST	low
O13	10	Miocene	0.000077	str mean	ST	low
O14	10	Miocene	0.000077	str mean	ST	low
O15	10	Miocene	0.000077	str mean	ST	low
O16	10	Miocene	0.000077	str mean	ST	low
O17	13	Lissie/Beaumont	0.000077	mean	ST	high 1
O18	13	Lissie/Beaumont	0.000077	mean	ST	high 1
O19	14	Lissie/Beaumont	0.000077	mean	ST tac	high 1
O20	15	Lissie/Beaumont	0.000251	mean	ST tac	high 1
O21	15	Lissie/Beaumont	0.000251	mean	ST tac	high 1
O22	16	Lissie/Beaumont	0.000251	tort	ST tac	high 1
O23	16	Lissie/Beaumont	0.000251	tort	ST tac	high 1
O24	16	Lissie/Beaumont	0.000251	tort	ST tac	high 1
O25	20	Beaumont	0.000111	low sin	ST tac	high 2
O26	20	Beaumont	0.000111	low sin	ST tac	high 2
O27	25	Beaumont	0.000031	low sin	ST tac	high 2
O28	29	Late Quaternary	0.000031	low sin	ST dac*	high 2

APPENDIX E

Aerial photograph interpretation

The following historic and recent aerial photographs display the condition of certain oxbows a few years to several decades after cutoff. The oxbows listed below were chosen for their cutoff date relative to the aerial photographs and/or the large number of aerial photographs showing changes through time of the oxbows. The aerial photographs are grouped by those lakes that have 4+ photographs shortly after cutoff (<10 years), lakes with 4+ photographs 10+ years after cutoff and lake with 2+ photographs after cutoff. These particular oxbow lakes, by examination of the different time periods, provide a snapshot of changing lake conditions through the decades after cutoff from the main channel.

Oxbow lakes with 4+ aerial photographs shortly after cutoff (<10 years). The date of cutoff is listed below the lake ID.

Lake O11
(1946)

1953

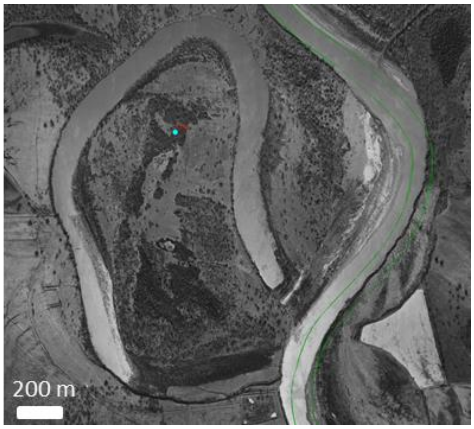

1960

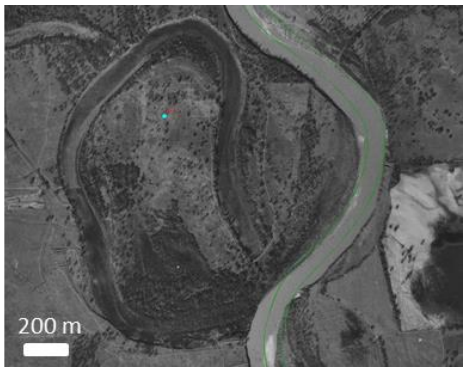

1972

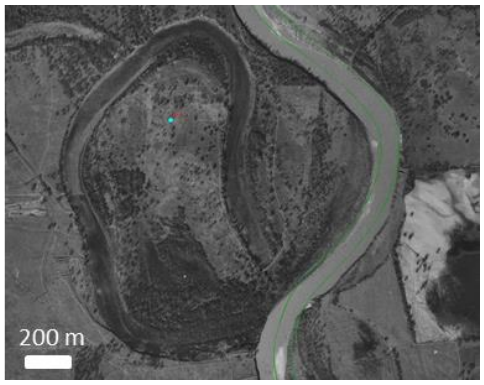

1984

2010

Lake O14
(1960)

1960

1966

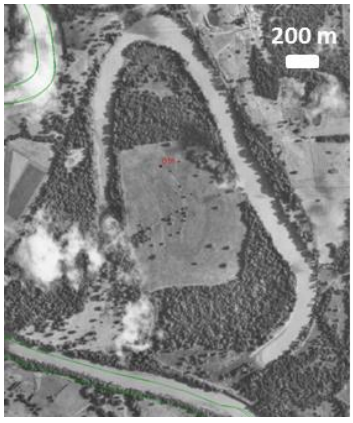

1978

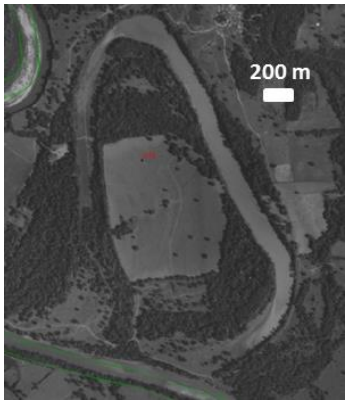

1984

2010

Lake O20
(1948)

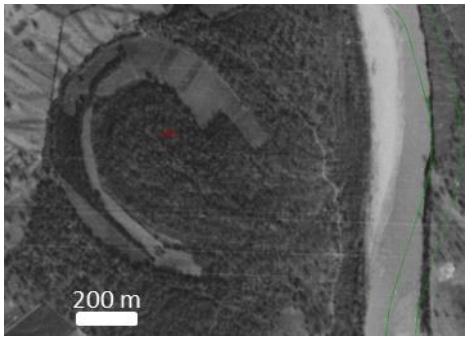

1952

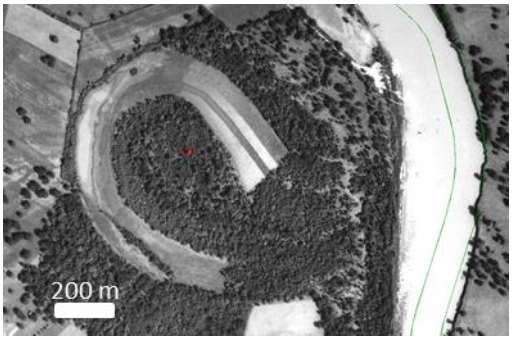

1966

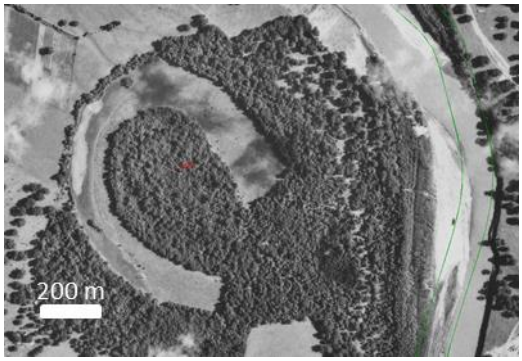

1978

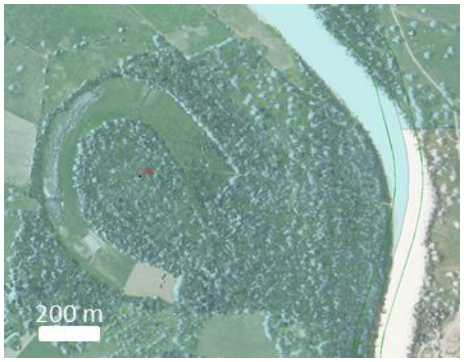

2010

Lake O21
(1948)

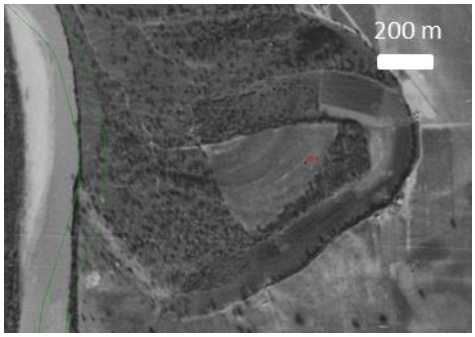

1952

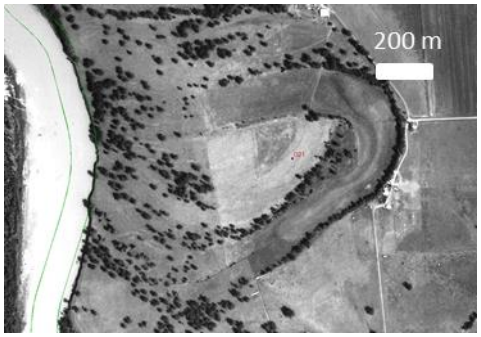

1966

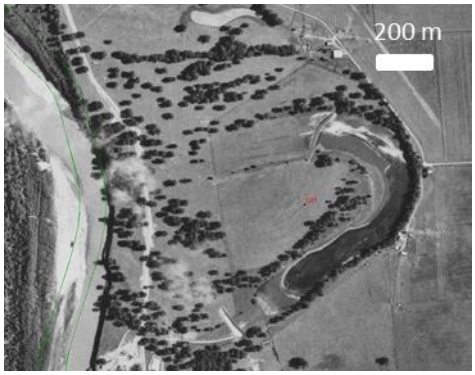

1978

2010

Oxbow lakes with 4+ aerial photographs and 10+ years after cutoff. The date of cutoff is listed below the lake ID.

Lake O5
(1920)

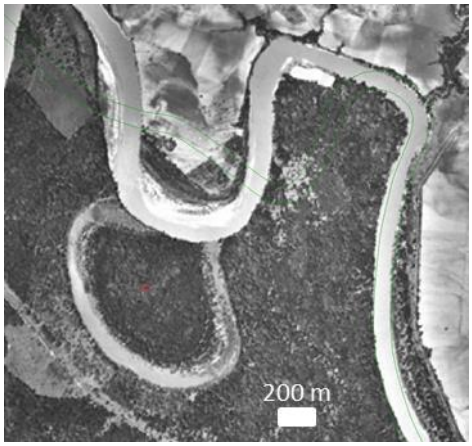

1940

1953

1964

2010

Lake O10
(1913)

1953

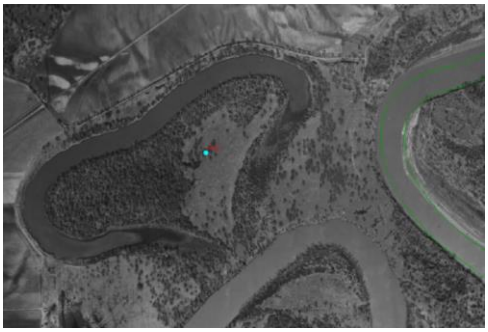

1960

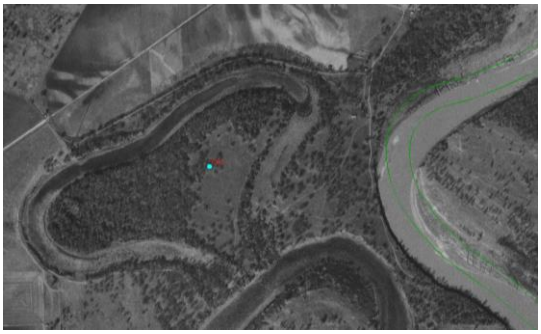

1972

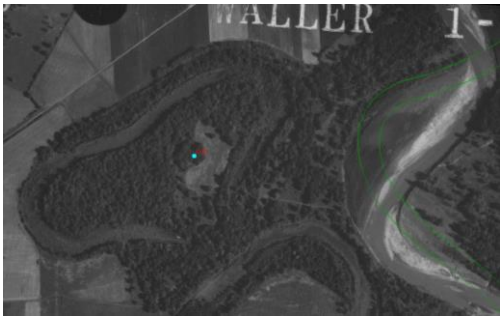

1984

2010

Lake O12
(1913)

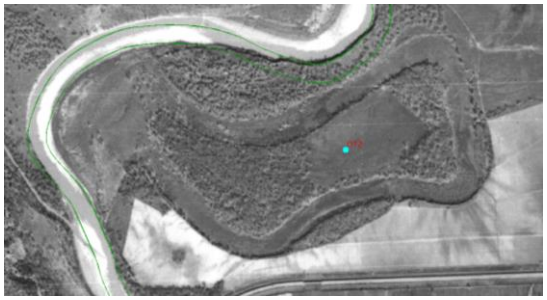

1953

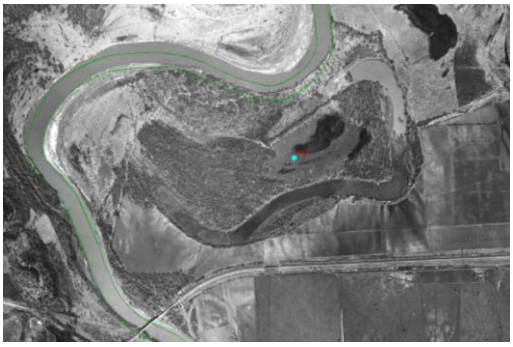

1960

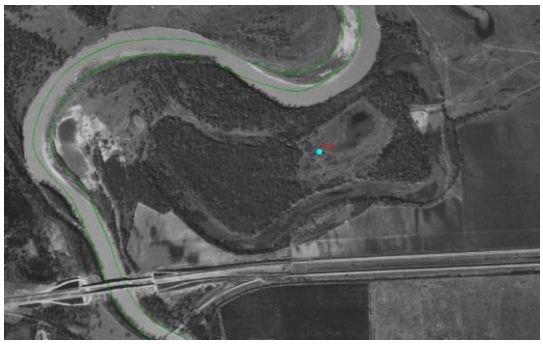

1972

2010

Lake O13
(1913)

1953

1960

1972

2010

Lake O18
(1917)

1953

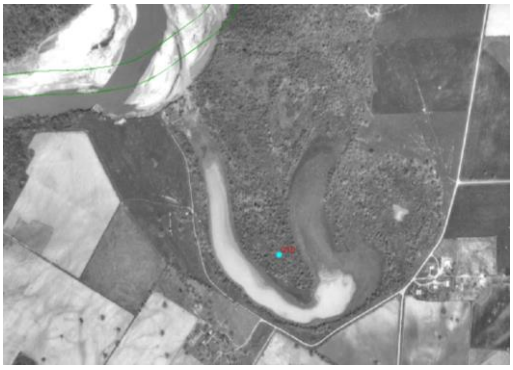

1966

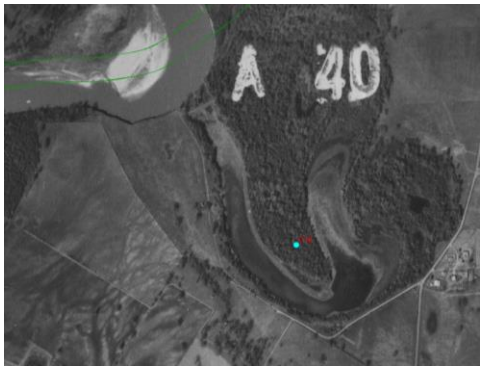

1972

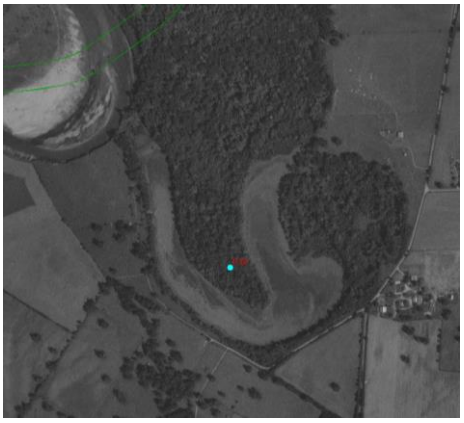

1984

2010

Lake O28
(1920)

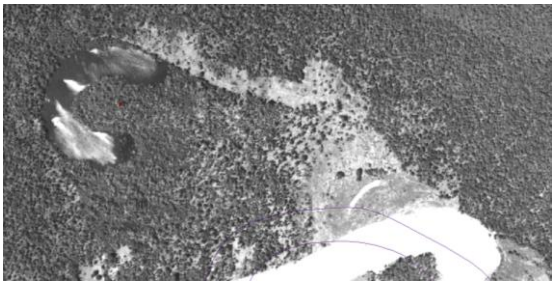

1944

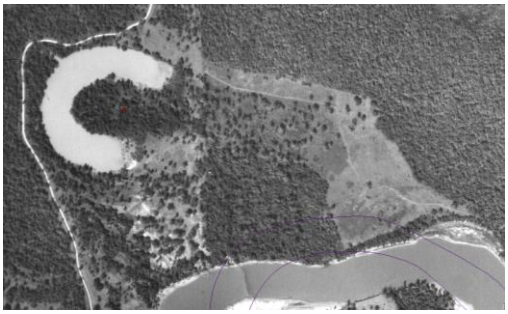

1965

1977

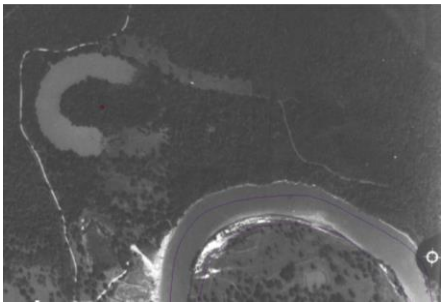

1987

2010

The following oxbow lakes have 2+ aerial photographs after the cutoff. The date is listed below the oxbow ID.

Lake O4
(1974)

1979

1988

2010

Lake O8
(1938)

1952

1972

2010

Lake O15
(1976)

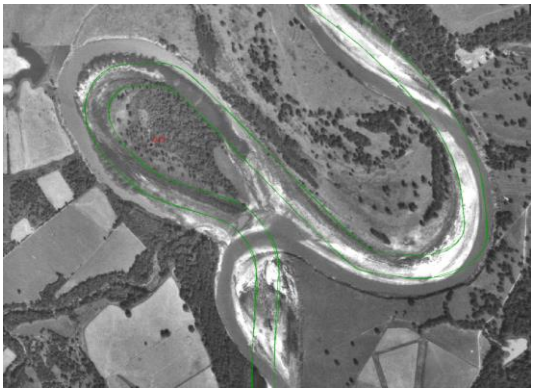

1976

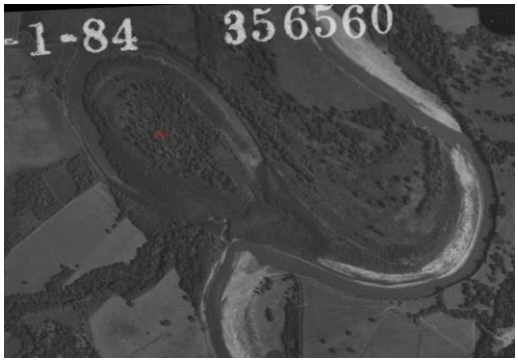

1984

2010

Lake O17
(1960)

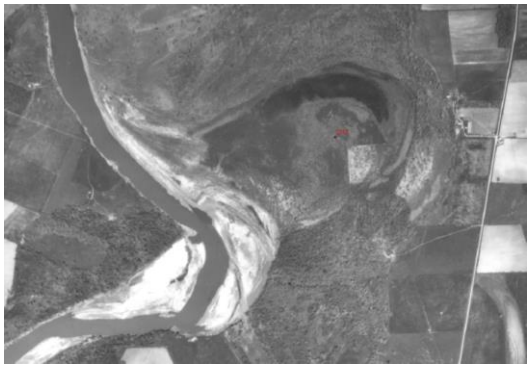

1966

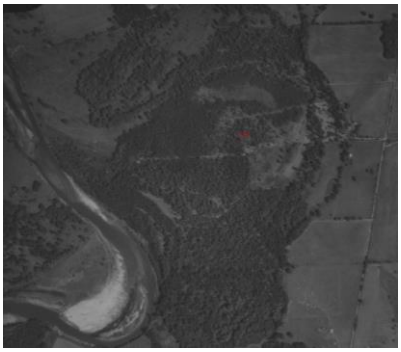

1984

2010